GENE REGULATION BY ARCA AND PHOB IN THE LIGHT-ORGAN SYMBIONT *VIBRIO FISCHERI*

by

JULIE L. STOUDENMIRE

(Under the Direction of Eric V. Stabb)

ABSTRACT

Bacterial pheromone signaling was discovered in *Vibrio fischeri*, where it controls activation of the *lux* operon responsible for bioluminescence and pheromone production. Although a threshold population density is required for pheromone signaling, environmental factors are also critical. For example, when *V. fischeri* enters its light-organ symbiosis with the Hawaiian Bobtail squid, the symbiotic *V. fischeri* cells are 1000-fold brighter than cells in laboratory cultures, even at the same population density. This observation prompted interest in understanding the regulators and environmental cues underlying *lux* regulation. Two such controls are the PhoBR and ArcAB two-component regulatory systems. The response regulators PhoB and ArcA control the *lux* operon in response to low phosphate and redox conditions, respectively; however it is unknown whether they are relevant to symbiotic bioluminescence induction, nor is the cue underlying Arc activation well understood. In this dissertation, I describe development of sensitive and specific fluorescent reporters to interrogate the regulatory status of PhoB and ArcA in *V. fischeri* cells both in and out of symbiosis. By adding a modified tag to a green fluorescent protein (GFP) and thereby targeting it for protease degradation, I decreased the half-life of the protein from over 24 hours to 81 minutes, making it a better proxy

for recent transcriptional activity. Using a novel, iterative and semi-randomized approach I generated a synthetic transcriptional promoter-*gfp* fusion optimized to be induced when PhoB is active. This construct was induced in low-phosphate conditions and showed heterogeneous activation in light-organ infections, suggesting non-uniform phosphate availability and the potential for low-phosphate conditions to contribute to symbiotic luminescence. I used the same synthetic promoter-*gfp* construct in conjunction with a chimeric ArcA-PhoB protein, using the receiver domain from ArcA fused to the DNA binding domain of PhoB, to explore Arc activation. I show that ArcB activates the ArcA-PhoB chimera in culture, but there is also ArcB-independent activation, which surprisingly appears to be dominant during colonization. Finally, I present data suggesting a role for acetyl-phosphate in activating the ArcA-PhoB chimera. Together, these studies pioneer the optimization of transcriptional regulators for assessing *V. fischeri* regulation *in situ*.

INDEX WORDS: *Aliivibrio, Euprymna scolopes*, *Photobacterium,* Regulation, Reporter

GENE REGULATION BY ARCA AND PHOB IN THE LIGHT-ORGAN SYMBIONT *VIBRIO FISCHERI*

by

JULIE L. STOUDENMIRE

B.S., University of Georgia, 2009

M.S., Georgia State University, 2011

A Dissertation Submitted to the Graduate Faculty of The University of Georgia in Partial Fulfillment of the Requirements for the Degree

DOCTOR OF PHILOSOPHY

ATHENS, GEORGIA

2017

GENE REGULATION BY ARCA AND PHOB IN THE LIGHT-ORGAN SYMBIONT *VIBRIO FISCHERI*

by

JULIE L. STOUDENMIRE

Major Professor: Eric V. Stabb

Committee: Mark Eiteman
Ellen Neidle
Vincent Starai

Electronic Version Approved:

Suzanne Barbour
Dean of the Graduate School
The University of Georgia
December 2017

DEDICATION

I dedicate this dissertation to my parents, Jay and Jackie, who have provided me valuable examples of what positive loving relationships can be and their encouragement has motivated me to reach farther than I ever dreamed possible.

ACKNOWLEDGEMENTS

I am incredibly thankful to the entire Microbiology department, and others in the University of Georgia community, that supported me along this journey. First, I need to acknowledge my advisor, Eric Stabb, who has supported me in my pursuit to explore teaching and mentoring more deeply while in his lab and for his patient guidance of me during my PhD research. I would also like to acknowledge my committee, current and past members of the Stabb lab (especially Alecia Septer), and other members of the department for their continuous support and advice. Without the unwavering personal and professional support of Anna Karls, Ellen Neidle, and Vincent Starai, I would not be the scientist or person I am today. I would additionally like to thank Tim Hoover for believing in me and giving me the opportunity to grow as a science educator. My friends and family, especially my parents and close friend Lisa Burgee, have been endlessly supportive throughout my education, for which I am very grateful. Last, but certainly not least, I would like to thank my husband, Zac, for his love, support, encouragement, and patience throughout this journey of graduate school.

TABLE OF CONTENTS

Page

LIST OF TABLES

Page

LIST OF FIGURES

Page

CHAPTER 1

INTRODUCTION AND LITERATURE REVIEW

OVERVIEW

The marine gamma-proteobacterium *Vibrio fischeri* has proven to be a valuable model for studying two important bacterial behaviors. First, the discovery that *V. fischeri* uses pheromone signaling to control expression of bioluminescence led to this bacterium becoming a groundbreaking example of a widespread regulatory phenomenon termed "quorum sensing", wherein pheromone-dependent gene activation requires a high density or "quorum" of cells (1-3). Later, the monospecific symbiosis between *V. fischeri* and the Hawaiian bobtail squid, *Eupyrmna scolopes,* was developed as a tractable experimental system for studying the mechanisms underlying persistent and beneficial animal-bacterium associations (4-7). These two distinct areas of study converged with the findings that bioluminescence is required for full colonization of the host (8-10) and that *V. fischeri* strain ES114, typical of most isolates from *E. scolopes*, only induces pheromone production and bioluminescence once it is established in the host but not in high-density colonies outside the host (4).

These observations prompted interest in multiple research questions. Which regulators control bioluminescence and pheromone production in *V. fischeri* ES114? Which of these regulators are responsible for induction of bioluminescence during symbiotic infection? What environmental parameters underlie this regulation and what are the corresponding relevant

conditions in the host light organ? Finally, given that pheromone signaling allows communication between cells, could this regulatory system allow heterogeneous environmental cues to elicit population-wide responses? Research to answer these questions has been ongoing, yet important gaps in our knowledge remain, particularly with respect to the regulatory status of *V. fischeri* cells in the host light organ.

In the remainder of this chapter, I will describe the model symbiosis between *V. fischeri,* and *E. scolopes*, this bacterium's bioluminescence and its regulation, two global regulators known to regulate colonization factors within *V. fischeri* and other Proteobacteria, and finally, the techniques currently used to study gene expression of bacteria *in situ.*

THE *VIBRIO FISCHERI – EUPRYMNA SCOLOPES* SYMBIOSIS

V. fischeri is found both free living and in the light-emitting organs of certain marine fish and squid, where it provides the host with bioluminescence in exchange for a privileged growth-promoting environment. Although *V. fischeri* light-organ symbioses with monocentrid fish proved difficult to study experimentally, the light-organ symbiosis with *E. scolopes* was more amenable to examination, largely because these animals will readily breed and lay eggs in laboratory aquaria (6, 11). Symbionts are not transmitted through the eggs, but after hatching; juvenile squid placed in water with *V. fischeri* are infected with this bacterium (and only this bacterium) in a specialized and ventrally located light organ (7). In this way, the symbiotic association can be reconstituted in the lab with wild-type or genetically modified *V. fischeri*, and these infections can be further compared to uninfected animals kept in water lacking *V. fischeri*. Further, fluorescent markers can be observed in the transparent tissue of an intact light organ. Thus, in addition to being a natural infection, this symbiosis is uniquely experimentally tractable.

During establishment of this natural infection, the bacteria traverse and encounter various environments on and in the host. The *E. scolopes* light organ has two pairs of ciliated appendages, one on each side of the organ, and at the base of each pair six pores lead from the surface of the light organ to epithelium-lined crypt spaces within the organ (Figure 1.1, (12)). Upon hatching, the ciliated appendages move the surrounding water over the pores, and *V. fischeri* cells in the water form aggregates near the pores on host-derived mucus (13). *V. fischeri* cells eventually enter the pores and migrate through the ducts into the crypts where they begin to replicate rapidly with an initial doubling time of 20 min (14). Each day, in response to the light at dawn, *E. scolopes* vents up to 90% of the light-organ contents back into the environment (15-17). It has been proposed that this mechanism serves to maintain a fresh culture of *V. fischeri* to support luminescence the next evening (17) and it may additionally, or alternatively, seed the environment with potential symbionts for the next generation of squid. After colonization, symbionts trigger a developmental program in *E. scolopes* whereby the ciliated appendages regress and disappear, and the light organ retains a monospecific culture of *V. fischeri* throughout most or all of the animal's remaining life (18).

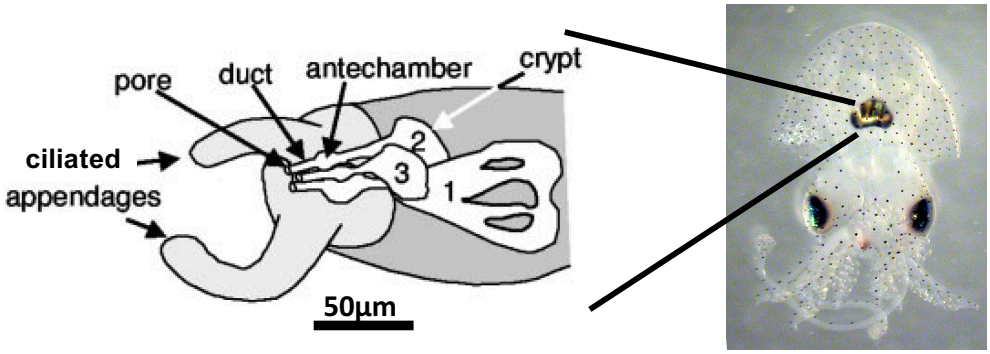

Figure 1.1: Organization of the microenvironments within the juvenile squid light organ. The light organ of a juvenile squid (right) is magnified and one lobe of the light organ is drawn in a schematic (left). There are three pores located at the base of the ciliated appendages, each lead to a duct, antechamber, and deep crypts, which ultimately house the bacteria (12). This figure is courtesy of Eric Stabb.

Luminescence and lux *regulation*

Like other host-associated bacteria, *V. fischeri* regulates many genes in response to the host environment. For example, as noted above, bioluminescence is induced upon infection and enables *V. fischeri* to colonize the host squid fully (8-10). Bacterial bioluminescence is an energetically expensive process and accordingly it is highly regulated. Briefly, *V. fischeri*'s luminescence is produced when luciferase (LuxAB) converts $FMNH_2$, O_2, and an aliphatic aldehyde to FMN, water, and an aliphatic acid (19). Luciferase drains $FMNH_2$ and O_2 pools, potentially from aerobic respiration, which may lead to decreased ATP production in the cell. LuxC, LuxD, and LuxE are responsible for (re)generating the aldehyde substrate in an ATP-dependent manner (20), while LuxG shuttles electrons to FMN to generate the $FMNH_2$ substrate (21). Moreover, the luciferase enzyme in fully induced cells may account for up to 5 percent of the total soluble protein (22). Since protein synthesis itself requires substantial energy, this is a large expense to the cell.

Production of luminescence in *V. fischeri* is in part controlled by pheromone-mediated regulation via LuxR and LuxI (Figure 1.2), with additional pheromone systems governed by AinSR and LuxS/LuxPQ also playing roles (1, 23-27). This regulation controls the *luxCDABEG* operon that underpins bioluminescence. LuxI, an autoinducer synthase, produces *N*-3-oxo-hexanoyl homoserine lactone (3-oxo-C6-HSL) (24), which diffuses freely between cells (28). As cell density increases, 3-oxo-C6-HSL accumulates. Once 3-oxo-C6-HSL reaches a threshold concentration, it combines with LuxR to activate transcription of the *luxICDABEG* operon (1, 25).

While high cell density may be necessary for inducing luminescence in *V. fischeri* during colonization of the *E. scolopes* light organ, it is not sufficient. Wild-type *V. fischeri* ES114

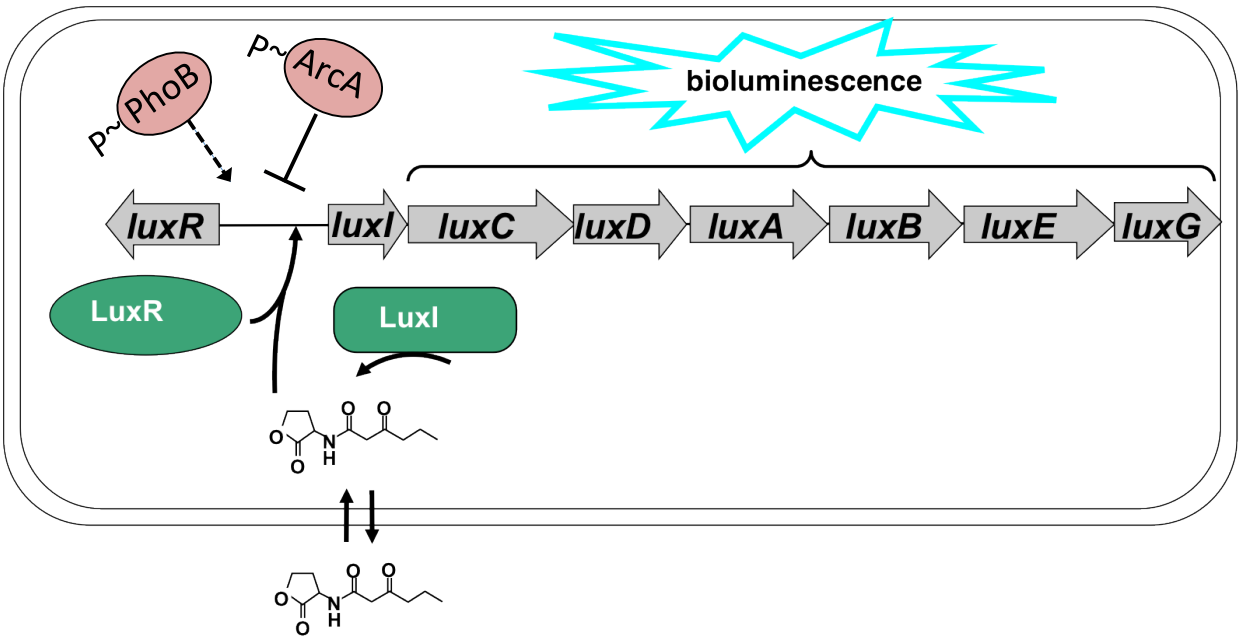

Figure 1.2: Regulation of the *lux* operon in *V. fischeri*. Luciferase (LuxAB) generates bioluminescence from $FMNH_2$, O_2, and an aliphatic aldehyde (19). LuxCDE (re)generates the aldehyde substrate (20), while and LuxG shuttles electrons to FMN (21). LuxI generates *N*-3-oxo-hexanoyl homoserine lactone (3OC6) (24), which diffuses across cell membranes (28). When intracellular concentrations of 3OC6 reach a critical threshold, 3OC6 combines with LuxR, and LuxR-3OC6 binds upstream of *luxI* and activates transcription through the *lux* operon (1, 25). Additional regulators, including phosphorylated ArcA and PhoB, can increase or decrease transcription through the *lux* operon under certain environmental conditions (28-30). The dotted line from P-PhoB indicates that the mechanisms of *lux* operon activation is unknown and probably indirect.

colonies on a plate are ~1000 fold dimmer than are cells within the host, despite reaching similar high cell densities (4). Several environmentally responsive regulators of luminescence have been studied. Among these are the global regulator CRP, which is involved in carbon metabolism (31-36), Fur, which is involved in iron acquisition and uptake (37), and ArcA, which coordinates metabolic shifts during transitions between aerobic and anaerobic environments (28, 29), and several others (30, 38-40). For the most part, the regulation of luminescence has been studied in cultured cells, and it is not always clear if these regulators are relevant for luminescence induction during symbiosis with the squid.

Two-component regulatory systems in V. fischeri

Many bacteria including *V. fischeri* respond quickly to changing environments through the sensing and signaling cascades of two-component regulatory systems (41, 42). Two-component regulators have been found in a variety of bacteria, and they directly or indirectly control the expression of genes associated with a wide range of processes and behaviors (41, 43). Among host-associated bacteria, two-component regulatory systems often control the induction of colonization or virulence factors (29, 38, 44, 45). The most common two-component regulators consist of a membrane-bound histidine kinase sensor and a cytoplasmic response regulator. Environmental signals trigger the sensor kinase to autophosphorylate, using ATP as a phospho-donor, at a conserved histidine residue. The phosphate group can then be transferred to a conserved aspartate residue on a cognate response regulator. Upon phosphorylation, the response regulator controls the transcription of genes through binding specific DNA sites, or, less commonly, directly controls protein function (46). While some response regulator DNA binding sites are conserved and easily identified bioinformatically (47-49), other response regulators' binding sites are less conserved and difficult to identify based on sequence.

As an additional control element, in the absence of their respective environmental signal, many sensor kinases have phosphatase activity capable of removing the phosphoryl group from their cognate response regulator (50). Further, phosphorylation and dephosphorylation of some response regulators is modulated by non-cognate sensors or by other mechanisms (51). Thus, the lack of a cognate signal does not necessarily result in the same output as is seen when the sensor kinase component is absent, and mutants lacking a sensor kinase or its cognate response regulator do not always have the same phenotype.

V. fischeri has forty predicted two-component regulatory systems (38). Among these, eight response regulators have an effect on luminescence under certain conditions; CheV, FlrC, GacA, PhoB, and YehT all positively regulate luminescence, whereas ArcA, LuxO, and PhoP repress luminescence (29, 30, 38, 39). Nine response regulators affect swimming motility, including CheY and FlrC, which are essential for motility, ArcA, CpxR, LuxO, NarP, and VpsR, which each positively regulate motility, and CheV, which represses motility (38). GacA's regulation of motility is complex and depends on the viscosity of the medium (39). As both luminescence and motility are required for establishing and maintaining colonization (8, 52-55), it is unsurprising that of the twelve response regulators with modified luminescence or motility, all but three (CpxR, PhoP, and YehT) contribute to colonization competitiveness (29, 38). Additionally, a mutant with a transposon insertion in the gene encoding PhoQ, the cognate sensor kinase to PhoP, is outcompeted in colonization (56). Moreover, mutations in five response regulator genes, *ntrC*, *expM*, VFA0179, VFA0181, and *sypG*, cause no known luminescence or motility defect in culture, yet the respective mutants still fail to colonize the squid competitively (38). Thus, it is clear that two-component regulators have a significant impact on the ability of *V. fischeri* to colonize its host, through their regulation of bioluminescence, motility, or other factors. However, it is not yet clear if and when each response regulator is active throughout the establishment and maintenance of symbiosis. Below I will describe in more detail two of the two-component regulatory systems in *V. fischeri* that are the focus of this dissertation: ArcAB and PhoBR.

ArcAB (anoxic redox control), which has primarily been studied in *Escherichia coli*, is a two-component regulatory system that responds to the redox state of the cell (57). While the conditions influencing the sensor kinase ArcB in *V. fischeri* may deviate from the paradigm in *E.*

coli, in that bacterium under reducing conditions ArcB phosphorylates ArcA, thereby activating it. Phosphorylated ArcA (P-ArcA) then regulates the expression of many metabolic genes as cells transition from aerobic to microaerobic or anaerobic metabolism (57). Arguably, this regulation could alternatively be described as the transition from respiratory to fermentative metabolism, as oxygen itself does not seem to be directly recognized by ArcB (58).

In culture, *V. fischeri arcA* and *arcB* mutants are ~500-fold brighter than wild type, achieving nearly symbiotic luminescence levels (29). This effect appears to be mediated by activated ArcA (P-ArcA) binding upstream of the *lux* operon and repressing its transcription (29). However, an *arcA* mutant is not brighter than wild type in the light organ (29), suggesting that ArcA does not significantly repress luminescence in symbiotic cells, at least at the times tested. On the other hand, wild-type cells have about a 4-fold competitive advantage over *arcA* mutants over two days of squid colonization (29). Taken together, these results indicate that Arc-mediated regulation could account for the disparity in luminescence levels between cells in culture and within the host, if the ArcA-mediated repression of the *lux* operon observed in culture is relieved during colonization. Yet it is clear that Arc must be active at some point during the first 48-hours of the symbiosis.

In considering these results it is important to note that the Lux circuit constitutes a positive feedback loop, because the 3-oxo-C6-HSL produced by LuxI, stimulates the *lux* operon to produce more LuxI (Figure 1.2). This positive feedback gives the regulatory circuit an element of hysteresis, making it more difficult to turn off once it has turned on (28, 59). Septer and Stabb demonstrated that direct repression of the *lux* operon by ArcA is relatively weak, and most of the 500-fold induction of luminescence in an *arcA* mutant is due to positive feedback (28). Moreover, they showed that once luminescence is induced and positive feedback is triggered,

ArcA is no longer effective at repressing it (28). These results were consistent with a hypothesis proposed by Bose *et al*. that redox conditions in the squid light organ affect the Arc system. They proposed that during initial stages of light-organ infection, ArcA, is inactive (or less active) allowing luminescence induction (Figure 1.2), but later during infection, as the crypts become crowded with symbionts, the Arc system is stimulated and contributes to colonization competitiveness but is unable to repress luminescence (29). Testing the activity of ArcA and ArcB *in situ*, in the symbiosis, will be critical for testing this hypothesis further.

Another two-component regulatory system of interest in *V. fischeri* is PhoBR. Like ArcAB, the PhoBR system contributes to both luminescence regulation and symbiotic competence. In many bacteria, the PhoBR two-component regulatory system responds to environmental phosphate concentrations and underpins a response to phosphate limitation (60). PhoR phosphorylates PhoB when environmental phosphate is low and removes the phosphoryl group when environmental phosphate is high (61). When phosphorylated, PhoB binds to specific "Pho Box" sequences in promoter regions and activates or represses the transcription of many genes, including those required for phosphate acquisition as well as genes underlying other processes such as virulence (62-65). *V. fischeri* cells grown in low-phosphate media display around 10-fold brighter luminescence relative to cells grown in phosphate-replete media and this effect is dependent on *phoB* (30).

Two lines of evidence suggest that the PhoB regulon contributes to the symbiotic competence of *V. fischeri*. First, a *phoB* mutant is outcompeted by wild type for colonization of the squid light organ (38). Second, mutants with transposon insertions in *pstA* and *pstC*, genes encoding the high-affinity phosphate importer, have a more pronounced competitive defect relative to wild-type during colonization than when grown in a phosphate-replete medium (56).

These data suggest that at some point in colonization, phosphate is low enough that the PhoB regulon is stimulated in symbiotic *V. fischeri*. However, transcriptomic analysis of symbionts vented from the juvenile squid light organ suggested the PhoB regulon is not induced (66). These conflicting results could be reconciled if PhoB is activated in a spatially or temporally dependent manner during light-organ colonization. Again, methods for assessing gene expression *in situ*, in the symbiosis, will be critical for exploring such possibilities.

IN SITU GENE EXPRESSION TECHNOLOGY

Much research has been dedicated to assessing which bacterial genes are differentially regulated during growth inside and outside a host, using both global and single-gene approaches. Common methods of studying gene expression within bacteria include the use of reporter genes such as *lacZ*, *inaZ*, or *gfp,* encoding β-galactosidase, ice nucleation protein, and green fluorescent protein, respectively, placed downstream of a promoter of interest (67-71). To assess transcription globally, popular approaches include quantifying mRNA transcripts within a population of cells (72-74) and *in vivo* expression technology (75, 76), both of which result in a collective snapshot of all of the genes being expressed at a particular time or time frame. To visualize spatial distribution of bacterial gene expression in live host samples, different techniques are required. Below, I will describe common methods to assess transcriptional regulation within bacterial cells in culture and in the host, ending with methods that have been used to investigate transcriptional regulation in *V. fischeri*.

Transcriptional reporters

The use of transcriptional reporter systems has increased our knowledge of gene regulation since the first published transcriptional reporter in 1975 (71). The *lac* operon's *lacZ*, encoding a β-galactosidase, fused to a promoter has been widely used since. Improvements on the initial reporter system have been made, including the transition to plasmid-based transcriptional fusions in 1980, allowing for faster *in vitro* construction (77). Alternative reporter genes have also been introduced. To name a few, in 1985, alkaline phosphatase (*phoA*) was used to analyze export signals and sequences (67), in 1990 luciferase (*luxAB*) fusions were constructed as a sensitive and even visible reporter (68), and in 1994 green fluorescent protein (*gfp*) was introduced and shown to produce green fluorescence in bacterial cells proportional to promoter induction (69). A benefit of fluorescence-based reporters is the ability to visualize promoter activity within an individual bacterial cell in its native state, including within symbiosis. GFP-based reporter systems are now used heavily to study transcriptional and translational regulation in both prokaryotic and eukaryotic systems.

Initially discovered in 1961, GFP has been optimized to study transcriptional activation within cells (69, 78). Since its discovery and isolation, mutations have been made to *gfp* to increase GFP fluorescence (79-83), shift excitation/emission spectra (81, 84), and decrease GFP misfolding (85) or folding time (86). GFP and its derivatives do not require cell lysis or the addition of reagents to be detected, only excitation by relatively short wavelength (usually <500 nm) light (79, 87). Additionally, GFP is a stable protein, thereby yielding relatively strong fluorescence when induced (88, 89). These properties have made GFP useful as a reporter, for determining if a promoter is activated in live bacterial cultures (90), or for detecting symbiont gene expression within host tissues, including both plants (91) and animals (92). However, the

stable nature of GFP could obscure down-regulation of gene expression in live bacteria. In other words, GFP may linger, long after transcription of the reporter has ceased. This complexity in interpretation is a potentially confounding factor for any reporter, but it has been a notable concern for the use of GFP. Destabilizing GFP variants or increasing their rate of recycling within the cell has addressed this issue. By adding variants of the eleven-amino acid SsrA tag to the C-terminus of the protein sequence, GFP is targeted to the ClpXP protease, reducing the half-life in some systems to between 40 and 110 min from more than 24 hours (70, 88).

Despite having sensitive methods to determine which genes are activated during host colonization, deciphering specific regulation patterns within the microenvironments of the host remains challenging. Using a *gfp*-transcriptional reporter, Brandl *et al*. saw large variations in gene expression when looking at bacteria recovered from a plant 48 hours after inoculation (93). Further, when looking at the spatial patterns of individual cells using confocal microscopy, they noticed heterogeneous expression and different fluorescence intensities within different physical or chemical microenvironments of the host tissue (93). In a similar study using a destabilized GFP variant, researchers successfully used *Erwinia herboicola* as a bioreporter to localize fructose availability on leaf surfaces (94). By using a destabilized GFP reporter, this study had the potential advantage of capturing more dynamic expression patterns. Thus, use of GFP and its derivatives has the potential to improve our understanding of the gene expression in microenvironments of intact symbiont tissues.

Investigating V. fischeri *gene regulation during colonization of juvenile squid*

Induction of the *lux* operon is just one example of genes expressed differently in the light-organ symbiosis relative to growth in laboratory culture. To identify other genes expressed

(or differentially expressed) in *V. fischeri* during symbiosis, several approaches have been utilized. Global transcriptomic approaches were applied to *V. fischeri* recovered from adult squid tissues (74) or from juvenile-squid ventate (66). Insertion sequence technology also has been used to identify *V. fischeri* genes important for competitive colonization (95), which indirectly suggests that these genes are expressed during colonization. These studies provide valuable information on the relative transcription of genes in the symbiosis and/or the genes required for successful maintenance in the squid during symbiosis. However, such approaches assess the bulk population of symbionts and do not take into account the possibility of different transcriptional responses to, or fitness effects in, distinct light-organ microenvironments. With respect to the transcripomic analysis of vented symbionts, each crypt of the squid light organ is not vented each day to the same degree. While crypt 1, and a large portion of crypt 2, is almost completely vented each night, crypt 3 is largely maintained and not vented (Figure 1.1, (96)). Further, as an example of microenvironment specificity, there is a delay in the expression of *lux* genes in crypt 3 (97). Therefore, by looking at the transcript levels of symbionts in squid ventate or transcripts from *V. fischeri* collected from the squid light organ as a whole, there is a possibility of missing regulatory responses found only in a distinct subset(s) of cells.

To determine if a gene or operon of interest is being expressed by particular *V. fischeri* cells in the squid light organ, *gfp*-transcriptional gene fusions have been used (97, 98). In this way, the above-mentioned microenvironment-specific expression of *lux* genes was discovered (97). A similar technique has also been used to determine the state of a global regulator, CRP, in symbiotic cells. Specifically, a CRP-dependent promoter was inserted upstream of a promoterless *gfp*, and in this case the amount of fluorescence indicated whether this global regulator was active. As predicted, this reporter was turned off when glucose was available but

was activated during growth without exogenous glucose and during light-organ colonization (32). These studies, however, used a stable GFP, which, as noted above, could potentially mask different dynamic transcription patterns of cells.

RATIONALE AND OBJECTIVES FOR THIS STUDY

Previous work with *V. fischeri* has identified numerous regulators of luminescence, motility, and other light-organ colonization factors (30, 38). However, in many cases it is still unclear if these regulators are important for transcriptional activation in symbiosis, and if so, when and where they are activated within the light organ. The goal of this dissertation was to develop transcriptional reporters for PhoB and ArcA that provide an optimal readout of regulator activity and are suitable for use in and out of symbiosis. Our goal was to generate *gfp*-based transcriptional reporters with promoters that are activated by a specific transcriptional regulator while maintaining low background expression. I wanted to augment this approach with constitutive *mCherry* expression, allowing me to localize and detect bacteria in symbiosis based on this protein's red fluorescence, regardless of whether *gfp* is expressed or not.

The approach of using native promoters driving transcriptional reporters to probe the activity of a global regulator such as ArcA or PhoB has the potential to give a weak and/or non-specific signal. My goal in Chapter 2 was to design a PhoB-dependent promoter that yields high GFP expression in low phosphate (PhoB-activating) conditions, and low background expression in phosphate-replete environments. I describe a method using the well-characterized "pho box" of PhoB binding sites with key transcriptional promoter elements surrounded by semi-randomized nucleotides, followed by iterative screening of promoter variants, to arrive at a promoter with optimal properties. I show that with initial data informing the design for a second

round of screening, improvements can be made to both increase reporter gene expression and decrease background. I demonstrate that this PhoB-dependent promoter can be used to probe phosphate- and PhoB-dependent activation in a variety of Proteobacteria, and propose that the iterative design technique is applicable to other reporters of transcriptional regulators. I also show that the addition of a modified SsrA tag decreases GFP half-life from over 24 hours to 81 min., allowing a reporter readout that is more closely connected to recent transcriptional activity.

In Chapter 3, I develop a chimeric protein to interrogate Arc activation in *V. fischeri*. Exploiting the PhoB-dependent reporter described above, I generated a chimeric protein that is activated in an ArcB-dependent manner, yet activates transcription from the PhoB-dependent promoter. ArcB activates this chimeric protein in *V. fischeri*, but surprisingly I found ArcB-independent activation of the chimeric reporter. Moreover, my data suggest that ArcB-independent activation is the primary mechanism of activation when *V. fischeri* is in the squid. Based on these data, I propose a more complex model of ArcA activation in *V. fischeri* than we anticipated based on studies in *E. coli*.

Finally, in Chapter 4, I discuss the contributions I have made to our understanding of the roles global regulators PhoB and ArcA play in *V. fischeri* gene regulation both in culture and in the light-organ symbiosis with *E. scolopes.* Additionally, I consider some of the larger implications of this research in exploiting the techniques and tools developed for interrogating the state of other two-component regulators and transferring these tools into other bacterial systems.

CHAPTER 2

ITERATIVE SYNTHESIS OF AN OPTIMIZED PHOB-DEPENDENT TRANSCRIPTIONAL REPORTER IN *VIBRIO FISCHERI*[1]

[1] Stoudenmire, J.L., Essock-Burns, T., McFall-Ngai, M., Weathers, E.N., Solaimanpour, S., Mrazek, J., and E.V. Stabb. To be submitted to *Journal of Bacteriology*.

ABSTRACT

The creation of transcriptional reporters was a revolutionary innovation for studying gene regulation. The fusion of transcriptional promoters to reporter genes has been used alternatively to analyze transcription of a gene of interest or to examine the activity of a specific transcriptional regulator. The latter application has the shortcoming that native promoters did not evolve as optimal readouts for the activity of a particular regulator. We sought to synthesize an optimized transcriptional reporter for assessing PhoB activity in *Vibrio fischeri*, aiming for maximal "on" expression when PhoB is active, minimal background in the "off" state, and no control elements for other regulators. We designed specific sequences for promoter elements with appropriately spaced PhoB-binding sites, and at nineteen intervening positions for which we did not predict sequence-specific effects the nucleotides were randomized. Eighty-three such constructs were screened, enabling us to identify bases at particular randomized positions that significantly correlated with high "on" or low "off" expression. A second round of promoter design rationally constrained thirteen additional positions, leading to a reporter with high PhoB-dependent expression, essentially no background, and no other known regulatory elements. As expressed reporters, we used both stable and destabilized GFP, the latter with a half-life of eighty-one minutes in *V. fischeri*. In culture, PhoB induced the reporter when phosphate was depleted below 10 μM. During symbiotic colonization of its host squid *Euprymna scolopes*, the reporter indicated heterogeneous phosphate availability in different light-organ microenvironments. Finally, testing this construct in other Proteobacteria demonstrated its broader utility.

IMPORTANCE

Transcriptional reporters are powerful tools for assessing when particular transcriptional regulators are active; however, when native promoters are used for this purpose, outputs can be non-ideal. Optimal reporters should be specific to the particular regulator being interrogated and should maximize the difference between "on" and "off" states; properties distinct from the selective pressures driving the evolution of natural promoters. Synthetic promoters offer a promising alternative, but our understanding does not yet enable fully predictive promoter design, and the number of alternatives can be intractable. In a synthetic promoter region with over 3.4×10^{10} possible sequences, we identified bases correlated with favorable performance by screening only 83 candidates, allowing us to rationally constrain our design. We thereby generated an optimized reporter that is induced by PhoB and used it to elucidate the low-phosphate response of *V. fischeri*. This promoter-design strategy will facilitate the engineering of other regulator-specific reporters.

INTRODUCTION

Malcolm Casadaban's use of the *lac* operon as a transcriptional reporter in 1975 revolutionized the study of gene regulation, paving a new way to assess the activity of a transcriptional promoter by fusing it to a gene encoding a readily screened and measured phenotype such as β-galactosidase activity (71). Ultimately, transcriptional reporters became a mainstay of bacterial genetics, and fusing a gene's promoter to a transcriptional reporter has led to the discovery of conditions and regulators that activate or repress countless genes. In a twist on this original application, when a particular transcriptional regulator controls a promoter, the corresponding promoter-reporter fusion is also sometimes used to assess the activity of that

regulator (99-101); however, this approach has limitations as native promoters are generally not ideal for this purpose.

An ideal readout of regulator activity would have minimal expression in the "off" state, high "on" expression, and a strict specificity for the regulator in question; attributes that do not necessarily reflect the evolution of native promoters. For example, some leaky expression in the "off" state is necessary for *lac* operon function, and native promoters are often regulated by multiple transcription factors simultaneously (102-104). Co-regulation has been addressed, at least in part, by avoiding or removing unwanted regulatory elements (99, 105-109); however, given the complexity of gene regulation, and the challenge of cataloging all the regulatory mechanisms at a natural promoter, this approach may not always be effective.

Synthetic promoters offer another approach for generating regulator-specific reporters. Such promoters can be engineered to incorporate sequence motifs consistent with regulation by one mechanism while avoiding binding sites for other regulators. Online tools can aid in this process (32, 110, 111), but promoter-reporter performance is not entirely predictable. Sequences with no known function, other than spacing between established regulatory elements, can affect output (32), hampering the rational engineering of such transcriptional reporters.

We sought to develop a transcriptional reporter to monitor the activation state of PhoB in *Vibrio fischeri*. In this bacterium, PhoB is an activator of bioluminescence, which is a colonization factor in *V. fischeri*'s light-organ symbiosis with the Hawaiian bobtail squid, *Euprymna scolopes* (8, 10, 30). Mutations in *phoB*, or the phosphate uptake system that it controls, reduce colonization competitiveness (30, 56). PhoB is the response regulator portion of a two-component regulatory system that activates expression of several genes under low-phosphate conditions (112, 113). In *Escherichia coli,* PhoB is activated upon phosphorylation by

its cognate sensor-kinase PhoR in response to low (<4 μM) phosphate (114). Phosphorylated PhoB then binds to a "Pho box" sequence consisting of two well-conserved 7-bp direct repeats (5'-CTGTCAT-3') separated by 4-bp of AT-rich sequence (62, 114, 115). PhoB binding can compensate for a poor -35 promoter element and activate transcription. Previously, PhoB dependent reporters have been generated using native promoters for *pstS* and *phoA* (113, 116-119), but as noted above these may have shortcomings such as high background or shared control with other regulators (120, 121).

In this study, we describe the generation of a synthetic PhoB-dependent transcriptional promoter, which we linked to *gfp* as a reporter gene, enabling us to use green fluorescence as both a measure of expression and a visual marker in symbiotic *V. fischeri* cells. We also expanded the utility of GFP for assessing dynamic changes in gene expression in *V. fischeri* by evaluating destabilized GFP variants. Our constructs are useful for assessing the low-phosphate response in *V. fischeri* and other bacteria, and our general method of synthetic reporter design has potential to be effective for studying other regulators in a variety of bacteria.

RESULTS

Generating and screening semi-randomized variants of a synthetic promoter region

To generate a PhoB-dependent and PhoB-specific synthetic transcriptional reporter, we began with a basic framework based on canonical attributes of PhoB-activated promoters, such as those upstream of *phoB* and *pstS* in *E. coli* (122), and we interspersed randomized sequences separating the features relevant to PhoB activation of transcription. This initial semi-randomized sequence is shown in Figure 2.1A, and its design is described as follows. Multiple Pho boxes are common upstream of PhoB-activated genes (63, 64, 118, 123, 124), and we therefore placed two

closely spaced Pho boxes, with one overlapping a weak -35 promoter element, consistent with arrangements in native promoters. As noted above, the canonical Pho box includes 7-bp direct repeats; however, an additional 3' A nucleotide may play a role (62). Of the four repeats in the two Pho boxes we used, none deviates from the 8-bp sequence 5'-CTGTCATA-3' by more than a single mismatch. Within each Pho box, the A/T richness of sequences between the direct repeats appears to play a role in establishing a hierarchy of PhoB binding (125), and this spacer between repeats was set at 5'-AAT-3' in the Pho box distal to the reporter and semi-randomized as A or T (W) in the Pho box overlapping the -35 promoter element (positions 4-6, Figure 2.1A). The three nucleotides between Pho boxes were completely randomized (positions 1-3, Figure 2.1A) as were positions upstream and downstream of the -10 promoter element (positions 7-11 and 12-19, respectively; Figure 2.1A). Altogether, this promoter has 34,359,738,368 (4^{16} x 2^3) different possible sequence variants.

We cloned and sequenced eighty-three variants of the construct illustrated in Figure 2.1A upstream of a promoterless *gfp* in a vector expressing *mCherry* constitutively. The GFP expression for each construct was measured in *V. fischeri* ES114 (WT) and its Δ*phoB* derivative JLS9 grown in batch cultures in defined minimal medium with low or high PO_4 (FMM, see Methods). Figure 2.1B shows the GFP expression for a promoterless negative control and four promoter variants that represent the observed wide range of variation in GFP output.

Although most clones displayed some of the desired low-PO_4- and *phoB*-dependent activation, the degree of activation varied, as did the level of undesirable background GFP expression in the Δ*phoB* mutant and/or in high-PO_4 conditions (e.g., Figure 2.1B). In some constructs, PhoB-dependent activation in low PO_4 was too weak to be useful (e.g., variant 1, Figure 2.1B). In others, background GFP expression was higher than optimal (e.g., variant 2,

A.

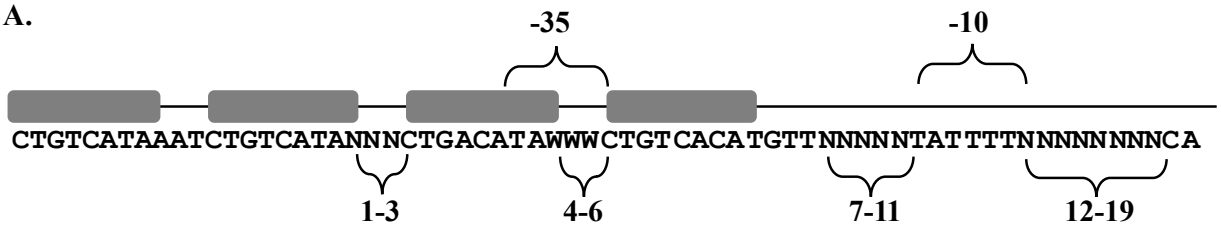

B.

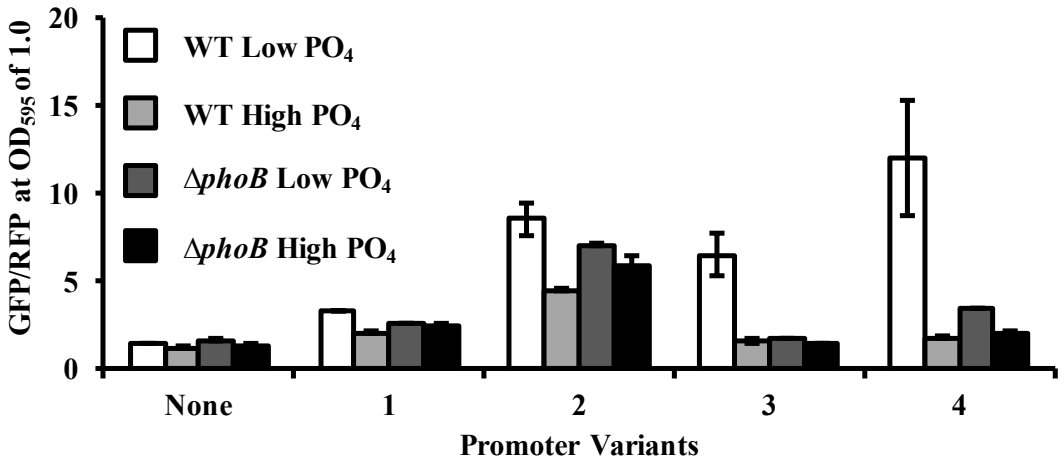

C.

	WT- Low PO_4	WT- High PO_4	Δ*phoB*- Low PO_4	Δ*phoB*- High PO_4	Nucleotide chosen for Round 2
1		1.7 C*; -2.3 T***	1.9 C*; -2.5 T***	1.5 C*; -2.0 T**	T
2	-2.2 A*	3.1 T ***; -2.1 A***; -2.0 G **	3.5 T***; -2.5 A***; -2.2 G**	3.6 T ***; -2.3 A***; -2.5 G***	G/C
3	1.35 A/G*				A/G
4	2.7 T**	1.7 T*	1.5 T*	1.8T*	T
5				0.87A*	A/T
6					A/T
7	-1.8 A*				T/C/G
8		2.2 G**			A/T/C
9	-2.2 A*				T/C/G
10		2.1 C*; -2.1 G ***	2.1 C*; -2.0 G**	2.1C*; -2.1 G***	G
11			-1.4 A*		N
12	-3.0 C**	1.1 G*			A/T/G
13					N
14		-1.1 G*	1.6 T**; -1.0 G*	1.4 T*	G
15			1.4 C*		N
16	-2.3 A*	1.8 C*	-1.6 A/G**	-1.4 A/G*	G
17		1.0 C**; -1.0 A**	1.0 C*; -1.6 A**	-1.3 A/T*	A
18					N
19		1.6 G*	2.0 G**; -1.2 A**	1.8 G**	A/T/C

Figure 2.1. Generation and screening of synthetic PhoB-dependent promoter variants. (A) Synthetic constructs included four PhoB-binding sites (grey boxes) as well as -35 and -10 promoter elements. Randomized or semi-randomized positions are numbered, corresponding to numbering in panel C. Sixteen randomized positions (labeled 1-3 and 7-19) are indicated by N. Positions 4-6 were restricted to A or T (W). Eighty-three different variations of the synthetic fragment in panel A were cloned upstream of *gfp* in pJLS27 and screened for activity, with the results for four representatives shown in panel B. Specific GFP activity was measured for constructs in ES114 and JLS9 (Δ*phoB*) grown in minimal media with high (378 μM) or low (37.8 μM) added PO_4. Strains carrying the promoterless parent vector were assayed to show background fluorescence (labeled "None"). Values were taken at an OD_{595} of 1.0, and error bars indicate standard deviation (n=3). One representative experiment of three is shown. (C) Each variable nucleotide position (1-19) was subjected to a Mann-Whitney U non-parametric statistical test comparing the average GFP/RFP output associated with each individual nucleotide (A,T,C, or G) against the average value for constructs with the other nucleotides in that position. We similarly compared pairs of nucleotides at a position (A/T vs. G/C; C/T vs. A/G; G/T vs. A/C; and C/G vs. A/T). The average GFP/RFP for all promoters without the nucleotide(s) being interrogated was subtracted from the average GFP/RFP for every promoter containing the nucleotide(s) with p-values lower than 0.05. For each of the four growth conditions, nucleotides correlated with significantly higher or lower GFP activity are indicated by green or red, respectively; *, **, and *** indicate $p<0.05$, <0.01, and <0.001. The last column in panel C indicates how randomization was further constrained for the next set of variants (Round 2). At position 2, C is colored blue to indicate that it was underrepresented in the screened variants (in only one of the eight-three variants) and therefore was included in Round 2.

Figure 2.1B). Some variants displayed significant activation with reasonably low-background (e.g., variants 3 and 4, Figure 2.1B); however, assessing eighty-three clones out of over 34 billion possibilities had not come close to saturating the screen, and we hoped that further analysis of sequences corresponding to desirable properties could allow us to constrain our design and isolate more optimal constructs.

Optimization of the synthetic promoter

To assess the prospects for improving the PhoB-dependent promoter, we analyzed whether the identity of any of the nineteen variable nucleotides (Figure 2.1A) correlated with GFP expression. Specifically, at each of the nineteen positions, we used Mann-Whitney tests to compare reporter output corresponding to each nucleotide relative to the output from constructs

with the other three possible nucleotides (A versus CGT, C versus AGT, G versus ACT, or T versus ACG). We subtracted the average GFP/RFP expression of the other three possible nucelotides from the nucleotide being interrogated, giving us the magnitude of the change. We likewise made comparisons based on possible pairs of nucleotides at a position, for example an A or C at a position versus a G or T at the same position. Variable nucleotide positions 4, 5, and 6 were limited to A or T (W) by design (Figure 2.1A), so only those two comparisons were made in those cases.

Figure 2.1C provides a summary of the significant ($p<0.05$, $p<0.01$, or $p<0.001$) correlations between nucleotide identity at each of the nineteen variable positions in the promoter and reporter output under each of the four strain/medium combinations tested. Given that four hundred and sixty comparisons were interrogated for significance, some of those indicated in Figure 2.1C may appear significant by chance, particularly at the $p<0.05$ level. On the other hand, in some positions all three background conditions (wild type high PO_4, Δ*phoB* mutant high or low PO_4) yielded similar results suggesting reproducibility and value of the data. Importantly, our goal was to determine how we might rationally constrain our sequence design to optimize output, not to definitively state a role for the sequence at any position, and the results shown in Figure 2.1B suggested a rational approach to further optimization was possible.

Our data suggested several further sequence constraints that might contribute to desirable reporter properties: high PhoB-dependent activation in low-PO_4 conditions or low background under the other conditions. For example, a C or a T at position 1 were correlated with above- or below-average background levels, respectively (Figure 2.1C), and therefore we defined this position as a T in our second-generation construct. As another example, a C at position 10 was correlated with below average expression in wild type under low-PO_4 conditions, so this position

was constrained to A, T, or G, in the second generation construct. Using this approach, most positions were defined more narrowly in the second round of screening. Three of the nineteen positions (positions 6, 13, and 18) yielded no indication that sequence affected performance, and three others (positions 5, 11, and 15) were relatively unconvincing, as significance was only seen in one of three background conditions at the $p<0.05$ level. These six positions were left unchanged in our design. For the most part, nucleotide representation at each randomized position had been evenly distributed, however, only one of the eighty-three promoters had a C at position 2, so C was included again at this position in the second round of promoter design.

A second round of synthetic inserts was engineered to contain the same conserved sequences as in round 1 (Figure 2.1A) along with the newly constrained positions (right column, Figure 2.1C). The resulting constructs were assayed in the same manner as the first-generation reporters. Many of the ninety-nine resulting promoters that were screened exhibited an increase in GFP expression in the "on" state (wild type low-PO_4) and/or decreased background in other conditions relative to earlier constructs. Figure 2.2 illustrates the best second-generation reporter (pJLS1088) compared to the ideal promoter from round 1 (pEW6AQ). The newer reporter exhibited significantly higher "on" activation and lower background (Figure 2.2). The difference in GFP expression between wild type and the *phoB* mutant in low PO_4 conditions was 11-fold for cells carrying pJLS1088, compared to 3-fold induction for the best first-round construct, and the PhoB-independent background was eliminated.

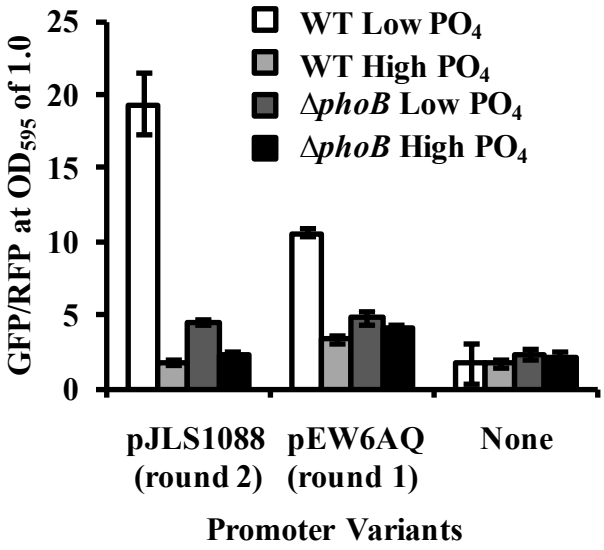

Figure 2.2. Iterative optimization of PhoB-dependent reporter performance. A representative of the best promoters from the first set of semi-randomized variants (pEW6AQ; also, number 4 in Figure 2.1B) was compared to an optimal variant (pJLS1088) generated after constraining additional positions as indicated in Figure 2.1C. Reporters were evaluated in ES114 and Δ*phoB* strains and were grown in minimal media under "high" or "low" PO_4 conditions. The promoterless parent vector pJLS27 (labeled "None") is included to show background. Fluorescence values were taken at an OD_{595} of 1.0, and error bars indicate standard deviation (n=3). Data shown represents one experiment of three performed.

Reporter responsiveness to environmental phosphate

To evaluate at what level of PO_4 the PhoB-specific reporter was activated, we measured GFP expression from pJLS1088 and phosphate levels during growth of wild-type strain ES114 in batch cultures using the empty vector (pJLS27) as a negative control (Figure 2.3). Due to the rapid depletion of PO_4 during exponential growth phase, measuring the exact PO_4 concentration when the GFP is first detectable proved difficult. However, GFP expression was consistently first seen when PO_4 levels were depleted to between 1 and 10 μM (Figure 2.3), similar to the activation of PhoB in *E. coli* below an environmental concentration of 4 μM PO_4 (114).

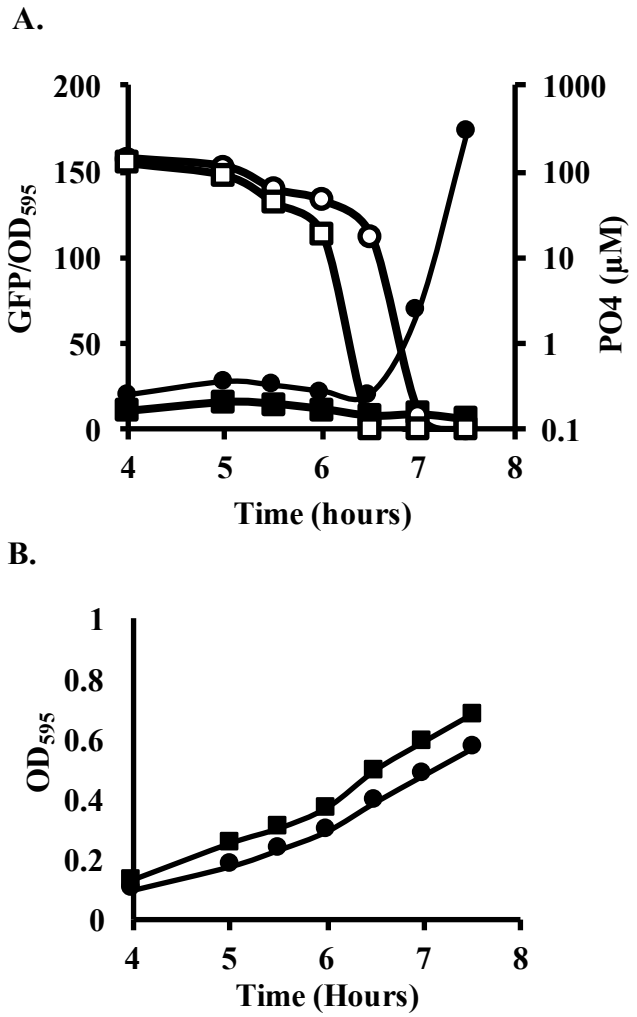

Figure 2.3. Reporter is induced upon PO_4 depletion in batch culture. (A) GFP/OD_{595} values and supernatant phosphate levels were measured over time in cultures of wild-type cells containing either the promoterless parent vector (pJLS27; squares) or the optimized PhoB-reporter (pJLS1088, circles) grown in batch cultures in FMM amended at the outset with 37.8 µM phosphate for a final concentration of 100 µM total phosphate. Filled shapes represent the GFP/OD_{595} fluorescence, whereas open shapes represent extracellular PO_4 concentration. (B) Growth of the cultures in panel A shown as cell density (OD_{595}) over time. One representative experiment of three is shown.

The PhoB-dependent reporter responds to low PO_4 in other proteobacteria

Because the Pho regulon is well conserved among proteobacteria (126), we tested whether the optimized reporter functions in bacteria other than *V. fischeri*. The reporter plasmid pJLS1088, and its parent pJLS27, have two origins of replication; the R6K gamma origin (127) and the origin from pES213, which replicates well in members of the *Vibronaceae* without the

need to maintain antibiotic selection(97, 128). For the plasmid to replicate in a variety of backgrounds, we added the *pir* gene to the parent vector and reporter, which should enable the R6K origin to replicate in a broad range of non-Vibrio hosts (129).

We tested GFP induction of our reporter in *Vibrio cholerae*, *Escherichia coli*, *Salmonella enterica*, and *Rugeria pomeroyi*, each of which encode PhoB. Figure 2.4 shows the red and green fluorescence of colonies grown on solid media with relatively high- or low-PO_4 levels. Red fluorescence is the result of constitutive *mCherry* expression from the plasmids, whereas green fluorescence corresponds to reporter GFP expression, with pJLS27 and pJLS71 serving as promoterless-*gfp* negative controls. Each strain displayed green fluorescence only when grown with the reporter on low-phosphate plates (Figure 2.4). Moreover, GFP expression in *V. cholerae* was eliminated in a *phoB* mutant (Figure 2.4).

Development of a reduced half-life GFP in V. fischeri

The stability of the GFP protein can lead to its accumulation and render this reporter non-ideal for assessing dynamic changes in gene expression, especially in symbiosis. In some bacteria, adding an SsrA tag to the C-terminus of GFP increases its recycling via an AAA+ protease (70, 88, 130), such as ClpAP or ClpXP (131). Variations in the last three amino acids of the eleven-residue SsrA peptide sequence (AANDENYALAA) can alter the efficiency with which the protein is recycled (88). We generated modified versions of *gfp*, encoding C-terminal *ssrA* tags terminating in the tripeptides LAA, ASV, or AAV, and expressed these from an isopropyl β-D-1-thiogalactopyranoside (IPTG) inducible promoter in the wild-type strain and three transposon mutants with insertions in *clpA, clpX,* or *clpS*, the last of which encodes an

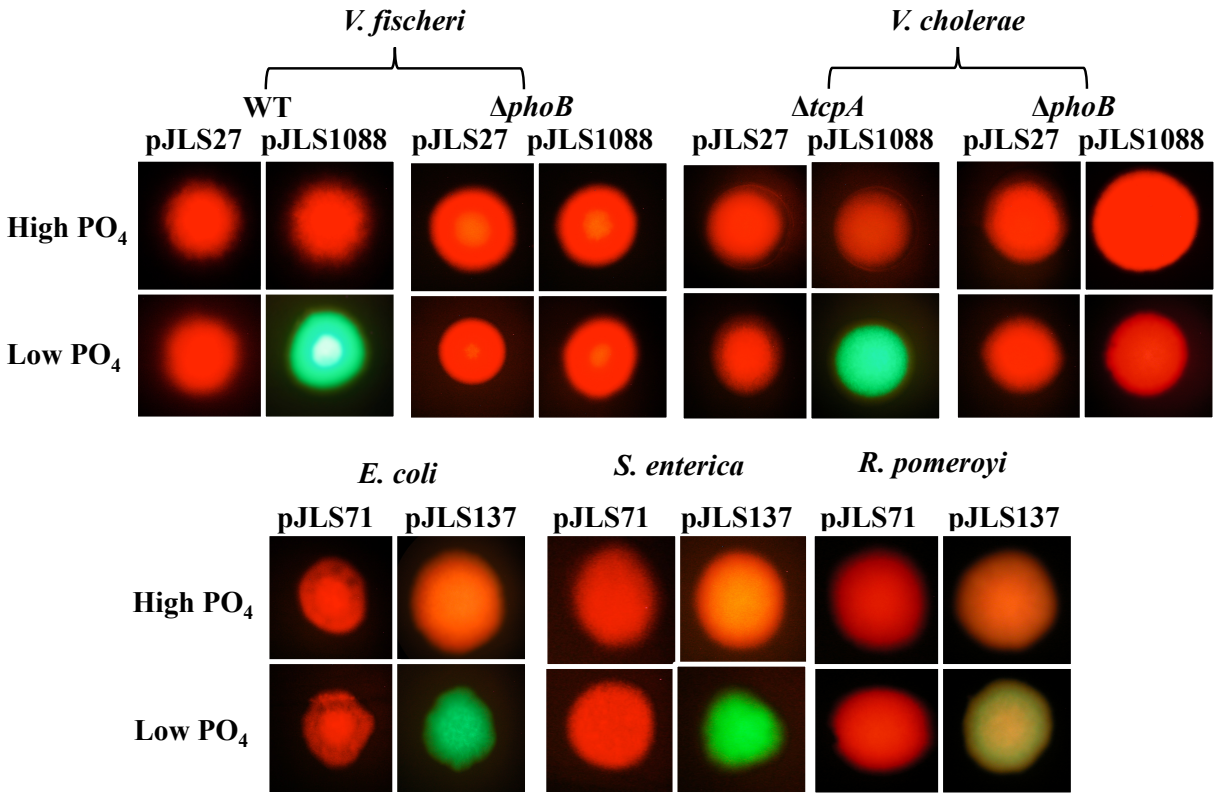

Figure 2.4. Response of reporter to low PO_4 in other proteobacteria. Red and green fluorescence from colonies of *V. fischeri*, *V. cholerae*, *E. coli*, *S. enterica*, or *R. pomeroyi* carrying a promoterless parent vector (pJLS27 for vibrios or pJLS71 for non-vibrios) and a vector containing the PhoB-activated promoter (pJLS1088 for vibrios or pJLS137 for non-vibrios). Strains include *V. fischeri* ES114 and JLS9 (Δ*phoB*), *V. cholerae* AC2764 (Δ*tcpA*) and AC3236 (Δ*phoB*), *E. coli* MG1655, *S. enterica* MS1868, and *R. pomeroyi* DSS-3. Strains were grown on agar plates with defined media containing "low" or "high" amounts of added PO_4 (see Methods). Colonies of similar sizes were imaged using a Nikon Eclipse E600 microscope with a 51005v2 filter, which enabled simultaneous visualization of both the constitutive red fluorescence and the green fluorescence of the reporter.

adapter that delivers proteins to ClpAP (132, 133). The stable parental GFP and the *ASV SsrA variant produced high fluorescence in all backgrounds (Figure 2.5). The *LAA and *AAV SsrA-tagged GFP variants yielded reduced or nearly undetectable fluorescence in wild type as well as the *clpA* and *clpS* mutants. In the *clpX* mutant background, fluorescence from the *AAV and *LAA variants was higher than in wild type (Figure 2.5). These results suggested that SsrA

tagging directed GFP turnover by ClpXP in *V. fischeri*; however, fluorescence from the *LAA and *AAV derivatives was too low in wild type to be useful.

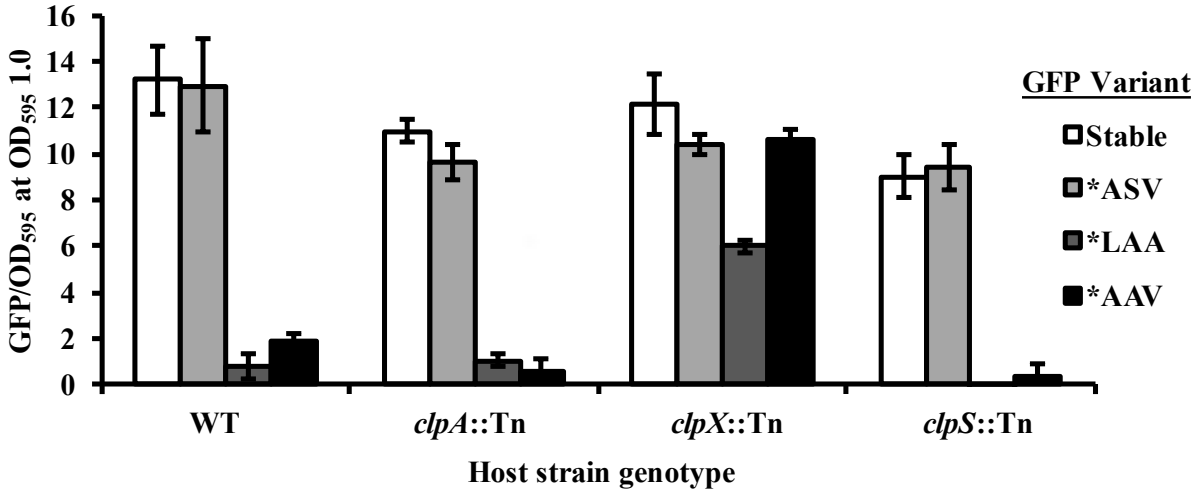

Figure 2.5. Effects of *clpX* and specific SsrA tags on GFP fluorescence in *V. fischeri.* Specific fluorescence is shown for wild-type strain ES114 or mutants with transposon insertions disrupting *clpA, clpX*, or *clpS*. pJLS153 (white bars; stable) has *gfp* without an *ssrA* tag. pJLS150 (light gray bars; *ASV), pJLS151 (dark gray bars; *LAA), and pJLS152 (black bars, *AAV) all have *gfp* with a modified *ssrA* tag, exchanging the last three amino acids as indicated. Strains were grown in SWTO medium with 2 mM IPTG to induce *gfp* expression. GFP/OD_{595} values were taken at an OD_{595} of 1.0, and error bars indicate standard deviation (n=3). One representative experiment of three performed is shown.

The *ASV variant of GFP yielded similar fluorescence values as the parental GFP when IPTG was added to induce their expression (Figure 2.5); however, when IPTG was washed away the fluorescence from the parental and *ASV-tagged GFP diverged (Figure 2.6). The parental GFP was remarkably stable, whereas fluorescence from the *ASV-tagged GFP decayed (Figure 2.6). The slope constant, μ, and half-life ($T_{1/2}$ = - ln 2/μ) for fluorescence were determined for each biological replicate (a total of twelve across four experiments) and averaged. The fluorescence values for the parental GFP were unchanged for the duration of the experiment, so a half-life could not be calculated, but fluorescence from the ASV SsrA-tagged GFP had an estimated half-life of 81 min. Taken together, our results suggest that GFP*ASV should be a

useful reporter in *V. fischeri*, displaying sufficient fluorescence when expressed but decaying quickly to capture dynamic changes in gene expression that would be missed using the parental GFP.

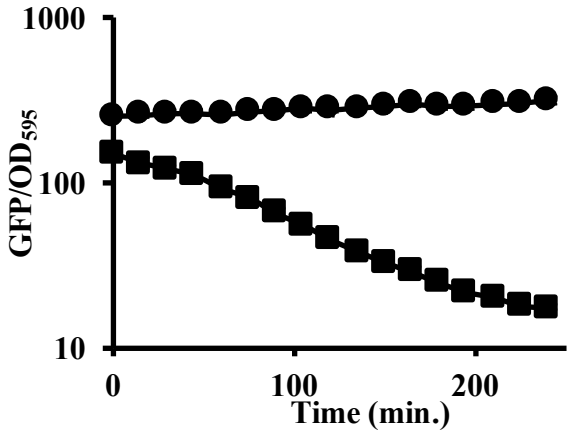

Figure 2.6. Addition of an SsrA tag to GFP increases turnover rate in *V. fischeri*. ES114 cells carrying pJLS150 (GFP*ASV; squares) or pJLS153 (parental GFP with no SsrA tag; circles) were grown in SWTO + 2 mM IPTG or SWTO with no inducer to an OD_{595} of 1.5 before being washed and resuspended in SWTO without IPTG. GFP/OD_{595} values were taken every 15 min. for 4 hours. Non-induced values (no IPTG added) were subtracted as background from induced values. Error bars indicating standard deviation (n=3) are smaller than the symbols. One representative experiment of four performed is shown.

Variability in expression of the PhoB-dependent reporter within symbiont populations

To assess the state of PhoB in the juvenile squid light organ, we infected juveniles with either ES114 or JLS9 (Δ*phoB*) harboring the empty vector from round 1, pJLS27, or the best reporter from round 1, pEW6AQ. In aposymbiotic, or uncolonized, squid the light organ has minimal green or red fluorescence (Figure 2.7A, "Aposymbiotic"), and juveniles infected with JLS9 or ES114 carrying the empty vector display red, but not green, fluorescence (data not shown and Figure 2.7A, "WT promoterless"). Juvenile squid infected with ES114 pEW6AQ, displayed variability in reporter expression, both within and between juveniles. For example, some light organs displayed homogenous red fluorescence (Figure 2.7B, top panel), while other juveniles had heterogeneous display of fluorescence with distinct areas with visible red and

green fluorescence (Figure 2.7B, bottom panels). Using an epifluorescence microscope, however, we were unable to distinguish the microenvironments being colonized. The stable GFP was used in these experiments, which would further compromise our ability to distinguish temporal regulatory changes.

We combined our PhoB-dependent promoter with the destabilized GFP*ASV variant and used this construct to assess PhoB activation in *V. fischeri* cells colonizing the host. Within the bi-lobed *E. scolopes* light organ symbionts colonize distinct microenvironments. Six pores on the organ surface lead through ducts and antechambers to six epithelium-lined crypts, three in each lobe, designated 1, 2, and 3 based on their progression in development (12). Using confocal microscopy, we were able to see the bacteria within the individual crypt spaces. Again, in animals infected with JLS9 carrying the reporter, pJLS298, all crypt spaces displayed only red fluorescence (data not shown). Several of the animals imaged using confocal had detectible *mCherry* expression in the crypts, yet had no visible GFP fluorescence (data not shown). Similar to the results with the epifluorescence microscope, we saw heterogeneous GFP-expression within the crypts of the light organ in animals infected with ES114 carrying the reporter, pJLS298. In each case, however, crypt 2 displayed strong GFP fluorescence, while crypt 1 had a smaller population of the cells expressing GFP and crypt 3 had no cells expressing GFP (Figure 2.7C and data not shown).

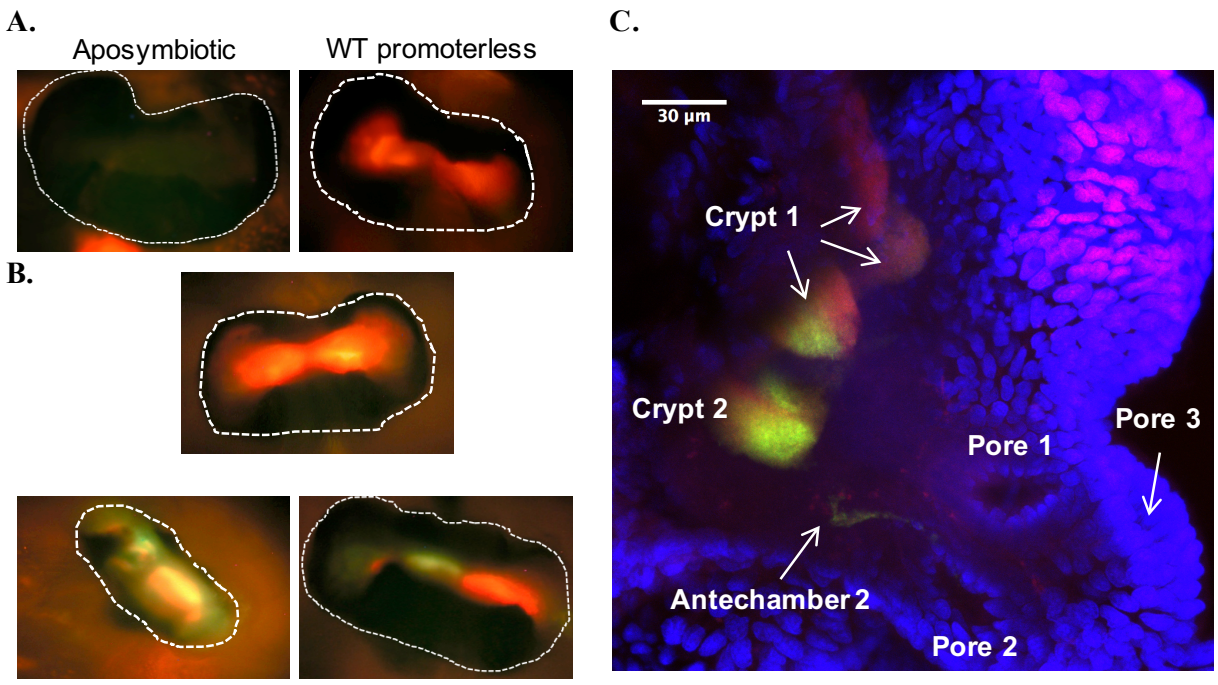

Figure 2.7. Expression of PhoB-dependent reporter in symbiotic *V. fischeri* cells. Juvenile squid were left aposymbiotic (A, left image) or infected with *V. fischeri* containing either the promoterless (pJLS27; A, right image) or the reporter, pEW6AQ (B). Light organs (~250 µm, dotted white lines) were visualized by epifluorescence microscopy with a red/green filter, 24 hours post-inoculation. The confocal image of a juvenile squid light organ (C) is one half of squid light organ from a juvenile infected with ES114 cells harboring the PhoB-dependent promoter (pJLS298) driving the expression of a destabilized GFP. The squid tissue is stained in blue, and the pores, antechambers, and crypts are labeled when visible.

DISCUSSION

Synthetic regulator-specific transcriptional reporters offer a promising approach to assess the regulator status under different conditions. We used such an approach to study the PhoBR two-component regulatory system in *V. fischeri*, both in culture and in symbiosis with the Hawaiian Bobtail squid, *E. scolopes*. First, we generated an improved PhoB-dependent reporter that has high expression when activated by PhoB but low background expression. We began with a rationally designed sequence (Figure 2.1A), based on known elements of transcriptional promoters and PhoB-dependent activation; however, our results underscored the limitations of

ability to predict an optimal sequence. We randomized, or semi-randomized, nucleotide positions for which we did not foresee a sequence-specific role in promoter optimization, yet constructs with different nucleotides at these positions had highly variable performance. While some of the eighty-three constructs initially screened worked reasonably well, others did not, and had we chosen a single defined sequence for a reporter it would most likely have been only marginally effective.

Our inability to predictively design an optimal reporter highlights gaps in our understanding of how specific sequences influence a PhoB-dependent promoter or promoters in general. As noted above, the individual nucleotide identities highlighted in Figure 2.1C should be viewed cautiously, particularly at the $p<0.05$ level, given the number of comparisons being made, but in aggregate the data make a compelling case that positions we did not predict would influence the reporter were important. Even in retrospect, some of the nucleotide identities that appear to impact promoter performance (Figure 2.1C) seem inexplicable, especially for the positions outside of the Pho boxes or the promoter elements. In one notable example, a guanosine at position 10, in the gap between Pho boxes and the -10 element, significantly correlated with decreased fluorescence in all three background conditions ($p<0.01$ to $p<0.001$). Although there is precedence for promoter spacer region sequence affecting transcription (134-136), to our knowledge it remains difficult to predict such effects in a synthetic promoter.

Similarly, the mechanisms underlying the differences in promoter reporter performance are unknown. The sequence-specific effects we observed may be due to subtle changes in DNA topology or context-specific effects on RNAP or PhoB binding and/or interaction. Additionally, there may be alternative weak promoters and transcriptional start sites aside from the promoter highlighted in Figure 2.1A, and changes that minimize their activity would decrease PhoB-

independent background. Although we cannot rule out the possibility that we have created binding sites for additional regulators, this mechanism seems improbable. Moreover, a non-PhoB activator of the reporter would itself have to be activated by PhoB, because activation is specifically PhoB dependent.

A second round of further-constrained promoter library screening enabled us to increase the reporter output in low phosphate conditions and decrease the background expression (Figure 2.2). While a similar combination of rational and randomized nucleotide screening method to design promoters for reporter use has been used previously (32), this study shows that by screening only eighty-three unique promoters out of over thirty-four billion possible, rational changes could be made to optimize reporter performance. The very best possible variant was likely not screened, and some aspects of the optimized sequence may be too dependent on the sequence context to be identified by our approach, but nonetheless we showed that improvements could be made by screening a manageable number of clones. Importantly, the round 2 promoters essentially eliminated the PhoB-independent background of the reporters (Figure 2.2). This elimination of background is particularly important for applications where a qualitative "active" or "inactive" is beneficial. Although background fluorescence can be subtracted readily in comparisons of batch cultures, in examining symbiotic cells *in situ* a low background allows for the sensitive detection of an "on" state of a reporter.

In addition to providing a proof of principle for optimizing a synthetic promoter, our reporter proved a useful tool for investigating the PhoB-mediated response to low phosphate in *V. fischeri*. The *E. coli* PhoBR system is activated upon sensing environmental phosphate levels of less than 4 μM (114), and we similarly observed the PhoB-dependent activation of the reporter to be between 1 and 10 μM phosphate (Figure 2.3). In the future, more samples could be

taken from batch cultures, or phosphate could be defined in chemostat conditions, to more precisely determine the threshold phosphate concentration required for activation. Furthermore, the threshold for reporter activation may not be constant for all bacteria. Among various proteobacteria, different concentrations of phosphate in the minimal media were required to visualize reporter activation (or lack thereof) (Figure 2.4). Therefore, it could be useful to determine the "break point", or the phosphate concentration below which the reporter turns on as we did in Figure 2.3, as it may be different in different organisms. Using different species, or engineered strains of *V. fischeri*, that induce their PhoB response at different phosphate concentrations could be a valuable approach for determining bioavailable phosphate levels in various environments and samples. It is worth noting that the PhoB-activated *pst* operon, which encodes the proteins for a high-affinity phosphate importer (114, 137), is often used in metatranscriptomic data sets as an indication for bacteria coming from phosphate-limiting conditions (138). Reporter strains added to such samples may help refine our understanding of bioavailable phosphate.

In this study, we also extended the utility of GFP as a reporter in *V. fischeri*. The use of GFP reporters can lead to an accumulation of fluorescent signal due to GFP's stability (88). We tagged *gfp* with the three variants used previously in *E. coli* (70, 88, 130), and our results are consistent with the SsrA tag likewise targeting proteins to the ClpXP protease in *V. fischeri* (Figure 2.5). Even in the *clpX* mutant background the GFP variant with the LAA-SsrA tag showed attenuated fluorescence (Figure 2.5), which could suggest either; 1) protein is also recycled by another protease, or 2) it is not properly folded resulting in less fluorescence. Regardless, and more importantly, we determined the half-life of the ASV-SsrA variant to be 81-min., and it showed a useful balance between fluorescence under inducing conditions (Figure

2.5) and decay of signal once inducer was removed (Figure 2.6). Our results parallel studies in *E. coli*, where the LAA-SsrA variant has the shortest half-life, followed by the AAV and ASV variants (88). This decreased half-life GFP variant should be particularly useful in *in situ* experiments assessing symbiotic *V. fischeri*, and it should be able to capture major changes in gene expression over the diurnal symbiotic cycle (15, 74).

Different reports suggest that PhoB in symbiotic *V. fischeri* might either be active (indicative of low phosphate availability) or inactive during colonization with *E. scolopes*. Mutants with a transposon insertion in *phoB* or the genes for the high-affinity phosphate importer, *pstA* and *pstS*, have decreased competitive fitness when competed against wild type for symbiotic colonization (38, 56), suggesting phosphate might be limiting. However, a separate study looking at the transcriptome of recently vented *V. fischeri*, the *pst* genes were not upregulated, suggesting PhoB was not in an activated state and that the light organ was not a phosphate-limited environment (66). A way to reconcile these two data sets could be if PhoB was activated in specific microenvironments of the light organ, as is the case with the *lux* operon (97). Sycuro *et al.* found that the crypts of the light organ are not vented equally (96), therefore if PhoB is activated more significantly in crypts 2 or 3, which are not vented as completely, the Pho regulon may not appear induced in the transcripomic dataset.

Here, we found that the PhoB-dependent reporter has heterogeneous expression between and within juvenile squid light organs at 24 hours (Figure 2.7B and C). Likewise, in infected animals displaying symbionts with green fluorescence, we saw noticeable partitioning of GFP expression within and between the crypts. For example, in Figure 2.7C, crypt 1 is shown in three regions with GFP detectable in only a portion of one of the region, yet crypt 2 shows most cells are expressing GFP with only a small section of cells with undetectable green fluorescence. Still,

some squid were well colonized by *V. fischeri* based on the homogenous mCherry fluorescence, yet showed little to no green fluorescence indicating the light organ is not in a phosphate stringent environment (Figure 2.7B top panel and data not shown). These data suggest that select region(s) of the light organ is phosphate limited at some point, which is consistent with the competitive defect seen when *phoB, pstA,* or *pstS* are disrupted. As only crypt 1 is mostly vented each morning (96), these data are also consistent with the transcriptomic study, as we were unable to detect PhoB-dependent activation in the majority or all of crypt 1 in each squid. Therefore, our data illustrate the power of considering the microenvironments of the squid light organ crypts in expression studies. Future studies should help to further define the spatial and temporal pattern of gene expression in symbiotic *V. fischeri*.

MATERIALS AND METHODS

Media and growth conditions

Vibrio fischeri strain ES114 was used as wild-type and parent for strain construction (4). *Escherichia coli* strains DH5α and DH5αλpir (128) were used as hosts for plasmids. *V. fischeri* was grown at either 24°C or 28°C in either lysogeny broth salt (LBS) medium (139), seawater tryptone (SWT) medium (4), or a modified Fischeri minimal medium (FMM) (98), with 37.8 μM K_2HPO_4 or 378μM K_2HPO_4 added for "low" and "high" phosphate conditions, respectively. Plasmids were maintained in *E. coli* grown in lysogeny broth (LB) (140) at 37°C. Solid media were prepared by adding 15 g l^{-1} agar. For selection of plasmids in *E. coli*, kanamycin (kn), chloramphenicol (cm), erythromycin (erm), or trimethoprim (tmp) was added to LB at final concentrations of 40, 20, 150 and 10 μg ml^{-1}, respectively. To maintain selection in *V. fischeri* on LBS, kn, cm, erm, or tmp were added at 100, 2, 5, and 10 μg ml^{-1}, respectively.

E. coli strain MG1655, *Salmonella typhimurium* strain MS1868, and *Vibrio cholerae* strains AC3236 and AC2764 were maintained and transformed using LB medium, and their response to PO_4 was assessed using a modified MOPS minimal medium at 37°C (141). V. cholerae strain AC2764 has a deletion of *tcpA*, reducing the strain virulence. To generate a base for the MOPS medium, we added no phosphate and used 1 g/L casamino acids. For "low" phosphate MOPS media, the base minimal medium was used with no added phosphate other than that in casamino acids and other components, whereas 800 μM K_2HPO_4 was added to the base medium for "high" phosphate conditions. *R. pomeroyi* strain DSS-3 was grown at 30°C on half-strength Yeast Tryptone Sea Salts medium (142), and to manipulate PO_4 availability it was grown in modified Marine Basal Medium (MBM,(143)) with either 0.2 mM K_2HPO_4 or 2 mM K_2HPO_4 added for "low" and "high" phosphate conditions, respectively. 80 μg ml^{-1} kn was included to maintain plasmid selection in DSS-3 (142, 143).

Plasmid and Strain Construction

Plasmids were mobilized from *E. coli* to *V. fischeri* by triparental mating using helper plasmid pEVS104 maintained in CC118λ*pir* (144), as previously described (145). Plasmids were moved into MG1655 and MS1868 by transformation. Plasmids were moved into AC3236 and AC2764 by conjugation using helper plasmid pEVS104 and by selecting for recipients on LB supplemented with kn (to select for the plasmid) and 2 μg ml^{-1} potassium tellurite (to select against *E. coli* donor cells). Plasmids were similarly moved into DSS-3 via conjugation using helper plasmid pEVS101 and by selecting on 1/2YTSS medium with kn and 2 μg ml^{-1} potassium tellurite.

JLS9, an in frame Δ*phoB* deletion mutant, was constructed through allelic exchange (10), and verified by PCR. To generate the Δ*phoB* allele, 2 kb upstream and downstream of *phoB* was

amplified (PhoBupF/PhoBupR and PhoBdnF/PhoBdnR, respectively) and cloned into pCR-Blunt TOPO, generating pSJB2 and pDC6, respectively. To generate the in-frame deletion, two small annealed oligos were inserted at the AscI site of both the upstream and downstream generating an NdeI site, yielding pJLS21 and pJLS22. pJLS22 was fused to pEVS118 at the KpnI site generating pJLS23, which was subsequently digested with ApaI and self-ligated to remove the ColE1 origin of replication (pJLS24). The resulting *phoB* upstream and downstream plasmids, pJLS21 and pJLS24 were fused together at the NdeI site. The resulting construct, pJLS25 was mobilized into ES114 to generate strain JLS9 via allelic exchange.

To generate the semi-randomized promoter regions for reporter-plasmid screening, oligonucleotides (Table 1) JLSPhoBPF2 and JLSPhoBPR (Round 1) or JLSPhoBPF3 and JLSPhoBPR2 (Round 2) were annealed together and filled in using DNA Polymerase I Klenow fragment to generate a blunt-ended double-stranded product. The filled in product was digested with SphI and SalI and ligated into similarly digested pJLS27. The resulting DH5α λpir transformants were screened by visualizing the plate under an epifluorescence microscope, using a red/green filter, selecting the green or yellow colonies. Fluorescence intensities were later screened in *V. fischeri* using a Synergy 2 plate reader (BioTek; Winooski, VT) excitation/emission wavelengths for GFP of 485nm/528 nm and *mCherry* at 530nm/590nm, normalizing GFP to mCherry (GFP/mCherry) or GFP to OD_{595} as indicated.

To increase the potential bacterial host range of the optimized reporter, we amplified the *pir* gene from pGRG36pir with primers JLSpirF3 and JLSpirR3 and cloned the SacII digested product into the “round 1” and “round 2” optimized reporters, generating pJLS70 and pJLS137. To generate an isogenic promoterless vector, we cut pJLS70 with SalI and ligated in oligos

JLSMCS1 and JLSMCS2 annealed together, which created a multiple cloning site and generated pJLS71.

The GFP variant used in the promoter screening process is a stable variant. To obtain closer to real-time data, an *ssrA* tag (VANDENYALAA) was added at the end of the *gfp* coding sequence. The *gfp-ssrA* variant was constructed using SOE PCR with primers DSgfp1, DSgfp2, DSgfp3, and DSgfp4 to amplify *gfp* and add an *ssrA* tag to the end of the protein just before the stop codon. The PCR product was digested with SacI and SpeI and was ligated into pVSV102 cut with the same enzymes to generate pRK12. A new vector (pJLS149) was constructed to enable the IPTG induction of GFP variants in *V. fischeri*, with *mCherry* expression from a consensus promoter (to be deposited in Genebank). To obtain different variants of the unstable gfp, primers JLSgfpf and either JLSssrA-ASV, JLSssrA-LAA, JLSssrA-AAV were used to amplify *gfp* from pRK12, digested with NheI and BamHI and ligated into pJLS149 cut with the same enzymes, generating pJLS150-pJLS152. A stable variant was constructed in the same manner using primers JLSgfpF and JLSgfpR plasmid DNA from pVSV33 as a template for the PCR generating plasmid pJLS153.

We then improved plasmid stability in both *E. coli* and *V. fischeri*, by increasing the length of the R6K and pES213 origins of replication, and removed $lacI^q$ from the promoter region of *gfp*, generating pJLS198 (to be deposited in Genebank). The promoter responding to PhoB activation from pJLS1088 was lifted and inserted into the SphI and SalI sites in pJLS198, generating pJLS203. Finally, to increase the red expression levels in symbiosis, a geneblock was generated containing the same promoter region as found in pJLS27, except the AvrII site was scrambled, was inserted into pJLS203 at the PacI and SbfI sites, generating pJLS298.

Table 2.1: Strains, Plasmids, and Oligonucleotides used in this study

Strain or Plasmid	Genotype[a]	Source
Escherichia coli		
CC118 λ*pir*	Δ(*ara-leu*) *araD* Δ*lac74 galE galK phoA20 thi-1 rpsE rpsB argE(*Am*) recA λpir*	(144)
DH5α	φ80d*lacZ*ΔM15 Δ(*lacZYA-argF*)U169 *deoR supE44 hsdR17recA1 endA1 gyrA96 thi-1 relA1*	(146)
DH5αλ*pir*	λ*pir* derivative of DH5α	(128)
MG1655	F- lambda- *ilvG- rfb*-50 *rph*-1	(147)
Rugeria pomeroyi		
DSS-3	Wild-type isolate from coastal seawater, Georgia (USA)	(148)
***Salmonella enterica* serovar Typhimurium**		
MS1868	*leuA414* (Am) *hsdSB*($r^- m^+$)$Fels^-$	(149)
Vibrio cholerae		
AC2764	E7946 Δ*tcpA*	A. Camilli
AC3236	E7946 Δ*phoB*	(65)
Vibrio fischeri		
ES114	Wild type isolate from *E. scolopes* light organ	(4)
JLS9	ES114 Δ*phoB*	This study
JLS38	ES114 Δ*phoU*	This study
VFS008C4	ES114 *clpA*::mini-Tn5 *ermR*	C. Whistler
VFS024A1	ES114 *clpS*::mini-Tn5 *ermR*	C. Whistler

VFS025G1	ES114 *clpX*::mini-Tn5 *ermR*	C. Whistler

Select Plasmids[b]		
pEVS101	conjugative helper plasmid; $oriV_{ColE1}$, $oriT_{RP4}$, erm^R	(145)
pEVS104	conjugative helper plasmid; $oriV_{R6K\gamma}$, $oriT_{RP4}$, kn^R	(145)
pEW6AQ	$oriV_{R6K\gamma}$, $oriT_{RP4}$, pES213, *mCherry,* kn^R, P_{phoB}-cm^R- *gfp* (Round 1)	This study
pJLS25	Δ*phoB* allele; $oriV_{ColE1}$, $oriV_{R6K\gamma}$, $oriT_{RP4}$, kn^R, cm^R	This study
pJLS27	$oriV_{R6K\gamma}$, $oriT_{RP4}$, pES213, *mCherry,* kn^R, promoterless- cm^R- *gfp*	(32)
pJLS70	$oriV_{R6K\gamma}$, $oriT_{RP4}$, pES213, *mCherry,* kn^R, *pir,* P_{phoB}-cm^R- *gfp* (Round 1)	This study
pJLS71	$oriV_{R6K\gamma}$, $oriT_{RP4}$, pES213, *mCherry,* kn^R, *pir,* promoterless- cm^R- *gfp*	This study
pJLS137	$oriV_{R6K\gamma}$, $oriT_{RP4}$, pES213, *mCherry,* kn^R, *pir,* P_{phoB}-cm^R- *gfp* (Round 2)	This study
pJLS149	$oriV_{R6K\gamma}$, $oriT_{RP4}$, pES213, *mcherry*, P_{con}-tmp^R, $lacI^q$-P_{tac}	This study
pJLS150	$oriV_{R6K\gamma}$, $oriT_{RP4}$, pES213, *mcherry*, P_{con}-tmp^R, $lacI^q$-P_{tac}-*gfp-ssrA*-ASV	This study
pJLS151	$oriV_{R6K\gamma}$, $oriT_{RP4}$, pES213, *mcherry*, P_{con}-tmp^R, $lacI^q$-P_{tac}-*gfp-ssrA*-LAA	This study
pJLS152	$oriV_{R6K\gamma}$, $oriT_{RP4}$, pES213, *mcherry*, P_{con}-tmp^R, $lacI^q$-P_{tac}-*gfp-ssrA*-AAV	This study

pJLS153	*oriV*$_{R6K\gamma}$, *oriT*$_{RP4}$, pES213, *mcherry*, P$_{con}$-*tmp*^{R}, *lacI*^{q}-P$_{tac}$-*gfp*	This study
pJLS198	*oriV*$_{R6K\gamma}$, *oriT*$_{RP4}$, pES213, *mcherry*, P$_{con}$-*tmp*^{R}, promoterless-*gfp*-*ssrA*-ASV	This study
pJLS203	*oriV*$_{R6K\gamma}$, *oriT*$_{RP4}$, pES213, *mcherry*, P$_{con}$-*tmp*^{R}, P$_{phoB}$- *gfp*-*ssrA*-ASV	This study
pJLS298	*oriV*$_{R6K\gamma}$, *oriT*$_{RP4}$, pES213, *mcherry*, P$_{con}$-*tmp*^{R}, P$_{phoB}$- *gfp*-*ssrA*-ASV	This study
pJLS1088	*oriV*$_{R6K\gamma}$, *oriT*$_{RP4}$, pES213, *mCherry, kn*^{R}, P$_{phoB}$-*cm*^{R}- *gfp* (Round 2)	This study
pRK12	Kn^{R}, *oriV*$_{R6K\gamma}$, promoterless *cm*^{R}-*gfp*-*ssrA*	R. Kaul
pVSV33	Kn^{R}, *oriV*$_{R6K\gamma}$, promoterless *cm*^{R}-*gfp*	(97)
pVSV102	*oriV*$_{R6K\gamma}$, *oriT*$_{RP4}$, pES213, *kn*^{R}, *gfp*	(97)

Oligonucleotides	**Sequence**[c,d]	**Source**
PhoBupF	GGC GCC TAG AGT GTT GTC TGG ACG	This study
PhoBupR	ATG GCG CGC CGG ATC CTT CTA GCC ATT CTC	This study
PhoBdnR	GGC GTA TCC ATA GGT GCC AGA GAC TGA G	This study
PhoBdnF	ATG GCG CGC CGG TAT AAA GGT AAT GGT TGA GCG TC	This study
NdeIprimer1	CGC GAA ACA TAT GAA A	This study
NdeIprimer2	CGC GTT TCA TAT GTT T	This study
JLSMCS1	GCA TGC TGT AAA ACG ACG GCC AGT ACG TGC TAT GCG AGC TCG GGC CCG C	This study

JLSMCS2	GTC GAC GCT AGC CAT TGC GCA GCG CGC TCT AGA TAG CGG GCC CGA GCT CGC ATA GC	This study
JLSphoBPF2	TAG CAT GCC TGT CAT AAA TCT GTC ATA NNN CTG ACA TAW WWC TGT CAC ATG TT	This study
JLSphoBPR	TAG TCG ACT GNN NNN NNN AAA ATA NNN NNA ACA TGT GAC AG	This study
JLSphoBPF3	TAG CAT GCC TGT CAT AAA TCT GTC ATA TSR CTG ACA TAT WWC TGT CAC ATG TT	This study
JLSphoBPR2	TAG TCG ACT GDN CNH AAA ATA NCV DVA ACT AGT GAC AG	This study
JLSpirF3	TAC CGC GGT TGA CTC TCA TGT TAT TGG CG	This study
JLSpirR3	TAC CGC GGA CGC GTT CAC CCC TTA GCT TTT TTG GGA GG	This study
DSgfpP1	ACA CTA GTC ACT ACT CTG TGC TAT GG	This study
DSgfpP2	AGCTGCCAATGCGTAGTTTTCGTCGTTTGCGACGTT GTA CAG TTC ATC CAT GCC ATG	This study
DSgfpP3	GTC GCA AAC GAC GAA AAC TAC GCA TTG GCA GCT TGA GGA TCC CCG GGA ATT C	This study
DSgfpP4	ACC CGC GGG GAT CTT AGG	This study
JLSgfpF	ATG GCT AGC AAA GGA GAA GAA CTC T	This study
JLSssrA-ASV	TAT GGA TCC TCA AAC TGA TGC TGC GTA GTT TTC GTC GTT TGC GAC	This study
JLSssrA-LAA	TAT GGA TCC TCA AGC TGC CAA TGC GTA GTT	This study

	TTC GTC GTT TGC GAC	
JLSssrA-AAV	TAT GGA TCC TCA AAC TGC TGC TGC GTA GTT TTC GTC GTT TGC GAC	This study
JLSgfpR	GCA GGA TGG TCA GTT GTA CAG TTC ATC CA	This study
pJLS198mCherryPcon	475-bp synthetic DNA fragment[e]	This study

[a]Drug resistance abbreviations: *cmR*, chloramphenicol resistance (*cat*); *knR*, kanamycin resistance (*aph*); and *tmpR* trimethoprim resistance (*dfr*).
[b]Plasmids listed may contain the RP4 origin of transfer ($oriT_{RP4}$). Replication origin(s) are denoted as ColE1, pES213, and/ or R6Kγ.
[c]Oligonucleotide sequences are provided in the 5'-3' orientation.
[d]Non-standard nucleotides are as follows: N (ACGT), W (AT), D (AGT), H (ACT), V (ACG), S (CG), R (AG)
[e]Designed DNA "Gene block" ordered from Integrated DNA Technologies (Coralville, Iowa), sequence available on request

Sequence analyses

Sequences of over a hundred semi-randomized promoter regions were determined at the University of Michigan DNA Sequencing Core Facility. To determine whether nucleotide identity at a particular position was significantly correlated with above- or below-average fluorescence from the reporter, a Mann Whitney U test was utilized. The reporter data analyzed were the GFP/RFP value at an OD of 1.0 from ES114 and JLS9 cultures grown in FMM with 10 μM or 200 μM KH_2PO_4. At each position, each nucleotide was compared to the other three nucleotides, and similarly, pairs of nucleotides were compared at each position against the other pairs (See Results).

Fluorescence assays

To measure levels of GFP and mCherry, cultures were grown in 96-well black clear-bottom plates (Greiner Bio-One, Monroe, North Carolina) in the indicated media. Plates were placed in a Synergy 2 plate reader (BioTek) without shaking, and OD_{595}, GFP (480/20 excitation

and 528/20 emission), and mCherry (530/25 excitation and 590/35 emission) measurements were taken every 30 minutes for 12 hours. OD_{595} readings were divided by 0.46 so that the value corresponds to OD_{595} over a 1-cm path length. GFP/RFP measurements were compared at a corrected OD_{595} of around 1.0.

Phosphorus concentration assays

Inorganic phosphorous was measured using the ascorbic acid method (150). Briefly, 1 ml of cells was removed at different times during growth, and the cells were removed by centrifugation. The supernatant was assayed for inorganic phosphorous directly, or after dilution in distilled water, by amending a 500 µl sample with 10 µl 11 N sulfuric acid, 40 µl AM-APT (described below), and 20 µl fresh ascorbic acid. The AM-APT was made by dissolving 8 g ammonium molybdate and 0.2g antimony potassium tartrate in a final volume of 1 L. The ascorbic acid was prepared by adding 60 g to a final volume of 1 L of water and adding 2 mL acetone. After mixing the reagents well and incubating at room temperature for 5 min the absorbance of the samples at OD_{650} was determined and compared to a standard phosphorous curve.

Microscopy

Bacteria were grown on FMM, MOPS medium, or MBM as indicated above with either no K_2HPO_4 added, or the amount of K_2HPO_4 indicated, for 24 to 48 hours at 28, 30, or 37°C as appropriate for the bacterial species being assessed. Colonies of similar size were imaged using a Nikon Eclipse E600 microscope with filter set 51005v2 to visualize simultaneously both the constitutive red fluorescence and the green fluorescence of the reporter. To asses *V. fischeri*

strains in the juvenile squid light organ, strains were grown in static SWT cultures to an OD_{600} of between 0.4 and 0.7 before diluting to between 3,000 and 7,000 CFU ml^{-1} in sterile instant ocean maintained at 36 ppt. Juvenile squid were exposed to the prepared inocula for 24 hours before either dissecting and imaging with the epifluorescent microscope, or fixing for 3 hours in 4% paraformaldehyde in mPBS for confocal imaging. Animals used for confocal imaging were then washed three times for 30 min. each in mPBS, dissected to expose their light organ, and stained overnight with a nuclear dye (Hoechst 33342). Dissected animals were mounted in vectashield to preserve fluorophores before imaging. Confocal microscopy was performed using a Zeiss LSM 510 or 710 confocal microscope. Samples were excited at 488 nm or 561 nm, and visualized at an emission wavelength of 495-556nm or 566-669nm for GFP and mCherry, respectively.

ACKNOWLEDGEMENTS

We thank Alecia Septer and Reni Kaul for generating pRK12, Hannah Bullock and William Whitman for assisting with growth and manipulation of *R. pomeroyi* DSS-3, and Andrew Camilli and Anna Karls for sharing strains. The National Science Foundation supported this research under grants IOS-1121106, IOS-1557964, and MCB-1716232. The research in this article was partially supported by a grant jointly funded by the University of Georgia Franklin College of Arts & Sciences, Office of the Vice President for Research, and Department of Microbiology.

CHAPTER 3

ASSESSING ARCA-DEPENDENT REGULATION IN THE LIGHT-ORGAN SYMBIONT *VIBRIO FISCHERI*[1]

[1] Stoudenmire, J.L., Septer, A.N., and E.V. Stabb. To be submitted to *Journal of Bacteriology*.

ABSTRACT

The ArcAB two-component regulatory system represses the *lux* operon responsible for bioluminescence in the light-organ symbiont *Vibrio fischeri*. This regulation could largely account for the difference between bioluminescent symbiotic cells and the dimmer state of *V. fischeri* outside the host; however, the conditions affecting ArcA regulation in *V. fischeri* in culture and in symbiotic cells require investigation. Here we developed a reporter system to probe ArcA activity in *V. fischeri*. To generate an ArcA-specific reporter, we fused the receiver domain of ArcA to the DNA binding domain of PhoB and showed that ArcB can control this chimeric response regulator to activate a previously developed specific and responsive PhoB-dependent transcriptional reporter. This activation required the canonical target for phosphorylation by ArcB, Asp54, in the ArcA receiver domain. In *Escherichia coli,* oxidized ubiquinone is thought to repress the kinase activity of ArcB, and consistent with that model, *ubiCA* mutants showed increased reporter activity. Unexpectedly, we observed ArcB-independent activation of the reporter in late-log phase cultures, in *ubiCA*/*arcB* mutants, and in symbiotic *V. fischeri* cells. This ArcB-independent activation required the response regulator but not its Asp54 residue. Based on experiments with *pta*/*ack* mutants and cultures amended with acetate, we hypothesize that acetyl-phosphate or acetyl-CoA might activate the ArcA receiver domain *in vivo*. Finally, our results suggested that *arcA* and *arcB* mutants should not have the same phenotype in symbiosis, which was corroborated in colonization competition experiments. We hypothesize that regulation mediated by ArcA in symbiotic *V. fischeri* cells involves a significant ArcB-independent component.

INTRODUCTION

The light-organ symbiosis between the bioluminescent bacterium *Vibrio fischeri* and the Hawaiian bobtail squid, *Euprymna scolopes*, is a useful model for studying bacteria-host interactions. Like other host-associated bacteria, *V. fischeri* regulates many genes in response to the host environment (4, 74). Notably, the *lux* operon responsible for bioluminescence is induced upon infection and enables *V. fischeri* ES114 to colonize the squid host fully (8-10). Although luminescence induction is well known to be cell-density dependent (1-3), *V. fischeri*'s luminescence is dimmer in culture than in the host, even at equivalent cell density, suggesting regulation in response to the light-organ environment (4). Luminescence is controlled in part by the ArcA/ArcB two-component regulatory system, which directly represses the *lux* operon in culture and could account for the luminescence difference between cultured and symbiotic cells (29).

Control of the *lux* operon by ArcA, and presumably by other regulators, is influenced by a *lux*-encoded positive-feedback circuit. In addition to its role in luminescence, the *lux* operon directs synthesis of a pheromone that together with LuxR stimulates *lux* operon transcription. This positive feedback amplifies Arc-mediated de-repression of luminescence, and once this operon is induced Arc no longer effectively represses it (28). Therefore, the observation that ArcA does not repress luminescence in the symbiosis could mean either that ArcA-mediated repression of *lux* is relieved, even temporarily, or that another regulator activates *lux*, triggering positive feedback and overriding Arc-mediated *lux* repression. In light of these observations, we became interested in assessing the regulatory status of Arc in symbiotic and other environments.

The mechanisms of ArcA/ArcB function in *V. fischeri* have been largely inferred from studies of this system in *Escherichia coli*. In *E. coli*, ArcB is activated by growth in reducing

conditions and it phosphorylates an aspartate (D54) in the receiver domain of the response regulator, ArcA, which in turn modulates the expression of many metabolic genes as cells transition from aerobic to microaerobic or anaerobic metabolism (57, 151). A current prevailing model is that oxidized quinones decrease ArcB autophosphorylation by oxidizing cysteines in the ArcB signal sensing, or PAS, domain (57). As O_2 becomes scarce, the quinone pool shifts to a more reduced state, ArcB autophosphorylation increases, and ArcA is activated to bind DNA, either enhancing or repressing transcription through the downstream promoter (57, 108, 152, 153). Studies have also suggested ArcB is affected by menaquinones (152, 153) and fermentation acids (151, 154, 155).

In many ways, the Arc system in *V. fischeri* resembles its counterpart in *E. coli*, although there are differences. ArcA and ArcB share 57% and 84% amino acid similarity between these bacteria, respectively, including conservation of amino acids implicated in redox sensing and signal transduction (29). Functional conservation is suggested by the observation that *V. fischeri arcA* can complement an *E. coli arcA* mutant (29). Similarly, in both bacteria the transcriptional regulator FNR activates *arcA* (156, 157), and *arcA* mediates regulation of succinate dehydrogenase (29, 58). A comprehensive bioinformatic analysis further indicated that the *V. fischeri* regulon is similar to the experimentally determined regulon in *E. coli* (158). On the other hand, the *V. fischeri* Arc system appears more active in well-aerated cultures than one would predict based on studies in *E. coli* (29, 57).

We wanted to explore the activity of the Arc system in *V. fischeri* more closely in order to understand the impact Arc plays on both bioluminescence and persistence of *V. fischeri* in the squid host. Both the *cydAB* and the *sdhCDAB* promoters, which are activated and repressed by ArcA, respectively, are frequently used with reporter genes to assess Arc activity; however, these

promoters are co-regulated with other global transcriptional regulators, such as FNR and CRP (99, 105-109, 159, 160). Our initial attempts to generate an ArcA-specific reporter were ineffective; however, we recently developed a specific and responsive synthetic reporter for the response regulator PhoB (Chapter 2). In this study, we exploited this PhoB-dependent reporter and an ArcA-PhoB chimera to investigate Arc activation.

RESULTS

Construction and design of an ArcA-dependent reporter

In order to assess the activation state of ArcA in symbiotic and cultured *V. fischeri* cells, we sought an ArcA-dependent and -specific reporter with low background in the "off" state, and high activation by ArcA. Initial attempts to synthesize a promoter to accomplish this objective were unsuccessful; however, we recently developed a highly responsive PhoB-dependent transcriptional reporter with essentially no PhoB-independent background activity. Both ArcA and PhoB are classified as OmpR-type response regulators (42), and we predicted swapping the DNA binding domain of ArcA with that of PhoB could generate a chimeric protein responding to the phosphorylation signal from ArcB and binding to DNA in a PhoB-specific manner, as has been done previously (161) Most response regulators have two domains, the N-terminal receiver domain with a conserved aspartate residue accepting the phosphorylation signal from the sensor kinase, and a C-terminal DNA binding domain (42, 162). By exchanging the native receiver domain with alternative sequences including a flexible peptide linker sequence, ESFHPPMDEFRGS, a chimeric PhoB can still bind to consensus PhoB binding sites in manner that is dependent on the non-native receiver domain and independent of phosphate concentration and PhoB's cognate sensor kinase PhoR (161).

To generate an ArcA-PhoB chimeric protein, we PCR amplified DNA encoding the N-terminal receiver domain of ArcA, amino acids 1-123 (163), and fused it to DNA encoding the C-terminal DNA binding domain of PhoB, amino acids 128-231 (164), with a 13-amino acid flexible linker (161, 165) (Figure 3.1a). We predicted the Asp 54 residue in the receiver domain of the chimeric protein will be phosphorylated in an ArcB-dependent manner, and upon phosphorylation the chimera will activate transcription of a *gfp* reporter with a PhoB-dependent promoter (Figure 3.1b).

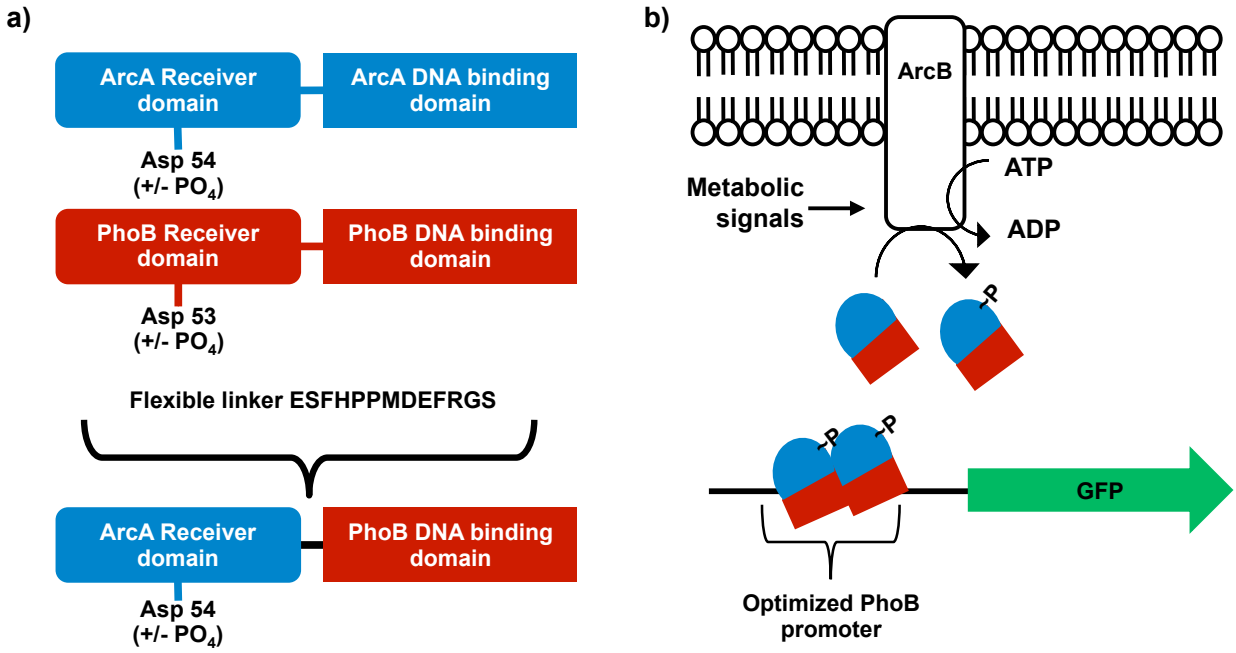

Figure 3.1. Generation of a chimeric response-regulator reporter system. (A) A chimeric response regulator was generated from the *V. fischeri* ArcA receiver domain (amino acids 1-123), a 13-amino acid flexible linker (ESFHPPMDEFRGS), and the PhoB DNA-binding domain (amino acids 128-231 from PhoB). (B) Our prediction was that the conserved target for ArcA phosphorylation, Asp54, would be phosphorylated by ArcB in response to metabolic cues (e.g., the status of the ubiquinone pool), resulting in multimers of the chimera binding the PhoB-specific promoter and activating the transcription of the *gfp* reporter gene.

DNA encoding the ArcA-PhoB chimera was inserted onto a previously characterized PhoB-dependent reporter plasmid, pJLS203 (Chapter 2), downstream of a consensus promoter. This reporter plasmid has constitutive *mCherry* expression and *gfp* expression under the control

of the PhoB-dependent promoter. In the wild-type strain, the native PhoB should increase GFP expression in response to low phosphate conditions; however, if the ArcA-PhoB chimera is independent of PhoR and the phosphate-starvation response, the reporter should not be activated in response to low-phosphate in a Δ*phoB* background. Wild-type *V. fischeri,* ES114, and a *phoB* deletion strain, JLS9 (chapter 2), each harboring the chimeric reporter plasmids with and without the PhoB-dependent promoter, were grown in "high" (378 μM PO_4) and "low" (37.8 μM PO_4) phosphate minimal media. GFP was measured at an OD_{600} of 1.0, as done previously (chapter 2). The GFP/OD_{600} expression in wild type cells is significantly higher in a low phosphate medium than compared to a high phosphate medium ($P < 0.005$), but the medium-specific increase in GFP/OD_{600} is lost in Δ*phoB* cells ($P > 0.3$, Figure 3.2). To ensure there is not activation of the reporter in a PhoB-dependent manner, all remaining experiments were conducted in a Δ*phoB* background.

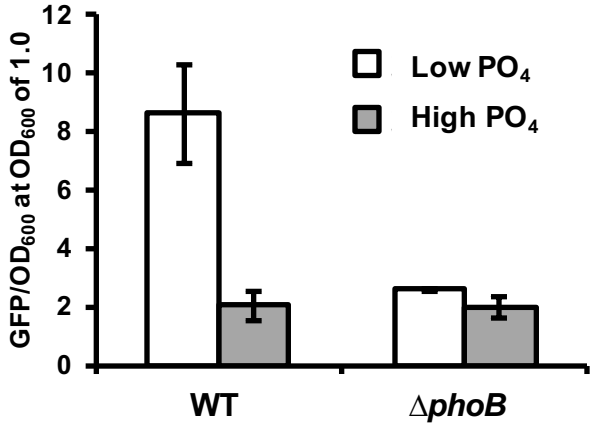

Figure 3.2. Chimeric ArcA-PhoB reporter is not responsive to phosphate levels. GFP and OD_{600} values were measured for cultures of ES114 (wild type, WT), and JLS9 (Δ*phoB*), JLS9, each containing the chimeric ArcA-PhoB protein and the optimized PhoB reporter encoded on pJLS217. Cultures were grown in FMM with low (37.8 μM, white bars) or high (378 μM, grey bars) phosphate. The GFP/OD_{600} values of the strains containing the promoterless vector (pJLS215) were subtracted from the values shown. The Δ*phoB* mutant is not significantly different in low or high phosphate media ($P > 0.3$), whereas there is significant activation of the PhoB-dependent reporter in ES114 low-phosphate FMM ($p < 0.005$). GFP/OD_{600} values were taken at an OD_{600} of 1.0, and error bars indicate standard deviation (n=3). Data shown are from one representative experiment of three performed.

Specific ArcB-dependent activation of the ArcA-PhoB chimeric reporter

In *V. fischeri*, ArcA- and ArcB-dependent repression of luminescence is detectable in aerobic cultures grown in rich media (28, 29). To determine if the chimeric protein is phosphorylated in an ArcB-dependent manner and able to activate transcription of a reporter gene, *gfp*, we compared the GFP-fluorescence from the reporter in JLS9 (Δ*phoB*) and JLS59 (Δ*phoB* Δ*arcB*) grown in the same complex medium, SWTO, in which we see strong ArcA- and ArcB-dependent repression of luminescence, with one modification (166). GFP fluorescence is quenched by acidity, and *V. fischeri* acidifies the medium (167, 168). Therefore, we added 100 mM MOPS pH 7.4 to SWTO to buffer the acid production. We see a significant ($p<0.005$) decrease in GFP expression from the reporter associated with the Δ*arcB* mutation when cells were grown in aerobic cultures to an OD_{600} of 2.5 compared to the Δ*phoB* mutant (Figure 3.3, chimera, $p<0.005$). This decrease in fluorescence in JLS59 (Δ*phoB* Δ*arcB*) approaches background fluorescence in control vectors lacking either the PhoB-dependent promoter or the ArcA-PhoB chimera gene (Figure 3.3). ArcB phosphorylates ArcA at a conserved aspartate residue (D54) (29, 169) and replacing this aspartate residue with an alanine eliminated chimera activity under these conditions (Figure 3.3).

V. fischeri *quinone mutants' activation of the ArcA-PhoB chimera*

In *E. coli*, ArcB is thought to respond to the redox state of the quinone pool (57, 108, 152, 153), with autophosphorylation of ArcB prevented through conformational changes induced by quinone-mediated cysteine oxidation in ArcB's PAS domain, or signal sensing domain (57). If the quinone pool is reduced, for example, by a lack of electron acceptors for respiration, ArcB autophosphorylation is favored, leading to activation of ArcA (57, 108). Further, Alvarez *et al.*

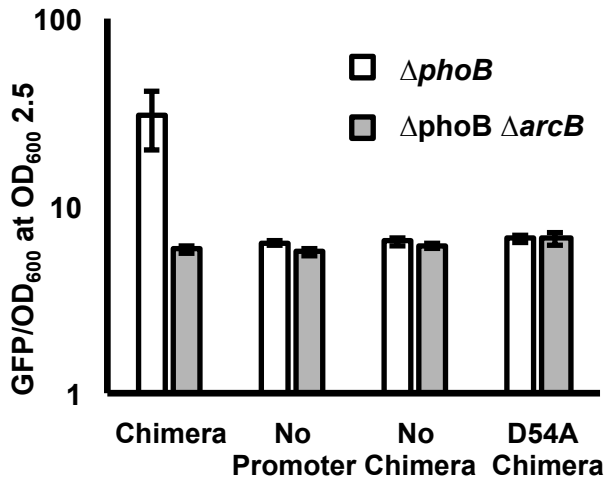

Figure 3.3. ArcA-PhoB reporter specificity in *V. fischeri*. JLS9 (Δ*phoB*; white bars) and JLS59 (Δ*phoB* Δ*arcB*; grey bars) carrying plasmid pJLS217 were grown aerobically in buffered SWTO. The GFP/OD_{600} values at an OD_{600} of 2.5 are shown, with error bars representing the standard deviation (n=4). The Δ*phoB* Δ*arcB* mutant with the chimera and reporter (Chimera) is not significantly different from itself or the Δ*phoB* mutant with the chimera containing a D54A mutation, no promoter, or no chimera. However, with the chimera and PhoB-promoter, the reporter in the Δ*phoB* Δ*arcB* mutant is less active than the reporter in the Δ*phoB* mutant (Chimera, $p < 0.005$). Shown is a representative graph of three experimental replicates.

demonstrate that menaquinones are required for activation of ArcB upon shifting to anoxic conditions, while ubiquinone is primarily responsible for silencing the kinase activities of ArcB during aerobic growth (152). To test if the *V. fischeri* ArcAB system is regulated in a similar manner, we deleted genes required for ubiquinone synthesis, *ubiCA*, and a gene required for menaquinone synthesis, *menA*.

In the *E. coli* model, mutants unable to synthesize menaquinone are unable to fully activate ArcA (152). Since ArcA appears active in aerobic *V. fischeri* culture, we investigated the effects of a mutation in *menA,* required for menaquinone synthesis, on the ability of the ArcA-PhoB chimera to activate the reporter under these conditions; however, deletion of *menA* had no discernable effect under these conditions (Fig. 3.4). Further, based on the model of ArcB being inhibited by oxidized ubiquinone (152), we predicted that a deletion of *ubiCA* would prevent ubiquinone synthesis and lead to an increase in fluorescence from the GFP reporter compared to

JLS9 (Δ*phoB*) in aerobic culture. Figure 3.4 shows a significant increase in reporter expression associated with the Δ*ubiCA* mutations. Surprisingly however, this activation is ArcB-independent (Figure 3.4).

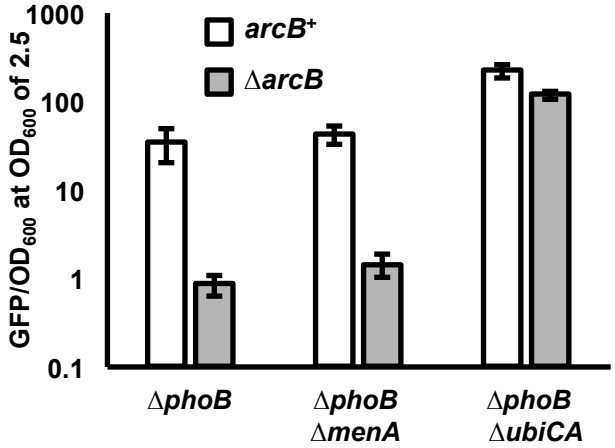

Figure 3.4. Effects of Δ*ubiC*A and Δ*menA* mutations on reporter activity. JLS9 (Δ*phoB*), JLS59 (Δ*phoB* Δ*arcB*), JLS60 (Δ*phoB* Δ*menA*), JLS61 (Δ*phoB* Δ*arcB* Δ*menA*), JLS64 (Δ*phoB*, Δ*ubiCA*), and JLS65 (Δ*phoB* Δ*arcB* Δ*ubiCA*) were grown aerobically in buffered SWTO, where the OD_{600} and GFP fluorescence values were measured at an OD_{600} of 2.5. The Δ*menA* mutants (JLS60 and JLS61) are not statistically different than the Δ*phoB* or Δ*phoB* Δ*arcB* mutants (JLS9 and JLS59). However, the Δ*ubiCA* mutants (JLS64 and JLS65) have increased GFP/OD_{600} from JLS9 (Δ*phoB*) and JLS59 (Δ*phoB* Δ*arcB*) ($p < 0.0002$). Data shown are from one representative experiment of four, and error bars represent standard deviation of biological replicates (n=4).

ArcB-independent activation of the ArcA-PhoB chimeric reporter in V. fischeri

We were interested in investigating the ArcB-independent effect seen in the Δ*ubiCA* background (Figure 3.4). Given the connection between Arc activation and fermentative products, we considered the possibility that the Δ*ubiCA* mutants, lacking effective respiration, might have an increase in fermentative end products. When grown in unbuffered SWTO medium, the Δ*ubiCA* mutants (JLS64 and JLS65) dropped the pH of the medium significantly faster than the parent grown in the same medium (data not shown). Fermentative end products, such as lactate and acetate, have been shown to accelerate the rate of ArcB autophosphorylation

(170) leading to higher ArcA phosphorylation (171), and inhibit the rate of ArcB phosphatase activity (172); however, these mechanisms are still dependent on ArcB.

We hypothesized that acetyl-phosphate (acetyl-P) or acetyl-CoA might play a role in direct activation of the chimera. There is some precedence for this concept, as acetyl-P has been used (in the low millimolar range) to phosphorylate ArcA (99) and other response regulators (173-178) *in vitro* (176-178). *V. fischeri* cells grown in SWTO medium can accumulate acetate to more than 5 mM, or up to 14 mM in some mutant strains lacking *acs*, which is in part responsible for the metabolism of acetate to acetyl-CoA (167). Furthermore, the intracellular concentration of acetyl-P in *E. coli* has been determined to range as high as 3 mM to more than 15 mM depending on growth conditions (179). Acetate metabolism occurs through two main pathways in gammaproteobacteria. First, acetate can irreversibly be converted to acetyl-CoA via acetyl-CoA synthase (Acs) (180). Second, acetate can be reversibly converted to acetyl-P via AckA, which can then be further converted to acetyl-CoA in a reversible reaction by phosphotransacetylase, Pta (180).

To explore whether acetyl-P is contributing to chimeric-dependent activation *in vivo*, we deleted the genes in the pathway to make acetyl-P, *pta* and *ackA*, in both the Δ*phoB* and Δ*phoB* Δ*arcB* backgrounds. At an OD_{600} of 2.5, we did not see a significant effect of the Δ*pta/ackA* deletion on reporter activity. However, at slightly higher OD_{600} values (e.g. 2.8), we see the Δ*arcB* mutant (JLS59) display fluorescence over background, and this increase was significantly less in JLS69 (Δ*phoB* Δ*arcB* Δ*pta/ackA*) (Figure 3.5). This above-background fluorescence was both chimera- and PhoB-promoter dependent (data not shown), yet independent of the conserved aspartate at position 54 in the receiver domain (Figure 3.5).

Since acetyl-P can be made from acetate, we also predicted that exogenous acetate in the medium might increase chimera-dependent ArcB-independent reporter activation. Consistent with this prediction, JLS59 (Δ*phoB* Δ*arcB*) has a 2-fold increase in chimera-dependent reporter activation with 40 mM acetate added to buffered SWTO (Figure 3.6, Δ*arcB*).

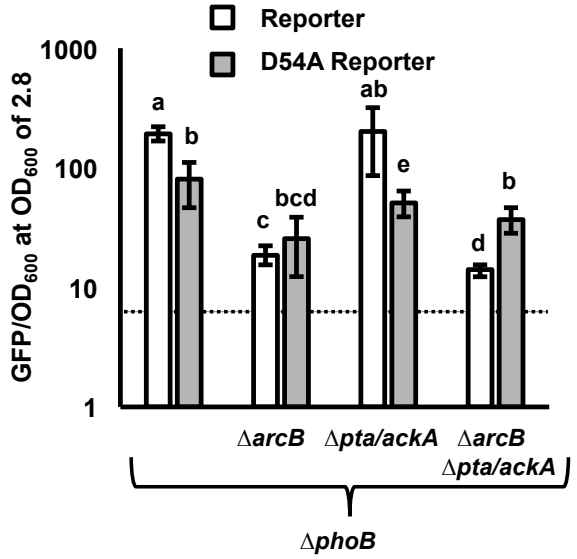

Figure 3.5. Chimera activation in an ArcB-independent manner is decreased in a Δ*pta/ackA* mutant. Specific fluorescence is shown for JLS9 (Δ*phoB*) or mutants JLS59 (Δ*phoB* Δ*arcB*), JLS67 (Δ*phoB* Δ*pta/ackA*), and JLS69 (Δ*phoB* Δ*arcB* Δ*pta/ackA*), harboring the reporter with both the chimera and PhoB-promoter (reporter, white bars) of the D54 chimera with promoter (light gray bars). Strains were grown in SWTO medium and GFP/OD_{600} values were taken at an OD_{600} of 2.8. The no promoter and no chimera control values are represented by the dotted line. An ANOVA ($p<0.05$) was performed and error bars indicate standard deviation (n=4). Data shown are from one representative experiment of three performed.

Symbiotic activation of the ArcA-PhoB chimera

We examined the reporter system in symbiotic cells to assess the activation state of ArcA in the symbiosis (Figure 3.7). To ensure the GFP reporter is not activated independently of the Arc-PhoB chimera in symbiosis, we examined a no-chimera control, which as predicted

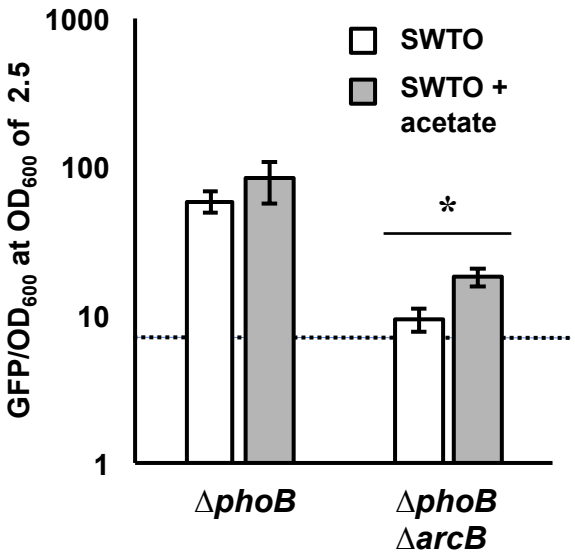

Figure 3.6. Exogenous acetate increases ArcB-independent reporter activation. The Δ*phoB* and Δ*phoB* Δ*arcB* mutants (JLS9 and JLS59) were grown in buffered SWTO with and without 40 mM acetate added (dark gray bars and white bars, respectively). Specific fluorescence is shown for the OD_{600} value of 2.5. The dotted line represents the approximate specific fluorescence of the promoterless reporter, * represents $p < 3.5E-05$, error bars represent standard deviation (n=4), and this is a representative graph of three biological replicates.

displayed only the constitutive mCherry fluorescence and not GFP (Figure 3.7). We then infected animals with different mutant strains that had the full reporter system (chimera and promoter). At 72-hours post-inoculation, these juvenile squid all had symbionts displaying both (constitutive) red mCherry fluorescence, and green GFP reporter fluorescence (Figure 3.7). Surprisingly, however, deleting *arcB* resulted in stronger GFP fluorescence, and this activation was unaffected by the D54A mutation in the receiver domain of the chimeric response regulator (Figure 3.7). Moreover, the D54A substitution in the receiver domain did not seem to affect symbiotic activation of the reporter when *arcB* was present. Finally, the Δ*pta/ackA* mutation, which should decrease acetyl-P levels in the cells had little effect on reporter activation in either *arcB*+ or Δ*arcB* backgrounds.

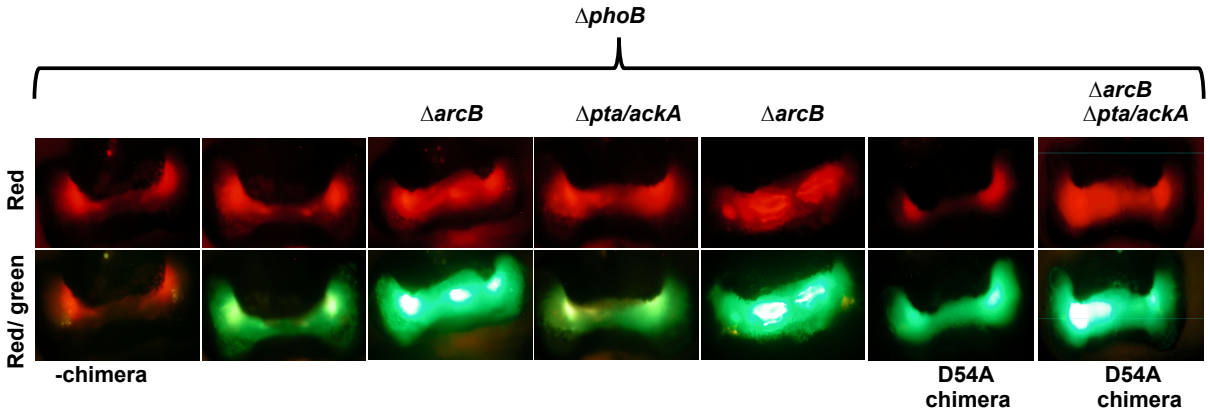

Figure 3.7. Symbiotic activation of the ArcA-PhoB chimera. Juvenile squid were infected with *V. fischeri* mutants JLS9, JLS59, JLS67, or JLS69 harboring the ArcA-PhoB chimeric reporter or reporter variants lacking the chimera or with the D54A mutation in the chimera. Light organs were visualized with an epifluorescent microscope under a red or red/green filter 72 hours post inoculation. Images are a representative light organ. At least 5 animals were dissected for each treatment.

The arcA *and* arcB *mutants do not phenocopy in symbiosis*

Bose *et al*. saw that an *arcA* mutant was outcompeted by approximately 4-fold during symbiotic competition against wild-type *V. fischeri* (29); however, given the ArcB-independent activation of the chimeric reporter, we predicted an *arcB* mutant might be more competitive, as it seems dispensable for ArcA activation in the symbiosis. We infected juvenile squid with a 1:1 ratio of mutant, AMJ2 (Δ*arcA*) or ANS71 (Δ*arcB*), to AKD200, a chloramphenicol resistant ES114-derivative. Forty-eight hours after inoculation, the Δ*arcA* mutant was 3.5-fold outcompeted with an average Relative Competitive Index (RCI, or the final ratio divided by the initial inocula ratio), of 0.3 (Figure 3.8a), similar to the results seen by Bose *et al.* (29); however, the Δ*arcB* mutant was significantly more competitive, being outcompeted only 1.6-fold with an average RCI of 0.6 (Figure 3.8b).

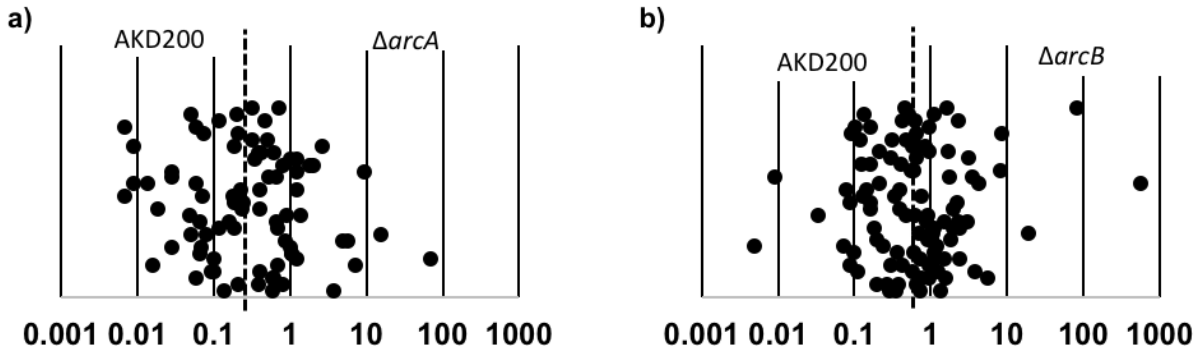

Figure 3.8. *arcA* and *arcB* mutants are outcompeted during host colonization. The *arcA* mutant (panel a, AMJ2) or the *arcB* mutant (panel b, ANS71), were competed with AKD200, a symbiosis-proficient chloramphenicol-resistant derivative of wild-type strain ES114, in a ~1:1 ratio. The bacteria were recovered from the squid after 48 hours of infection. Each symbol represents the RCI calculated from an individual squid (Δ*arcA* n=84, Δ*arcB* n= 103). The dotted lines represent the average RCI; 0.3 for the Δ*arcA* mutant and 0.6 for the Δ*arcB* mutant. Each mutant was significantly outcompeted by AKD200 ($p < 8E-05$). Data shown are the combination of at least three independent experiments, each with similar results.

DISCUSSION

The ArcAB two-component regulatory system has been extensively studied in the model organism *E. coli* (181). ArcA can activate many genes as a global regulator, including those for virulence, conjugation, hydrogenase and other genes regulating metabolism in various bacteria, including those in mutualistic or parasitic associations with hosts (57, 182-185). Given the link between redox and Arc-mediated repression of luminescence in *V. fischeri*, Bose *et al.* speculated that pioneer bacteria in the light organ experience oxidative conditions not conducive to ArcAB activation, allowing derepression of the *lux* operon (29). Supporting this model, Septer and Stabb demonstrated that ArcA cannot repress luminescence after the LuxIR positive feedback loop is initiated inducing bright luminescence (28). In this study, we aimed to generate an ArcA-activated reporter to probe the activation state of ArcA in *V. fischeri* within the host Hawaiian bobtail squid, *Euprymna scolopes*, light organ.

We designed a chimeric protein that would respond to ArcB-dependent activation of ArcA via phosphorylation of the Asp54 residue, but that would also bind to a PhoB binding site (Figure 3.1). Using this chimeric protein with a previously optimized PhoB-specific reporter (chapter 2) in a *phoB* mutant background, we see activation of the chimera in aerobically grown cultures that is both chimera- and promoter-dependent (Figure 3.3), consistent with the aerobic activation conditions identified previously (29). Further, we show that activation under these conditions is dependent on the conserved Asp54 residue in the ArcA receiver domain (Figure 3.3), suggesting ArcB can successfully phosphorylate the Asp 54 residue of the ArcA-PhoB chimera. This chimeric protein design with the optimized PhoB-dependent promoter should be applicable to other two-component response regulators, particularly the OmpR-type family of response regulators in which both ArcA and PhoB are classified. Swapping the receiver domain of the chimera with other OmpR-type receiver domains could lead to the development of additional sensitive and specific reporters for other two-component systems.

The *E. coli* model of ArcB activation hinges on ArcB sensing the redox state of the quinone pool (57, 108, 152, 153). Briefly, quinone mediated changes in the PAS domain of ArcB via oxidation of cysteine residues, are thought to lock the ArcB dimer in an "off" state under oxidative conditions (57). Upon transitioning to micro- or anaerobic conditions, ArcB can autophosphorylate and transfer the phosphate group to ArcA at the conserved Asp54 residue (57, 169). More specifically, ubiquinone is predicted to be responsible for repressing ArcB kinase activity in aerobically grown cultures, whereas menaquinone is required for the anaerobic activation of ArcB (152).We found that a deletion of *menA* in *V. fischeri* had no discernible effect in aerobic cultures (Figure 3.4), which is consistent with the *E. coli* model. Likewise, deleting *ubiCA* resulted in the chimera being activated both earlier (data not shown) and to a

greater extent (Figure 3.4), again consistent with the *E. coli* model. Surprisingly, however, in the Δ*ubiCA* background we observed high *arcB*-independent reporter activation (Figure 3.4). These data suggest that while the ArcAB system seems to be similar to *E. coli*, ArcA activation in an ArcB-independent manner may be playing a role in *V. fischeri*. Although, Loui *et al.* saw unexplained ArcB-independent activation of ArcA in *E. coli* (186), which could suggest ArcB-independent activation is more widespread than currently identified, this effect has not been reported under most lab conditions.

We hoped to gain a better understanding of the possible mechanism of ArcB-independent activation of ArcA by looking into *V. fischeri* metabolism. It is possible acetyl-P could act *in vivo* to phosphorylate ArcA in an ArcB-independent manner. Acetyl-P is commonly used to phosphorylate response regulators *in vitro* at concentrations in the low-to-mid millimolar range (176-178), and has been reporter to accumulate to 15 mM, or more, under some growth conditions (179). Acetyl-P is converted to acetate via AckA (180), and *V. fischeri* accumulates up to 5 mM acetate in wild type cultures before consuming the acetate and converting it to acetyl-CoA (167). We deleted *pta* and *ackA,* which are required for the reversible conversion of acetyl-CoA to acetate through acetyl-P (180), and saw ArcB-independent activation at late stationary phase cells (Figure 3.5), and though slight, there was a significant reduction of chimeric activation in the Δ*phoB* Δ*arcB* Δ*pta/ackA* mutant (Figure 3.5). These data suggest acetyl-P may influence the ArcB-independent activation of the reporter, but it does not appear to be solely responsible for ArcB-independent activation, unless there is an alternative source of acetyl-P in the cell.

Since acetyl-P is an intermediate in the metabolism of acetate and we see some effect of acetyl-P on the phosphorylation of the chimera, we predicted the addition of exogenous acetate

may increase the ArcB-independent activation of the reporter. With the addition of 40 mM acetate, we see a significant increase in chimera activation in the *arcB* mutant; while we see a consistent slight increase in the parent strain, it is not statistically significant (Figure 3.6). Together, these data suggest that an accumulation of acetate, such as later in the growth cycle in culture (167) or in the squid light organ (74), leads to activation of ArcA in an ArcB-independent manner. Acetate can be metabolized to acetyl-CoA, which is then fed into the TCA cycle via two independent ways. First, as mentioned before, acetate can be first converted to acetyl-P via AckA, which is then immediately converted to acetyl-coA via Pta (179). The second pathway includes a direct conversion from acetate to acetyl-coA via Acs (179). We see ArcB-independent activation of the chimeric reporter independent of the Asp54 residue, and therefore, we do not know what post-translational modification is occurring to elicit the necessary conformational change for the chimeric response regulator to become active. Based on the increase in chimera activation due to the presence of acetate (Figure 3.6), it is possible this increase is due to acetyl-P, however, the decrease in chimera activation in JLS69 (Δ*phoB* Δ*arcB* Δ*pta/ackA*) mutant compared to JLS59 (Δ*phoB* Δ*arcB*) was minimal (Figure 3.5). It is perhaps more likely the post-translational modification is due to an increase in acetyl-CoA and could involve acetylation, rather than phosphorylation of the chimeric protein.

Based on the results of Bose *et al.* (29), it is unsurprising that we saw the ArcA-PhoB chimeric reporter activated in symbiosis with the Hawaiian Bobtail Squid (Figure 3.7). Importantly, this activation was chimera dependent, but surprisingly we saw stronger activation in the absence of *arcB* suggesting the possibility that ArcB is playing a stronger role in deactivating ArcA in symbiosis than in culture. We show that even in a Δ*pta/ackA* mutant background there is still ArcA-PhoB chimera activation, which still is stronger in the Δ*pta/ackA*

Δ*arcB* mutant background further suggesting that while acetyl-P may be playing a role in the activation of the chimeric protein in an ArcB-independent manner, it is not the only mechanism of activating the reporter in an ArcB-independent manner. Further, we determined that the ArcB-independent activation in symbiosis was independent of the D54 residue in the ArcA receiver domain. Together these data suggest the ArcB-independent mechanism of ArcA activation in symbiosis is significant, and this activity is independent of the conserved aspartate residue in ArcA.

In light of the detected ArcB-independent chimera activation (Figure 3.5 and Figure 3.6), we predicted an *arcB* mutant would be able to compete against the wild type strain more efficiently than an *arcA* mutant. In a Tn-seq data set generated by Brooks *et al.*, an *arcB* mutant was detected 7-fold less in the bacterial library coming out of symbiosis when compared to the library used to infect the squid (95). Whereas an *arcA* mutant was detected 26-fold less in the output, although neither effect was deemed a robust and statistically conclusive indication of symbiotic attenuation (95). Consistent with the results of Bose *et al.* (29), we saw a 3.5-fold decrease in competitive fitness (3.5-fold) in an *arcA* mutant (AMJ2) 48 hours after inoculation (Figure 3.8). Consistent with our prediction, we saw only a 1.6-fold drop in competitive fitness with an *arcB* mutant (Figure 3.8). These data further support a role for ArcB-independent activation of ArcA in the host light organ.

In summary, the *V. fischeri* ArcAB two-component regulatory system has many similarities to the published work on this system in *E. coli*, with some marked differences. We identified ArcB-independent activation of a chimeric reporter protein and while we have not identified an ArcB-independent mechanism of ArcA activation, we have generated evidence to suggest it may relate to acetate metabolism in the cell. Future work should identify the ArcB-

independent modifications to the chimeric protein, which will help determine the underlying mechanism. Additionally, other two-component regulators are important in host colonization (38), and we predict this chimeric reporter design of exploiting an optimized PhoB-Dependent reporter could be useful in identifying their roles during symbiosis.

MATERIALS AND METHODS

Growth conditions and media

Vibrio fischeri ES114 was used as the parent and wild-type strain for all strain constructions (4). *V. fischeri* was grown at 28°C, and all experiments were carried out in one of three standard media, LBS (139), FMM (98), or SWTO (29), with SWTO modified with 100mM MOPS at pH 7.4, except where indicated. *Escherichia coli* strains DH5α (144) and DH5α λ*pir* (146), were used for all cloning experiments described below, and *E. coli* was grown in either LB medium (187) or BHI medium (Difco) at 37°C. To maintain antibiotic selection, kanamycin (kan), chloramphenicol (cm), erythromycin (erm), trimethoprim (tmp), or ampicillin (Amp) was added to media at final concentrations of 40, 20, 150, 10 μg ml^{-1}, 100 μg ml^{-1}, respectively for *E. coli,* and 100, 2, 5, and 10 μg ml^{-1}, respectively for *V. fischeri*. Ampicillin was not used for selection in *V. fischeri*.

Plasmid and strain construction

All bacterial strains, plasmids, and oligonucleotides used in this study are presented in Table 1. Plasmids were maintained in *E. coli* and mobilized into *V. fischeri* using triparental mating as previously described (145). Chromosomal mutations in *V. fischeri* were constructed through allelic exchange (10) and verified using PCR. To generate the Δ*arcB* allele, primers

ASarcBupF and ASarcBupR were used to amplify ~1.5 kb upstream of *arcB* and primers ASarcBdownF and ASarcBdownR were used to amplify ~1.5 kb downstream of *arcB*. These two fragments were fused and amplified using SOE (Splicing by Overlap Extension) PCR (188), and the resulting product was blunt-end cloned directly into pCR-BluntII-TOPO, generating plasmid pAS122. To add the origin of transfer required for mating into *V. fischeri*, plasmids pAS122 and pEVS118 were each digested with XhoI and then fused, generating pAS125. The Δ*arcB* allele on pAS125 was placed in ES114 (wild type) and JLS67 (Δ*phoB* Δ*pta/ackA)*, to generate ANS71(Δ*arcB)* and JLS69 (Δ*phoB* Δ*arcB* Δ*pta/ackA)*.

Strain JLS59 (Δ*phoB* Δ*arcB*) and JLS67 (Δ*phoB* Δ*pta/ackA*) were generated through allelic exchange using the Δ*phoB* allele on pJLS25 (chapter 2) mobilized into ANS71 (Δ*arcB*) and Δpta/ackA (Δ*pta/ackA*), respectively. The Δ*menA* allele was generated in a similar method by amplifying ~1.5 kb upstream and downstream of *menA* using primer pairs ASmenAupF/ASmenAupR and ASmenAdownF/ASmenAdownR, respectively. The final SOE-PCR product was directly cloned into pCR-BluntII-TOPO, generating pAS67. Plasmids pAS67 and pEVS118 were then fused at their respective KpnI sites to generate pAS70. The Δ*menA* allele on pAS70 was mobilized into JLS9 (Δ*phoB*) and JLS59 (Δ*phoB* Δ*arcB*), to generate JLS60 (Δ*phoB* Δ*menA*) and JLS61 (Δ*phoB* Δ*arcB* Δ*menA*), respectively.

To generate the Δ*ubiCA* allele, the ~1.5 kb upstream and downstream of *ubiCA* were amplified using primer pairs JBUBI1/JBUBI2 and JBUBI3/JBUBI4 and each cloned into pCR-BluntII-TOPO to generate plasmids pJLB136 and pJLB137, respectively. To add the required origin of transfer, plasmid pJLB136, containing the upstream of *ubiC,* and pEVS94 were fused at their XbaI sites, to generate pJLB147. Plasmid pJLB147 was then digested with SpeI and self-ligated to remove the ColEI origin of replication and the kanamycin resistance gene, generating

pJLB148. To fuse the upstream and downstream sequences together, plasmids pJLB137 and pJLB148 were fused at the NheI site, generating the Δ*ubiCA* allele in pJLB153. Plasmid pJLB153 was used for allelic exchange by mobilizing into JLS9 (Δ*phoB*) and JLS59 (Δ*phoB* Δ*arcB*), generating JLS64 (Δ*phoB* Δ*ubiCA*) and JLS65 (Δ*phoB* Δ*arcB* Δ*ubiCA*). In order to get successful Δ*ubiCA* mutants, the single recombinants had to be grown in a microaerobic environment.

The Δ*pta/ackA* mutation was generated in a similar manner. Around 1600bp of upstream sequence (ptaupF/ptaupR) was cloned into pCR-BluntII-TOPO, ptaup, while around 1650bp of downstream sequence (ptadownF/ptadownR) was cloning into pDMA61, ptadown. Vectors ptaup and ptadown were fused together at the AvrII site, forming the deletion construct pΔpta/ackA, which was then moved into ES114 to make the Δpta/ackA mutant.

To generate the reporter plasmids, the chimeric *arcA-phoB* sequence was constructed. First, the N-terminal regulatory domain comprised of the first 123 amino acids of ArcA (as predicted by (163)) was cloned into pCR-BluntII-TOPO using primers JLSArcAF2 and JLSArcA123R3, generating pJLS11. The DNA binding domain of PhoB (as predicted by (137)) was amplified using primers JLSPhoB128F3 and JLSPhoBR2, which also added a thirteen amino acid linker, ESFHPPMDEFRGS (165), to the 5' end of the product, generating pJLS12. Plasmids pJLS11 and pEVS118 were fused at the KpnI site, and subsequently digested with XbaI and self-ligated generating plasmids pJLS13 and pJLS14. Plasmids pJLS12 and pJLS14 were fused together at the XmnI site, to generate the *arcA-phoB* chimeric allele in pJLS17. The chimera was amplified with primers JLSarcAF5 and JLSPhoBR5, which added an AgeI site upstream of the ATG start codon and flanking SalI sites. This fragment was then cloned into the XhoI site of pJLS203, generating plasmid pJLS215. Oligonucleotides JLSPconAgeI3 and

JLSPconAgeI4 were annealed and inserted into the AgeI site of pJLS215, inserting a near consensus promoter with ribosome binding site, generating plasmid pJLS217. To test the effects of a mutation to the conserved D54 allele in ArcA, a D54A mutation was made in the chimeric protein. First, pJLS217 was digested with SphI and NruI, and a PCR product containing the chloramphenicol resistance gene and promoter, amplified by JLScamF and JLScamR, was ligated in, generating plasmid pJLS251. Plasmid pJLS251 was again digested with SphI and NruI and a fragment containing the D54A mutation was ligated in from a synthesized geneblock, JLSArcAD-A, generating pJLS255.

Table 3.1: Strains, Plasmids, and Oligonucleotides used in this study

Strain	Genotype[a]	Source
Escherichia coli		
CC118 λ*pir*	Δ(*ara-leu*) *araD* Δ*lac74 galE galK phoA20 thi-1 rpsE rpsB argE(*Am*) recA λpir*	(144)
DH5α	φ80d*lacZ*ΔM15 Δ(*lacZYA-argF*)U169 *deoR supE44 hsdR17 recA1 endA1 gyrA96 thi-1 relA1*	(146)
DH5α λ*pir*	λ*pir* derivative of DH5α	(128)
Vibrio fischeri		
Δpta/ackA	ES114 Δ*pta/ackA*	A. Dunn
ANS71	ES114 Δ*arcB*	A. Septer
AKD200	ES114 cm^R	(189)
ES114	Wild type isolate from *E. scolopes* light organ	(4)
JLS9	ES114 Δ*phoB*	Chapter 2

JLS59	ES114 Δ*phoB* Δ*arcB*	This study
JLS60	ES114 Δ*phoB* Δ*menA*	This study
JLS61	ES114 Δ*phoB* Δ*arcB* Δ*menA*	This study
JLS64	ES114 Δ*phoB* Δ*ubiCA*	This study
JLS65	ES114 Δ*phoB* Δ*arcB* Δ*ubiCA*	This study
JLS67	ES114 Δ*phoB* Δ*pta*/*ackA*	This study
JLS69	ES114 Δ*phoB* Δ*arcB* Δ*pta*/*ackA*	This study

Select Plasmids[b]		
pΔpta/ackA	Δ*pta*/*ackA* allele; $oriV_{colE1}$, $oriV_{R6K\gamma}$, $oriT_{RP4}$, kan^R, cm^R	A. Dunn
pAS70	Δ*menA* allele; $oriV_{colE1}$, $oriV_{R6K\gamma}$, $oriT_{RP4}$, kan^R, cm^R	A. Septer
pAS125	Δ*arcB* allele; $oriV_{colE1}$, $oriV_{R6K\gamma}$, $oriT_{RP4}$, kan^R, cm^R	A. Septer
pEVS94	$oriV_{R6K\gamma}$, $oriT_{RP4}$, erm^R	(145)
pEVS104	conjugative helper plasmid; $oriV_{R6K\gamma}$, $oriT_{RP4}$, kan^R	(145)
pEVS118	$oriV_{R6K\gamma}$, $oriT_{RP4}$, cm^R	(145)
pJLB153	Δ*ubiCA* allele; $oriV_{colE1}$, $oriV_{R6K\gamma}$, $oriT_{RP4}$, kan^R, erm^R	J. Bose
pJLS17	$arcA^{1\text{-}123}$ESFHPPMDEFRGS$phoB^{128\text{-}231}$ allele; $oriV_{colE1}$, $oriV_{R6K\gamma}$, $oriT_{RP4}$, kan^R, cm^R	This study
pJLS25	Δ*phoB* allele; $oriV_{colE1}$, $oriV_{R6K\gamma}$, $oriT_{RP4}$, *kanR*, *cmR*	Chapter 2
pJLS198	$oriV_{R6K\gamma}$, $oriT_{RP4}$, pES213, *mcherry*, P_{con}-tmp^R, *gfp*-ssrA-ASV	Chapter 2
pJLS203	$oriV_{R6K\gamma}$, $oriT_{RP4}$, pES213, *mcherry*, P_{con}-tmp^R, P_{phoB} *gfp*-ssrA-ASV	Chapter 2

pJLS215	*oriV*$_{R6K\gamma}$, *oriT*$_{RP4}$, pES213, *mcherry*, P$_{con}$-*tmp*^{R}, *gfp*-ssrA-ASV, P$_{con}$ *arcA*$^{1-123}$ESFHPPMDEFRGS*phoB*$^{128-231}$ allele	This study
pJLS217	*oriV*$_{R6K\gamma}$, *oriT*$_{RP4}$, pES213, *mcherry*, P$_{con}$-*tmp*^{R}, P$_{phoB}$ *gfp*-ssrA-ASV, P$_{con}$ *arcA*$^{1-123}$ESFHPPMDEFRGS*phoB*$^{128-231}$ allele	This study
pJLS255	*oriV*$_{R6K\gamma}$, *oriT*$_{RP4}$, pES213, *mcherry*, P$_{con}$-*tmp*^{R}, P$_{phoB}$ *gfp*-ssrA-ASV, P$_{con}$ *arcA*$^{1-123}$ESFHPPMDEFRGS*phoB*$^{128-231}$*D54A* allele	This study

Oligonucleotides[c]	Sequence	Source
ASarcBdownF	GAATATTATCAGGGTATGTTTATGGTCGACTAAGGAA TAATATGAAGAAGGTAC	A. Septer
ASarcBdownR	AGAGCTTTATCTTGTTATTGAC	A. Septer
ASarcBupF	CTTATTGTGACGTGCAAAC	A. Septer
ASarcBupR	GTCGACCATAAACATACCCTGATAATATTC	A. Septer
ASmenAdownF	TATTCACTATTTTTGCGATGCTATGCCTAGGTAAAAAC GAAAGCGGCTTATC	A. Septer
ASmenAdownR	AAAGAACGTCAGATGTTGGTA	A. Septer
ASmenAupF	CACAAGACTATTATCAACAATGCA	A. Septer
ASmenAupR	TTACCTAGGCATAGCATCGCAAAAATAGTGAATA	A. Septer
JBUBI1	CGCATTATCAAACCCTAGAGCAGGAC	J. Bose
JBUBI2	GCTAGCCATATTCTCTATAACCTCTTTCACATATATTGC	J. Bose
JBUBI3	GCTAGCTAACGTGTTGTTTTAAAAGAAAAGCCAG	J. Bose
JBUBI4	CCCTGCGGGTCCTATTTTCCGTCGC	J. Bose
JLSArcAF2	TACCCGGGATGCAAACCCCACAGATCC	This study

JLSArcAF5	CGTAGTCGACACCGGTATGCAAACCCCACAGATCC	This study
JLSArcA123R3	TAGAATGTATTCGTTCATTGAACGAGTTAATAAGTTACGTGC	This study
JLSPconAgeI3	CCGGGTTGACATAAAGTCCAAGATAGTCTATAATGCGGATAGCGCGCCTCTGAGGAAG	This study
JLSPconAgeI4	CCGGCTTCCTCAGAGGCGCGCTATTCGCATTATAGACTATCTTGGACTTTATGTCAAC	This study
JLSPhoBR2	TACCCGGGTTATGACGCTTGTACAGAGAAGCG	This study
JLSPhoBR4	CGTAGTCGACTTATGACGCTTGTACAGAGAAGCG	This study
JLSPhoB128F3	TAGAATACATTCCACCCACCAATGGATGAATTTAGAGGTTCAGAAGAGCTGATTGATG	This study
JLSCamF	ATGCCACGTGGCATGCCTGGGCCAACTTTTGGCG	This study
JLSCamR	ATGCGGATCCTCGCGAGCACCAGGCGTTTAAGGG	This study
Geneblock JLSArcAD-A	CACGAAGTTCGCGAGCAAGAAGAAGGCCATTTTTACCTGGCAGGTTAATAGCCATAATCACAAGATTAAGCTGCTGTTCAGAAAGCACTTTATGCATTTCTTCGCCATCGCTAGCTTCAAAAACATTGTAGCCTTCAGCTTCAAAAATGCTTTTTAACGTATTACGAGTTACGTGTTCATCTTCAACGATTAGGATCTGTGGGGTTTGCATACCGGCTTCCTCAGAGGCGCGCTATCCGCATTATAGACTATCTTGGACTTTATGTCAACCCGGTGTCGAGCCCGGGCATGCCTAGGTA	This study
ptadownF	AATCCTAGGTAATTTCATGCTCTAGAAATAGAGCGTAG	A. Dunn
ptadownR	GTC AAT GGC TCC ATT TAT GTC ATG TG	A. Dunn

ptaupF	ATTCACGTCAACACCAGCACTT	A. Dunn
ptaupR	AATCCTAGGAACCAGCTTAGACATGTATAAATACCTATTT	A. Dunn

[a]Drug resistance abbreviations: *ampR*, ampicillin resistance (*bla*); *cmR*, chloramphenicol resistance (*cat*); *kanR*, kanamycin resistance (*aph*); and *tmpR* trimethoprim resistance (*dfr*).
[b]Plasmids listed may contain the RP4 origin of transfer ($oriT_{RP4}$). Replication origin(s) are denoted as $oriV_{ColE1}$, pES213, and/ or $oriV_{R6K\gamma}$.
[c]Oligonucleotide sequences are provided in the 5'-3' orientation.

Growth and fluorescence assays

All growth and fluorescence assays were carried out in 96-well black plates, with clear bottoms (Greiner Bio-One) using the protocols described previously (Chapter 2), with the following modifications. The plates were shaken in the plate reader continuously, and the plates were read for a full 24 hours. Juvenile squid were inoculated as previously described (189). Prior to dissection 72 hours after inoculation to expose the light organ, juveniles were anesthetized with by adding MgCl. Light organs were visualized using a Nikon Eclipse E600 microscope with filter set 51005v2 to visualize both the green fluorescence of the reporter and the constitutive red fluorescence simultaneously.

Squid competition assays

Squid competition assays were performed with fresh juvenile squid (less than 24 hours old) as described previously (189). Briefly, hatchlings were moved to dishes containing 100 mL of Instant Ocean (Spectrum Brands, Blacksburg, VA) mixed to 36 ppt and containing an equal ratio of mutant to AKD200, which is a chloramphenicol marked derivative of wild type. After ~14 hours and ~32 hours post-inoculation, the juvenile squid were moved to filter-sterilized Instant Ocean. The experiments were stopped after 48 hours by placing the squid into the -80 C

freezer. The squid were later dilution plated onto LBS and colonies were patched onto LBS amended with chloramphenicol to calculate the mutant to AKD200 ratio. The relative competitive index (RCI) was calculated by dividing the mutant-to-AKD200 ratio in the final by the inoculum ratio. Log transformed values were used to calculate the average and the statistical significance.

ACKNOWLEDGEMENTS

We thank Anne Dunn and Jeffery Bose for generating the Δ*pta/ackA* and Δ*ubiCA* alleles, respectively, Alecia Septer for the generation of the Δ*arcB* and Δ*menA* alleles and helpful discussions, and Coralis Rodriguez-Garcia for technical assistance. The National Science Foundation supported this research under grants IOS-1121106, IOS-1557964, and MCB-1716232. The research in this article was partially supported by a grant jointly funded by the University of Georgia Franklin College of Arts & Sciences, Office of the Vice President for Research, and Department of Microbiology.

CHAPTER 4

CONCLUSIONS AND FUTURE DIRECTIONS

The purpose of this dissertation was to investigate the activation state of two global regulators, ArcA and PhoB, in the marine bacterium *Vibrio fischeri*. I developed reporters enabling me to measure ArcA- or PhoB-dependent activation in cells grown in different culture conditions, and to qualitatively visualize activation in symbiotic cells colonizing the Hawaiian Bobtail Squid, *Euprymna scolopes*. The squid-*Vibrio* symbiosis is a valuable natural symbiosis to study pheromone signaling and host-bacterial interactions, because it can be reconstituted in the lab (6, 11), the eggs are laid symbiont-free (7), and the bacteria are genetically tractable and easily cultured outside of symbiosis. Bioluminescence in *V. fischeri* is required for full colonization of the host (8-10), and it is pheromone regulated (1-3). However, bioluminescence from *V. fischeri* strain ES114, originally isolated from *E. scolopes*, is only induced to high levels inside the host and not in free-living cells (4). Two environmental regulators of bioluminescence in culture are PhoB and ArcA (28-30), and both PhoB and ArcA are required for *V. fischeri* to compete effectively to colonize *E. scolopes* (29, 38). My goals were to determine the state of these regulators during symbiotic colonization, as well as to explore the activation signals for ArcA.

In Chapter 2, I developed a transcriptional reporter to examine the when PhoB was active. A series of observations had led to the hypothesis that the PhoB-dependent low-phosphate

response is activated in symbiotic cells. As noted above, luminescence is induced in the symbiosis, and it is also induced about ~10 fold in culture when phosphate is low and *phoB* is present (30). Additionally, a *phoB* mutant and transposon-insertion mutants in *pstA* and *pstS*, genes encoding the high affinity phosphate transporter, have competitive colonization defects (30, 38). Therefore, Lyell *et al.* hypothesized that the light organ is a phosphate limiting environment for symbionts, which could contribute to the luminescence induction (30). More recently however, a transcriptomic study of *V. fischeri* cells vented from the host suggested the PhoB-regulon is not upregulated, and therefore the squid light organ is not phosphate limiting for *V. fischeri* (66). My observation that PhoB is in a conditionally active state within the squid light organ could be consistent with each of these apparently conflicting reports.

Inside the squid's bi-lobed light organ, symbionts encounter distinct microenvironments. The light organ has three deep crypts on each side, named 1, 2, and 3 (Figure 1.1, (12)). Dunn *et al.* showed that when hatchling squid are co-colonized with two different strains, the bacterial populations within the crypts largely segregate, with fewer than 10% of the crypts showing a mixture of the two strains (97). Thus, there appear to be physical barriers separating populations in these different compartments. Additionally, a delay in the induction of the *lux* operon in cells within crypt 3 was detected (97), suggesting sufficient variation between crypt spaces to produce transcriptional differences between the bacterial sub-populations colonizing them. Moreover, Sycuro *et al.* found that the crypts are not vented equally. The bacteria in crypt 1 are mostly vented, but the bacteria found in crypts 2 and 3 are largely retained (96). Together with my symbiotic PhoB-dependent reporter data, I propose that the phosphate levels vary between different colonized microenvironments of the squid light organ. Specifically, if the crypt 1 is more phosphate-replete than is crypt 2 or crypt 3, such a pattern would be consistent with both

the transcriptomic data collected by Thompson *et al.* (66), largely from cells vented from crypt 1, and with my results suggesting that crypt 2 is more phosphate-limited than crypt 1 (Figure 2.7). The number of juvenile squid examined with symbionts carrying my PhoB-dependent reporter should be expanded in the future to test the extent of crypt-specific PhoB-dependent activation; however, my results already underscore the power of using *gfp* to examine expression *in situ*.

In Chapter 3, I sought to further investigate the state of the Arc system in culture and in symbiosis. Previous work suggested that the ArcAB system in *V. fischeri* has both similarities to and differences from the well-studied system in *Escherichia coli*. Bose *et al*. showed that ArcA from *V. fischeri* can complement an *arcA* mutant in *E. coli*, suggesting some functional similarity (29). However, they also showed that ArcA represses luminescence in aerobic culture ~500-fold, suggesting ArcA is in an active state aerobically, which differs from the model of ArcA activation in *E. coli*, where ArcA appears to be activated in the transition from aerobic to microaerobic or anaerobic conditions (29, 57). These data raise the possibility of a different activation signal in *V. fischeri*, rather than the relative oxidized versus reduced state of the quinone pool as proposed in *E. coli* (57, 108, 152, 153). Bose *et al*., also showed that while *V. fischeri* ArcA does not repress luminescence in symbiosis, ArcA is required to be competitive in the squid in co-inoculations (29). More recently, Septer and Stabb showed that direct Arc-mediated repression of the *lux* operon is actually relatively weak, and they showed that de-repression of luminescence upon the loss of ArcA activity is amplified by the LuxIR positive feedback loop (28). These data suggest that while the ArcAB system is not repressing luminescence in symbiosis, it is active in the light organ at some point. Through the generation of an ArcA-dependent reporter, my goal was to further investigate the environmental cues activating Arc in *V. fischeri* and to assess the state of Arc in symbiosis.

In *E. coli*, after detecting an environmental signal consistent with a relatively reduced environment, ArcB autophosphorylates and that phosphate group can then be transferred to the Asp-54 residue on ArcA, which stimulates the Arc regulon (57, 151). I found that by replacing the aspartate residue at position 54 in the receiver domain of *V. fischeri*'s ArcA with an alanine, I can disrupt ArcA activation (Figure 3.3). Therefore, it appears as though ArcA is phosphorylated, and therefore activated, by ArcB in similar manner to *E. coli*. Surprisingly, the *arcB* mutant retains significant ArcA-dependent activation of a transcriptional reporter in symbiosis (Figure 3.7). This result was the opposite of our expectations, and further motivated us to identify the activating signal for ArcA. As mentioned above, the reduced state of the quinone pool has been shown to influence ArcB autophosphorylation in *E. coli* (57, 108, 152, 153). I found that the presence or absence of quinones does influence ArcA activation in *V. fischeri*, however, there appears to be significant ArcB-independent activation in a ubiquinone synthase mutant (Figure 3.4). Further, I show that this ArcB-independent activation is independent of the conserved Asp-54 residue in ArcA (Figure 3.5). Together, these data begin to shed light on an important aspect of *V. fischeri*'s Arc activation that is not accounted for in the current paradigm model of Arc activation in *E. coli*.

In addition to the proposed role of quinones in modulating ArcB activity, it also appears that fermentative acids, such as lactate and acetate, can accelerate the rate of ArcB-autophosphorylation in *E. coli* (151, 154, 155). The mechanism and significance of fermentation acids affecting Arc has been debated, but it may be important in *V. fischeri*. Doudoroff detected formic acid as the major acid produced during glucose fermentation in *V. fischeri*, with smaller contributions from acetate, lactate, and succinate (168). Acetate is produced in a reversible reaction from acetyl-CoA, with acetyl phosphate (acetyl-P) as an intermediate (180). Acetyl-P is

used to phosphorylate response regulators *in vitro* in the low millimolar range (176-178), and some suggest acetyl-P can accumulate in the cytoplasm of bacterial cells to levels between three and fifteen mM (179). Therefore, we focused on the potential for acetyl-P to act as the ArcB-independent signal activating ArcA. I show that a mutant in *V. fischeri* unable to produce acetyl-P via Pta or AckA has less ArcB-independent activation of the ArcA-dependent reporter; however, the reporter still shows some ArcB-independent activation (Figure 3.5) indicating acetyl-P production may not be the entire signal, or that there is another pathway for the cell to make acetyl-P. Furthermore, I show that the addition of 40 mM acetate to the culture medium increases the ArcB-independent activation of the ArcA-dependent reporter (Figure 3.6).

Because deletion of *pta* and *ackA*, which presumably leads to lower acetyl-P accumulation, did not prevent the activation of the ArcA-dependent reporter, another possible mechanism of Arc modulation is the acetylation of the ArcA receiver domain by acetyl-CoA. There is precedence for this mechanism, as dual post-translational control of a response regulator by both phosphorylation and acetylation has been previously demonstrated in CheY (190). Acs converts acetate directly to acetyl-CoA in an irreversible reaction. To test if acetylation of the response regulator is a possibility in *V. fischeri*, we are mutating genes in the two pathways for acetate metabolism to acetyl-CoA (*pta*/*ackA* and *acs*). If the increase in ArcB-independent activation of the reporter upon addition of acetate is minimized in these mutants, it is possible acetyl-CoA is acetylating the protein. Further, a poly-His tag is being added to the N-terminus of the chimeric protein used in the ArcA-dependent reporter. Mass spectroscopy of this protein purified from cells grown under ArcB-independent Arc-activating conditions would enable identification of any such post-translational modifications.

Overall, my research discovered ArcB-independent activation of ArcA in *V. fischeri*, which is present in late stationary phase in culture and in the squid light organ. These results add to our understanding of how Arc regulates transcription in *V. fischeri*, but the precise signal activating ArcA remains elusive. We have some indication that acetate metabolism may play a role, and future work will focus on testing these predictions further.

My research also developed techniques to optimize transcriptional reporters for *in situ* analyses. First, I generated the PhoB-dependent promoter by starting with a semi-randomized DNA sequence, screening fewer than 100 promoters, finding specific nucleotide positions that significantly correlated with optimal performance (low background and high signal), and honing in on an optimized promoter (Figures 2.1 and 2.2). I showed that this reporter is activated at physiologically relevant environmental phosphate levels (Figure 2.3), and demonstrated its activity in other proteobacteria (Figure 2.4). Additionally, I tested GFP derivatives and found one where the half-life in *V. fischeri* is decreased from over 24 hours to approximately 81 min (Figures 2.5 and 2.6). This "Goldilocks" GFP derivative is stable enough to be measureable, yet fluorescence output is more temporally relatable to transcriptional activity. This reporter design method, in conjunction with the destabilized GFP, should be applicable to other transcriptional regulators, and has been used in part previously to design a CRP-dependent promoter (32).

The high sensitivity of the PhoB-dependent promoter, with a high output and minimal background, has broad implications for monitoring gene expression in bacteria. For example, in Chapter 3, I designed a chimeric protein comprised of domains from the response regulators ArcA and PhoB. I showed that the chimeric protein is activated by ArcA's cognate histidine kinase, ArcB, yet activates transcription in a PhoB-dependent manner (Figures 3.1 and 3.2). In a similar way, transcriptional reporters for other response regulators can be generated, using the

PhoB DNA binding domain and the optimized PhoB-dependent reporter. Many response regulators change the transcription at native promoters minimally, and/or the native promoters are regulated by multiple transcription factors (29, 99, 105-109, 159, 160). By using a chimeric protein with a response regulator receiver domain fused to the PhoB DNA binding domain in conjunction with the PhoB-dependent promoter, the chances of coregulation are minimized and the distinction between reporter "on" and "off" states is clear.

It is clear that two-component regulatory systems are important for *V. fischeri* to thrive in the squid, as mutations in the response regulators of at least fifteen of the forty predicted systems led to decreased colonization competitiveness (29, 38). It will be interesting to study the activation state of these systems during symbiosis, and the chimeric response regulator approach described above would facilitate this research. Bacterial two-component response regulators are divided into four main groups: CheY-like, NarL-like, OmpR-like, and NtrC-like (42, 46). CheY-like response regulators are unique in that they lack DNA binding motifs (46), and would therefore make inappropriate targets for the chimeric reporter approach. Further, NarL-like and NtrC-like response regulators have different DNA binding domains from the winged helix-turn-helix (wHTH) domain of the OmpR-like response regulators (42, 46, 173), for which both ArcA and PhoB have been classified. Thus, I would predict the chimeric approach would work best for response regulators characterized as OmpR-like.

V. fischeri has thirteen predicted OmpR-like response regulators, and of these, only five have characterized homologs in other bacteria (38). Of the OmpR-like regulators, only ArcA and PhoB have known impacts on luminescence (29, 30), and only ArcA and CpxR appear to affect motility (38). Mutants lacking ArcA, PhoB, VFA_0179, and VFA_0181, are less competitive in colonizing the host (29, 38). Recently, a Tn-seq data set revealed that insertions in genes for two

of the regulators, *cpxR* and VF_0436, were depleted in every sample passaged through the squid when compared to the input (95). As noted above, I would predict the described response regulator chimera approach, exploiting the DNA-binding domain of OmpR-type regulator PhoB, would be most successful with other OmpR-type response regulators. I would start by interrogating the activation state of CpxR, VFA_0179, VFA0181, and VF_0436, as evidence suggests those response regulators have the greatest symbiosis-specific role in *V. fischeri*, yet they have not yet been characterized. In this way, the tools and methodologies developed in this dissertation should continue making contributions to our understanding of this model symbiosis.

REFERENCES

1. **Nealson KH, Platt T, Hastings JW.** 1970. Cellular control of the synthesis and activity of the bacterial luminescent system. J Bacteriol **104:**313-322.

2. **Eberhard A.** 1972. Inhibition and Activation of Bacterial Luciferase Synthesis. J Bacteriol **109:**1101-1105.

3. **Fuqua WC, Winans SC, Greenberg EP.** 1994. Quorum sensing in bacteria: the LuxR-LuxI family of cell density-responsive transcriptional regulators. J Bacteriol **176:**269-275.

4. **Boettcher KJ, Ruby EG.** 1990. Depressed light emission by symbiotic *Vibrio fischeri* of the sepiolid squid *Euprymna scolopes*. J Bacteriol **172:**3701-3706.

5. **Doino JA, McFall-Ngai MJ.** 1995. A Transient Exposure to Symbiosis-Competent Bacteria Induces Light Organ Morphogenesis in the Host Squid. Biological Bulletin **189:**347-355.

6. **Wei SL, Young RE.** 1989. Development of symbiotic bacterial bioluminescence in a nearshore cephalopod, *Euprymna scolopes*. Mar Biol **103:**541-546.

7. **McFall-Ngai MJ, Ruby EG.** 1991. Symbiont recognition and subsequent morphogenesis as early events in an animal-bacterial mutualism. Science **254:**1491-1494.

8. **Visick KL, Foster J, Doino J, McFall-Ngai M, Ruby EG.** 2000. *Vibrio fischeri lux* genes play an important role in colonization and development of the host light organ. J Bacteriol **182:**4578-4586.

9. **Koch EJ, Miyashiro T, McFall-Ngai MJ, Ruby EG.** 2014. Features governing symbiont persistence in the squid-vibrio association. Mol Ecol **23:**1624-1634.

10. **Bose JL, Rosenberg CS, Stabb EV.** 2008. Effects of *luxCDABEG* induction in *Vibrio fischeri*: enhancement of symbiotic colonization and conditional attenuation of growth in culture. Arch Microbiol **190:**169-183.

11. **Haygood MG.** 1993. Light organ symbioses in fishes. Crit Rev Microbiol **19:**191-216.

12. **Montgomery MK, McFall-Ngai M.** 1993. Embryonic Development of the Light Organ of the Sepiolid Squid *Euprymna scolopes* Berry. Biological Bulletin **184:**296-308.

13. **Nyholm SV, Stabb EV, Ruby EG, McFall-Ngai MJ.** 2000. Establishment of an animal–bacterial association: Recruiting symbiotic vibrios from the environment. Proceedings of the National Academy of Sciences **97:**10231-10235.

14. **Ruby EG, Asato LM.** 1993. Growth and flagellation of *Vibrio fischeri* during initiation of the sepiolid squid light organ symbiosis. Arch Microbiol **159:**160-167.

15. **Boettcher KJ, Ruby EG, McFallNgai MJ.** 1996. Bioluminescence in the symbiotic squid *Euprymna scolopes* is controlled by a daily biological rhythm. Journal of Comparative Physiology a-Sensory Neural and Behavioral Physiology **179:**65-73.

16. **Nyholm SV, McFall-Ngai MJ.** 1998. Sampling the light-organ microenvironment of *Euprymna scolopes*: description of a population of host cells in association with the bacterial symbiont *Vibrio fischeri*. Biol Bull **195:**89-97.

17. **Lee KH, Ruby EG.** 1994. Effect of the Squid Host on the Abundance and Distribution of Symbiotic *Vibrio fischeri* in Nature. Appl Environ Microbiol **60:**1565-1571.

18. **Montgomery MK, McFall-Ngai M.** 1994. Bacterial symbionts induce host organ morphogenesis during early postembryonic development of the squid *Euprymna scolopes*. Development **120:**1719-1729.

19. **Ziegler MM, Baldwin TO.** 1981. Biochemistry of Bacterial Bioluminescence. Current Topics in Bioenergetics **12:**65-113.

20. **Boylan M, Miyamoto C, Wall L, Graham A, Meighen E.** 1989. Lux C, D and E genes of the *Vibrio fischeri* luminescence operon code for the reductase, transferase, and synthetase enzymes involved in aldehyde biosynthesis. Photochem Photobiol **49:**681-688.

21. **Lin JW, Chao YF, Weng SF.** 1998. Characteristic analysis of the *luxG* gene encoding the probable flavin reductase that resides in the *lux* operon of *Photobacterium leiognathi*. Biochem Biophys Res Commun **246:**446-452.

22. **KARL DM, NEALSON KH.** 1980. Regulation of Cellular Metabolism During Synthesis and Expression of the Luminous System in *Beneckea* and *Photobacterium*. Microbiology **119:**285-285.

23. **Engebrecht J, Nealson K, Silverman M.** 1983. Bacterial bioluminescence: isolation and genetic analysis of functions from *Vibrio fischeri*. Cell **32:**773-781.

24. **Schaefer AL, Val DL, Hanzelka BL, Cronan JE, Jr., Greenberg EP.** 1996. Generation of cell-to-cell signals in quorum sensing: acyl homoserine lactone synthase activity of a purified *Vibrio fischeri* LuxI protein. Proc Natl Acad Sci U S A **93:**9505-9509.

25. **Eberhard A, Burlingame AL, Eberhard C, Kenyon GL, Nealson KH, Oppenheimer NJ.** 1981. Structural identification of autoinducer of *Photobacterium fischeri* luciferase. Biochemistry **20:**2444-2449.

26. **Hanzelka BL, Parsek MR, Val DL, Dunlap PV, Cronan JE, Jr., Greenberg EP.** 1999. Acylhomoserine lactone synthase activity of the *Vibrio fischeri* AinS protein. J Bacteriol **181:**5766-5770.

27. **Lupp C, Ruby EG.** 2004. *Vibrio fischeri* LuxS and AinS: comparative study of two signal synthases. J Bacteriol **186:**3873-3881.

28. **Septer AN, Stabb EV.** 2012. Coordination of the *arc* regulatory system and pheromone-mediated positive feedback in controlling the *Vibrio fischeri lux* operon. PLoS One **7:**e49590.

29. **Bose JL, Kim U, Bartkowski W, Gunsalus RP, Overley AM, Lyell NL, Visick KL, Stabb EV.** 2007. Bioluminescence in *Vibrio fischeri* is controlled by the redox-responsive regulator ArcA. Mol Microbiol **65:**538-553.

30. **Lyell NL, Dunn AK, Bose JL, Stabb EV.** 2010. Bright mutants of *Vibrio fischeri* ES114 reveal conditions and regulators that control bioluminescence and expression of the *lux* operon. J Bacteriol **192:**5103-5114.

31. **Lyell NL, Colton DM, Bose JL, Tumen-Velasquez MP, Kimbrough JH, Stabb EV.** 2013. Cyclic AMP Receptor Protein Regulates Pheromone-Mediated Bioluminescence at Multiple Levels in *Vibrio fischeri* ES114. J Bacteriol **195:**5051-5063.

32. **Colton DM, Stoudenmire JL, Stabb EV.** 2015. Growth on glucose decreases cAMP-CRP activity while paradoxically increasing intracellular cAMP in the light-organ symbiont *Vibrio fischeri*. Mol Microbiol **97:**1114-1127.

33. **Dunlap PV.** 1989. Regulation of luminescence by cyclic AMP in *cya*-like and *crp*-like mutants of *Vibrio fischeri*. J Bacteriol **171:**1199-1202.

34. **Dunlap PV, Callahan SM.** 1993. Characterization of a periplasmic 3':5'-cyclic nucleotide phosphodiesterase gene, *cpdP*, from the marine symbiotic bacterium *Vibrio fischeri*. J Bacteriol **175:**4615-4624.

35. **Dunlap PV, Greenberg EP.** 1985. Control of *Vibrio fischeri* luminescence gene expression in *Escherichia coli* by cyclic AMP and cyclic AMP receptor protein. J Bacteriol **164:**45-50.

36. **Dunlap PV, Greenberg EP.** 1988. Control of *Vibrio fischeri lux* gene transcription by a cyclic AMP receptor protein-*luxR* protein regulatory circuit. J Bacteriol **170:**4040-4046.

37. **Septer AN, Lyell NL, Stabb EV.** 2013. The Iron-Dependent Regulator Fur Controls Pheromone Signaling Systems and Luminescence in the Squid Symbiont *Vibrio fischeri* ES114. Appl Environ Microbiol **79:**1826-1834.

38. **Hussa EA, O'Shea TM, Darnell CL, Ruby EG, Visick KL.** 2007. Two-component response regulators of *Vibrio fischeri*: identification, mutagenesis, and characterization. J Bacteriol **189:**5825-5838.

39. **Whistler CA, Ruby EG.** 2003. GacA Regulates Symbiotic Colonization Traits of *Vibrio fischeri* and Facilitates a Beneficial Association with an Animal Host. J Bacteriol **185:**7202-7212.

40. **Cao X, Studer SV, Wassarman K, Zhang Y, Ruby EG, Miyashiro T.** 2012. The novel sigma factor-like regulator RpoQ controls luminescence, chitinase activity, and motility in *Vibrio fischeri*. MBio **3**.

41. **Hoch JA.** 2000. Two-component and phosphorelay signal transduction. Curr Opin Microbiol **3:**165-170.

42. **Stock AM, Robinson VL, Goudreau PN.** 2000. Two-component signal transduction. Annu Rev Biochem **69:**183-215.

43. **Monedero V, Revilla-Guarinos A, Zuniga M.** 2017. Physiological Role of Two-Component Signal Transduction Systems in Food-Associated Lactic Acid Bacteria. Adv Appl Microbiol **99:**1-51.

44. **Prüβ BM.** 2017. Involvement of two-component signaling in bacterial motility and biofilm development. J Bacteriol doi:10.1128/jb.00259-17.

45. **Derzelle S, Turlin E, Duchaud E, Pages S, Kunst F, Givaudan A, Danchin A.** 2004. The PhoP-PhoQ Two-Component Regulatory System of *Photorhabdus luminescens* Is Essential for Virulence in Insects. J Bacteriol **186:**1270-1279.

46. **Galperin MY.** 2006. Structural Classification of Bacterial Response Regulators: Diversity of Output Domains and Domain Combinations. J Bacteriol **188:**4169-4182.

47. **Schaaf S, Bott M.** 2007. Target Genes and DNA-Binding Sites of the Response Regulator PhoR from *Corynebacterium glutamicum*. J Bacteriol **189:**5002-5011.

48. **Hung DCI, Downey JS, Ayala EA, Kreth J, Mair R, Senadheera DB, Qi F, Cvitkovitch DG, Shi W, Goodman SD.** 2011. Characterization of DNA Binding Sites of the ComE Response Regulator from *Streptococcus mutans*. J Bacteriol **193:**3642-3652.

49. **Nowak-Lovato KL, Hickmott AJ, Maity TS, Bulyk ML, Dunbar J, Hong-Geller E.** 2012. DNA binding site analysis of *Burkholderia thailandensis* response regulators. J Microbiol Methods **90:**46-52.

50. **Georgellis D, Kwon O, De Wulf P, Lin EC.** 1998. Signal decay through a reverse phosphorelay in the Arc two-component signal transduction system. J Biol Chem **273:**32864-32869.

51. **Yamamoto K, Hirao K, Oshima T, Aiba H, Utsumi R, Ishihama A.** 2005. Functional characterization *in vitro* of all two-component signal transduction systems from *Escherichia coli*. J Biol Chem **280:**1448-1456.

52. **Graf J, Dunlap PV, Ruby EG.** 1994. Effect of transposon-induced motility mutations on colonization of the host light organ by *Vibrio fischeri*. J Bacteriol **176:**6986-6991.

53. **Millikan DS, Ruby EG.** 2004. *Vibrio fischeri* flagellin A is essential for normal motility and for symbiotic competence during initial squid light organ colonization. J Bacteriol **186:**4315-4325.

54. **Millikan DS, Ruby EG.** 2003. FlrA, a sigma54-dependent transcriptional activator in *Vibrio fischeri*, is required for motility and symbiotic light-organ colonization. J Bacteriol **185:**3547-3557.

55. **Millikan DS, Ruby EG.** 2002. Alterations in *Vibrio fischeri* motility correlate with a delay in symbiosis initiation and are associated with additional symbiotic colonization defects. Appl Environ Microbiol **68:**2519-2528.

56. **Lyell NL, Stabb EV.** 2013. Symbiotic characterization of *Vibrio fischeri* ES114 mutants that display enhanced luminescence in culture. Appl Environ Microbiol **79:**2480-2483.

57. **Malpica R, Franco B, Rodriguez C, Kwon O, Georgellis D.** 2004. Identification of a quinone-sensitive redox switch in the ArcB sensor kinase. Proc Natl Acad Sci U S A **101:**13318-13323.

58. **Iuchi S, Lin EC.** 1988. *arcA* (*dye*), a global regulatory gene in *Escherichia coli* mediating repression of enzymes in aerobic pathways. Proc Natl Acad Sci U S A **85:**1888-1892.

59. **Williams JW, Cui X, Levchenko A, Stevens AM.** 2008. Robust and sensitive control of a quorum-sensing circuit by two interlocked feedback loops. Mol Syst Biol **4:**234.

60. **Makino K, Shinagawa H, Amemura M, Nakata A.** 1986. Nucleotide sequence of the *phoR* gene, a regulatory gene for the phosphate regulon of *Escherichia coli*. J Mol Biol **192:**549-556.

61. **Makino K, Shinagawa H, Amemura M, Kawamoto T, Yamada M, Nakata A.** 1989. Signal transduction in the phosphate regulon of *Escherichia coli* involves phosphotransfer between PhoR and PhoB proteins. J Mol Biol **210:**551-559.

62. **Blanco AG, Sola M, Gomis-Ruth FX, Coll M.** 2002. Tandem DNA recognition by PhoB, a two-component signal transduction transcriptional activator. Structure **10:**701-713.

63. **Diniz MM, Goulart CL, Barbosa LC, Farache J, Lery LM, Pacheco AB, Bisch PM, von Kruger WM.** 2011. Fine-tuning control of *phoBR* expression in *Vibrio cholerae* by binding of PhoB to multiple Pho boxes. J Bacteriol **193:**6929-6938.

64. **Kimura S, Makino K, Shinagawa H, Amemura M, Nakata A.** 1989. Regulation of the phosphate regulon of *Escherichia coli*: characterization of the promoter of the *pstS* gene. Mol Gen Genet **215:**374-380.

65. **Pratt JT, Ismail AM, Camilli A.** 2010. PhoB regulates both environmental and virulence gene expression in *Vibrio cholerae*. Mol Microbiol **77:**1595-1605.

66. **Thompson LR, Nikolakakis K, Pan S, Reed J, Knight R, Ruby EG.** 2017. Transcriptional characterization of *Vibrio fischeri* during colonization of juvenile *Euprymna scolopes*. Environ Microbiol **19:**1845-1856.

67. **Manoil C, Beckwith J.** 1985. Tn*phoA*: a transposon probe for protein export signals. Proc Natl Acad Sci U S A **82:**8129-8133.

68. **Elhai J, Wolk CP.** 1990. Developmental regulation and spatial pattern of expression of the structural genes for nitrogenase in the cyanobacterium *Anabaena*. EMBO J **9:**3379-3388.

69. **Chalfie M, Tu Y, Euskirchen G, Ward WW, Prasher DC.** 1994. Green fluorescent protein as a marker for gene expression. Science **263:**802-805.

70. **Miller WG, Leveau JHJ, Lindow SE.** 2000. Improved *gfp* and *inaZ* Broad-Host-Range Promoter-Probe Vectors. Mol Plant-Microbe Interact **13:**1243-1250.

71. **Casadaban MJ.** 1975. Fusion of the *Escherichia coli lac* genes to the *ara* promoter: a general technique using bacteriophage Mu-1 insertions. Proc Natl Acad Sci U S A **72:**809-813.

72. **Lucchini S, Liu H, Jin Q, Hinton JCD, Yu J.** 2005. Transcriptional Adaptation of *Shigella flexneri* during Infection of Macrophages and Epithelial Cells: Insights into the Strategies of a Cytosolic Bacterial Pathogen. Infect Immun **73:**88-102.

73. **Joseph B, Przybilla K, Stuhler C, Schauer K, Slaghuis J, Fuchs TM, Goebel W.** 2006. Identification of *Listeria monocytogenes* genes contributing to intracellular replication by expression profiling and mutant screening. J Bacteriol **188:**556-568.

74. **Wier AM, Nyholm SV, Mandel MJ, Massengo-Tiasse RP, Schaefer AL, Koroleva I, Splinter-Bondurant S, Brown B, Manzella L, Snir E, Almabrazi H, Scheetz TE, Bonaldo Mde F, Casavant TL, Soares MB, Cronan JE, Reed JL, Ruby EG, McFall-Ngai MJ.** 2010. Transcriptional patterns in both host and bacterium underlie a daily rhythm of anatomical and metabolic change in a beneficial symbiosis. Proc Natl Acad Sci U S A **107:**2259-2264.

75. **Slauch JM, Camilli A.** 2000. IVET and RIVET: Use of gene fusions to identify bacterial virulence factors specifically induced in host tissues. Methods Enzymol **326:**73-96.

76. **Angelichio MJ, Camilli A.** 2002. *In Vivo* Expression Technology. Infect Immun **70:**6518-6523.

77. **Casadaban MJ, Cohen SN.** 1980. Analysis of gene control signals by DNA fusion and cloning in *Escherichia coli*. J Mol Biol **138:**179-207.

78. **Shimomura O, Johnson FH, Saiga Y.** 1962. Extraction, Purification and Properties of Aequorin, a Bioluminescent Protein from the Luminous Hydromedusan, Aequorea. Journal of Cellular and Comparative Physiology **59:**223-239.

79. **Heim R, Cubitt AB, Tsien RY.** 1995. Improved green fluorescence. Nature **373:**663-664.

80. **Cormack BP, Valdivia RH, Falkow S.** 1996. FACS-optimized mutants of the green fluorescent protein (GFP). Gene **173:**33-38.

81. **Heim R, Tsien RY.** 1996. Engineering green fluorescent protein for improved brightness, longer wavelengths and fluorescence resonance energy transfer. Curr Biol **6:**178-182.

82. **Zhang G, Gurtu V, Kain SR.** 1996. An Enhanced Green Fluorescent Protein Allows Sensitive Detection of Gene Transfer in Mammalian Cells. Biochem Biophys Res Commun **227:**707-711.

83. **Chiu W-l, Niwa Y, Zeng W, Hirano T, Kobayashi H, Sheen J.** 1996. Engineered GFP as a vital reporter in plants. Curr Biol **6:**325-330.

84. **Heim R, Prasher DC, Tsien RY.** 1994. Wavelength mutations and posttranslational autoxidation of green fluorescent protein. Proceedings of the National Academy of Sciences of the United States of America **91:**12501-12504.

85. **Siemering KR, Golbik R, Sever R, Haseloff J.** 1996. Mutations that suppress the thermosensitivity of green fluorescent protein. Curr Biol **6:**1653-1663.

86. **Pédelacq J-D, Cabantous S, Tran T, Terwilliger TC, Waldo GS.** 2006. Engineering and characterization of a superfolder green fluorescent protein. Nat Biotechnol **24:**79.

87. **Delagrave S, Hawtin RE, Silva CM, Yang MM, Youvan DC.** 1995. Red-shifted excitation mutants of the green fluorescent protein. Biotechnology (N Y) **13:**151-154.

88. **Andersen JB, Sternberg C, Poulsen LK, Bjorn SP, Givskov M, Molin S.** 1998. New unstable variants of green fluorescent protein for studies of transient gene expression in bacteria. Appl Environ Microbiol **64:**2240-2246.

89. **Tombolini R, Unge A, Davey ME, de Bruijn FJ, Jansson JK.** 1997. Flow cytometric and microscopic analysis of GFP-tagged *Pseudomonas fluorescens* bacteria. FEMS Microbiol Ecol **22:**17-28.

90. **Yu X, Xu J, Liu X, Chu X, Wang P, Tian J, Wu N, Fan Y.** 2015. Identification of a highly efficient stationary phase promoter in *Bacillus subtilis*. **5:**18405.

91. **Gage DJ, Bobo T, Long SR.** 1996. Use of green fluorescent protein to visualize the early events of symbiosis between *Rhizobium meliloti* and alfalfa (*Medicago sativa*). J Bacteriol **178:**7159-7166.

92. **Kikuchi Y, Fukatsu T.** 2014. Live imaging of symbiosis: spatiotemporal infection dynamics of a GFP-labelled *Burkholderia* symbiont in the bean bug *Riptortus pedestris*. Mol Ecol **23:**1445-1456.

93. **Brandl MT, Quiñones B, Lindow SE.** 2001. Heterogeneous transcription of an indoleacetic acid biosynthetic gene in *Erwinia herbicola* on plant surfaces. Proceedings of the National Academy of Sciences of the United States of America **98:**3454-3459.

94. **Leveau JH, Lindow SE.** 2001. Appetite of an epiphyte: quantitative monitoring of bacterial sugar consumption in the phyllosphere. Proc Natl Acad Sci U S A **98:**3446-3453.

95. **Brooks JF, Gyllborg MC, Cronin DC, Quillin SJ, Mallama CA, Foxall R, Whistler C, Goodman AL, Mandel MJ.** 2014. Global discovery of colonization determinants in the squid symbiont *Vibrio fischeri*. Proceedings of the National Academy of Sciences **111:**17284-17289.

96. **Sycuro LK, Ruby EG, McFall-Ngai M.** 2006. Confocal microscopy of the light organ crypts in juvenile *Euprymna scolopes* reveals their morphological complexity and dynamic function in symbiosis. J Morphol **267:**555-568.

97. **Dunn AK, Millikan DS, Adin DM, Bose JL, Stabb EV.** 2006. New *rfp*- and pES213-derived tools for analyzing symbiotic *Vibrio fischeri* reveal patterns of infection and *lux* expression *in situ*. Appl Environ Microbiol **72:**802-810.

98. **Septer AN, Wang Y, Ruby EG, Stabb EV, Dunn AK.** 2011. The haem-uptake gene cluster in *Vibrio fischeri* is regulated by Fur and contributes to symbiotic colonization. Environ Microbiol **13:**2855-2864.

99. **Lynch AS, Lin EC.** 1996. Transcriptional control mediated by the ArcA two-component response regulator protein of *Escherichia coli*: characterization of DNA binding at target promoters. J Bacteriol **178:**6238-6249.

100. **Shimada T, Fujita N, Yamamoto K, Ishihama A.** 2011. Novel Roles of cAMP Receptor Protein (CRP) in Regulation of Transport and Metabolism of Carbon Sources. PLOS ONE **6:**e20081.

101. **Muir RE, Gober JW.** 2005. Role of Integration Host Factor in the Transcriptional Activation of Flagellar Gene Expression in *Caulobacter crescentus*. J Bacteriol **187:**949-960.

102. **Martinez-Antonio A, Collado-Vides J.** 2003. Identifying global regulators in transcriptional regulatory networks in bacteria. Curr Opin Microbiol **6:**482-489.

103. **Balleza E, Lopez-Bojorquez LN, Martinez-Antonio A, Resendis-Antonio O, Lozada-Chavez I, Balderas-Martinez YI, Encarnacion S, Collado-Vides J.** 2009. Regulation by transcription factors in bacteria: beyond description. FEMS Microbiol Rev **33:**133-151.

104. **Feng Y, Cronan JE.** 2010. Overlapping Repressor Binding Sites Result in Additive Regulation of *Escherichia coli* FadH by FadR and ArcA. J Bacteriol **192:**4289-4299.

105. **Cotter PA, Melville SB, Albrecht JA, Gunsalus RP.** 1997. Aerobic regulation of cytochrome *d* oxidase (*cydAB*) operon expression in *Escherichia coli*: roles of Fnr and ArcA in repression and activation. Mol Microbiol **25:**605-615.

106. **Iuchi S, Matsuda Z, Fujiwara T, Lin EC.** 1990. The *arcB* gene of *Escherichia coli* encodes a sensor-regulator protein for anaerobic repression of the Arc modulon. Mol Microbiol **4:**715-727.

107. **Cotter PA, Gunsalus RP.** 1992. Contribution of the *fnr* and *arcA* gene products in coordinate regulation of cytochrome o and d oxidase (*cyoABCDE* and *cydAB*) genes in *Escherichia coli*. FEMS Microbiol Lett **70:**31-36.

108. **Bekker M, Alexeeva S, Laan W, Sawers G, Teixeira de Mattos J, Hellingwerf K.** 2010. The ArcBA two-component system of *Escherichia coli* is regulated by the redox state of both the ubiquinone and the menaquinone pool. J Bacteriol **192:**746-754.

109. **Sawers G, Kaiser M, Sirko A, Freundlich M.** 1997. Transcriptional activation by FNR and CRP: reciprocity of binding-site recognition. Mol Microbiol **23:**835-845.

110. **Estrada J, Ruiz-Herrero T, Scholes C, Wunderlich Z, DePace AH.** 2016. SiteOut: An Online Tool to Design Binding Site-Free DNA Sequences. PLoS One **11:**e0151740.

111. **Gilman J, Love J.** 2016. Synthetic promoter design for new microbial chassis. Biochem Soc Trans **44:**731-737.

112. **Yang C, Huang TW, Wen SY, Chang CY, Tsai SF, Wu WF, Chang CH.** 2012. Genome-wide PhoB binding and gene expression profiles reveal the hierarchical gene regulatory network of phosphate starvation in *Escherichia coli*. PLoS One **7:**e47314.

113. **Lubin EA, Henry JT, Fiebig A, Crosson S, Laub MT.** 2015. Identification of the PhoB Regulon and Role of PhoU in the Phosphate Starvation Response of *Caulobacter crescentus*. J Bacteriol **198:**187-200.

114. **Wanner BL.** 1996. Signal transduction in the control of phosphate-regulated genes of *Escherichia coli*. Kidney Int **49:**964-967.

115. **Okamura H, Hanaoka S, Nagadoi A, Makino K, Nishimura Y.** 2000. Structural comparison of the PhoB and OmpR DNA-binding/transactivation domains and the arrangement of PhoB molecules on the phosphate box. J Mol Biol **295:**1225-1236.

116. **Gebhard S, Cook GM.** 2008. Differential regulation of high-affinity phosphate transport systems of *Mycobacterium smegmatis*: identification of PhnF, a repressor of the *phnDCE* operon. J Bacteriol **190:**1335-1343.

117. **Munoz-Martin MA, Mateo P, Leganes F, Fernandez-Pinas F.** 2011. Novel cyanobacterial bioreporters of phosphorus bioavailability based on alkaline phosphatase and phosphate transporter genes of *Anabaena* sp. PCC 7120. Anal Bioanal Chem **400:**3573-3584.

118. **Makino K, Shinagawa H, Amemura M, Kimura S, Nakata A, Ishihama A.** 1988. Regulation of the phosphate regulon of *Escherichia coli*. Activation of *pstS* transcription by PhoB protein *in vitro*. J Mol Biol **203:**85-95.

119. **Cardemil CV, Smulski DR, Larossa RA, Vollmer AC.** 2010. Bioluminescent *Escherichia coli* strains for the quantitative detection of phosphate and ammonia in coastal and suburban watersheds. DNA Cell Biol **29:**519-531.

120. **Spira B, Yagil E.** 1999. The integration host factor (IHF) affects the expression of the phosphate-binding protein and of alkaline phosphatase in *Escherichia coli*. Curr Microbiol **38:**80-85.

121. **Taschner NP, Yagil E, Spira B.** 2006. The effect of IHF on sigmaS selectivity of the *phoA* and *pst* promoters of *Escherichia coli*. Arch Microbiol **185:**234-237.

122. **Aoyama T, Oka A.** 1990. A common mechanism of transcriptional activation by the three positive regulators, VirG, PhoB, and OmpR. FEBS Lett **263:**1-4.

123. **Kim SK, Kimura S, Shinagawa H, Nakata A, Lee KS, Wanner BL, Makino K.** 2000. Dual transcriptional regulation of the *Escherichia coli* phosphate-starvation-inducible *psiE* gene of the phosphate regulon by PhoB and the cyclic AMP (cAMP)-cAMP receptor protein complex. J Bacteriol **182:**5596-5599.

124. **Kasahara M, Makino K, Amemura M, Nakata A, Shinagawa H.** 1991. Dual regulation of the *ugp* operon by phosphate and carbon starvation at two interspaced promoters. J Bacteriol **173:**549-558.

125. **Gao R, Stock AM.** 2015. Temporal hierarchy of gene expression mediated by transcription factor binding affinity and activation dynamics. MBio **6:**e00686-00615.

126. **Yuan Z-C, Zaheer R, Morton R, Finan TM.** 2006. Genome prediction of PhoB regulated promoters in *Sinorhizobium meliloti* and twelve proteobacteria. Nucleic Acids Res **34:**2686-2697.

127. **Kolter R, Inuzuka M, Helinski DR.** 1978. Trans-complementation-dependent replication of a low molecular weight origin fragment from plasmid R6K. Cell **15:**1199-1208.

128. **Dunn AK, Martin MO, Stabb EV.** 2005. Characterization of pES213, a small mobilizable plasmid from *Vibrio fischeri*. Plasmid **54:**114-134.

129. **Wild J, Czyz A, Rakowski S, Filutowicz M.** 2004. γ origin plasmids of R6K lineage replicate in diverse genera of Gram-negative bacteria. Ann Microbiol **54:**471-480.

130. **Keiler KC, Waller PR, Sauer RT.** 1996. Role of a peptide tagging system in degradation of proteins synthesized from damaged messenger RNA. Science **271:**990-993.

131. **Sauer RT, Bolon DN, Burton BM, Burton RE, Flynn JM, Grant RA, Hersch GL, Joshi SA, Kenniston JA, Levchenko I, Neher SB, Oakes ESC, Siddiqui SM, Wah DA, Baker TA.** 2004. Sculpting the Proteome with AAA+ Proteases and Disassembly Machines. Cell **119:**9-18.

132. **Rivera-Rivera I, Roman-Hernandez G, Sauer RT, Baker TA.** 2014. Remodeling of a delivery complex allows ClpS-mediated degradation of N-degron substrates. Proc Natl Acad Sci U S A **111:**E3853-3859.

133. **Dougan DA, Reid BG, Horwich AL, Bukau B.** 2002. ClpS, a Substrate Modulator of the ClpAP Machine. Mol Cell **9:**673-683.

134. **Jensen PR, Hammer K.** 1998. The Sequence of Spacers between the Consensus Sequences Modulates the Strength of Prokaryotic Promoters. Appl Environ Microbiol **64:**82-87.

135. **Hawley DK, McClure WR.** 1983. Compilation and analysis of *Escherichia coli* promoter DNA sequences. Nucleic Acids Res **11:**2237-2255.

136. **Kammerer W, Deuschle U, Gentz R, Bujard H.** 1986. Functional dissection of *Escherichia coli* promoters: information in the transcribed region is involved in late steps of the overall process. The EMBO Journal **5:**2995-3000.

137. **Wanner BL.** 1993. Gene regulation by phosphate in enteric bacteria. J Cell Biochem **51:**47-54.

138. **Konopka A, Wilkins MJ.** 2012. Application of meta-transcriptomics and -proteomics to analysis of *in situ* physiological state. Frontiers in Microbiology **3:**184.

139. **Stabb EV, Reich KA, Ruby EG.** 2001. *Vibrio fischeri* genes *hvnA* and *hvnB* encode secreted NAD(+)-glycohydrolases. J Bacteriol **183:**309-317.

140. **Sambrook J, Fritsch EF, Maniatis T.** 1989. Molecular cloning, vol 2. Cold spring harbor laboratory press New York.

141. **Neidhardt FC, Bloch PL, Smith DF.** 1974. Culture medium for enterobacteria. J Bacteriol **119:**736-747.

142. **Gonzalez JM, Covert JS, Whitman WB, Henriksen JR, Mayer F, Scharf B, Schmitt R, Buchan A, Fuhrman JA, Kiene RP, Moran MA.** 2003. *Silicibacter pomeroyi* sp. nov. and *Roseovarius nubinhibens* sp. nov., dimethylsulfoniopropionate-demethylating bacteria from marine environments. Int J Syst Evol Microbiol **53:**1261-1269.

143. **Reisch CR, Moran MA, Whitman WB.** 2008. Dimethylsulfoniopropionate-dependent demethylase (*DmdA*) from *Pelagibacter ubique* and *Silicibacter pomeroyi*. J Bacteriol **190:**8018-8024.

144. **Herrero M, de Lorenzo V, Timmis KN.** 1990. Transposon vectors containing non-antibiotic resistance selection markers for cloning and stable chromosomal insertion of foreign genes in gram-negative bacteria. J Bacteriol **172:**6557-6567.

145. **Stabb EV, Ruby EG.** 2002. RP4-based plasmids for conjugation between *Escherichia coli* and members of the Vibrionaceae. Methods Enzymol **358:**413-426.

146. **Hanahan D.** 1983. Studies on transformation of *Escherichia coli* with plasmids. J Mol Biol **166:**557-580.

147. **Singer M, Baker TA, Schnitzler G, Deischel SM, Goel M, Dove W, Jaacks KJ, Grossman AD, Erickson JW, Gross CA.** 1989. A collection of strains containing genetically linked alternating antibiotic resistance elements for genetic mapping of *Escherichia coli*. Microbiol Rev **53:**1-24.

148. **Gonzalez JM, Kiene RP, Moran MA.** 1999. Transformation of sulfur compounds by an abundant lineage of marine bacteria in the alpha-subclass of the class *Proteobacteria*. Appl Environ Microbiol **65:**3810-3819.

149. **Grana D, Youderian P, Susskind MM.** 1985. Mutations that improve the ant promoter of *Salmonella* phage P22. Genetics **110:**1-16.

150. **United States. Environmental Protection Agency. Water Quality Office.** 1971. Methods for chemical analysis of water and wastes. Environmental Protection Agency, Analytical Quality Control Laboratory; for sale by the Supt. of Docs., U.S. Govt. Print. Off., Cincinnati,.

151. **Iuchi S.** 1993. Phosphorylation/dephosphorylation of the receiver module at the conserved aspartate residue controls transphosphorylation activity of histidine kinase in sensor protein ArcB of *Escherichia coli*. J Biol Chem **268:**23972-23980.

152. **Alvarez AF, Rodriguez C, Georgellis D.** 2013. Ubiquinone and menaquinone electron carriers represent the yin and yang in the redox regulation of the ArcB sensor kinase. J Bacteriol **195:**3054-3061.

153. **Georgellis D, Kwon O, Lin EC.** 2001. Quinones as the redox signal for the Arc two-component system of bacteria. Science **292:**2314-2316.

154. **Rolfe MD, Beek AT, Graham AI, Trotter EW, Asif HMS, Sanguinetti G, de Mattos JT, Poole RK, Green J.** 2011. Transcript Profiling and Inference of Escherichia coli K-12 ArcA Activity across the Range of Physiologically Relevant Oxygen Concentrations. J Biol Chem **286:**10147-10154.

155. **Georgellis D, Kwon O, Lin EC.** 1999. Amplification of signaling activity of the arc two-component system of Escherichia coli by anaerobic metabolites. An in vitro study with different protein modules. J Biol Chem **274:**35950-35954.

156. **Septer AN, Bose JL, Dunn AK, Stabb EV.** 2010. FNR-mediated regulation of bioluminescence and anaerobic respiration in the light-organ symbiont *Vibrio fischeri*. FEMS Microbiol Lett **306:**72-81.

157. **Compan I, Touati D.** 1994. Anaerobic activation of *arcA* transcription in *Escherichia coli*: roles of Fnr and ArcA. Mol Microbiol **11:**955-964.

158. **Ravcheev DA, Gerasimova AV, Mironov AA, Gelfand MS.** 2007. Comparative genomic analysis of regulation of anaerobic respiration in ten genomes from three families of gamma-proteobacteria (*Enterobacteriaceae, Pasteurellaceae, Vibrionaceae*). BMC Genomics **8:**54.

159. **Matsushika A, Mizuno T.** 2000. Characterization of three putative sub-domains in the signal-input domain of the ArcB hybrid sensor in *Escherichia coli*. J Biochem **127:**855-860.

160. **Park SJ, Tseng CP, Gunsalus RP.** 1995. Regulation of succinate dehydrogenase (*sdhCDAB*) operon expression in *Escherichia coli* in response to carbon supply and anaerobiosis: role of ArcA and Fnr. Mol Microbiol **15:**473-482.

161. **Mack TR, Gao R, Stock AM.** 2009. Probing the roles of the two different dimers mediated by the receiver domain of the response regulator PhoB. J Mol Biol **389:**349-364.

162. **West AH, Stock AM.** 2001. Histidine kinases and response regulator proteins in two-component signaling systems. Trends Biochem Sci **26:**369-376.

163. **Toro-Roman A, Mack TR, Stock AM.** 2005. Structural analysis and solution studies of the activated regulatory domain of the response regulator ArcA: a symmetric dimer mediated by the alpha4-beta5-alpha5 face. J Mol Biol **349:**11-26.

164. **Ellison DW, McCleary WR.** 2000. The Unphosphorylated Receiver Domain of PhoB Silences the Activity of Its Output Domain. J Bacteriol **182:**6592-6597.

165. **Harmer T, Wu M, Schleif R.** 2001. The role of rigidity in DNA looping-unlooping by AraC. Proceedings of the National Academy of Sciences of the United States of America **98:**427-431.

166. **Alkaabi KM, Yafea A, Ashraf SS.** 2005. Effect of pH on thermal- and chemical-induced denaturation of GFP. Appl Biochem Biotechnol **126:**149-156.

167. **Studer SV, Mandel MJ, Ruby EG.** 2008. AinS quorum sensing regulates the *Vibrio fischeri* acetate switch. J Bacteriol **190:**5915-5923.

168. **Doudoroff M.** 1942. Studies on the Luminous Bacteria: II. Some Observations on the Anaerobic Metabolism of Facultatively Anaerobic Species. J Bacteriol **44:**461-467.

169. **Georgellis D, Lynch AS, Lin EC.** 1997. *In vitro* phosphorylation study of the Arc two-component signal transduction system of *Escherichia coli*. J Bacteriol **179:**5429-5435.

170. **Georgellis D, Kwon O, Lin ECC.** 1999. Amplification of Signaling Activity of the Arc Two-component System of *Escherichia coli* by Anaerobic Metabolites. J Biol Chem **274:**35950-35954.

171. **Steinsiek S, Stagge S, Bettenbrock K.** 2014. Analysis of *Escherichia coli* Mutants with a Linear Respiratory Chain. PLOS ONE **9:**e87307.

172. **Rolfe MD, Ter Beek A, Graham AI, Trotter EW, Asif HM, Sanguinetti G, de Mattos JT, Poole RK, Green J.** 2011. Transcript profiling and inference of *Escherichia coli* K-12 ArcA activity across the range of physiologically relevant oxygen concentrations. J Biol Chem **286:**10147-10154.

173. **Stock J B.** 1995. Two-component signal transduction systems: structure-function relation ships and mechanisms of catalysis. Two-Component Signal Transduction**:**25-51.

174. **Lukat GS, McCleary WR, Stock AM, Stock JB.** 1992. Phosphorylation of bacterial response regulator proteins by low molecular weight phospho-donors. Proc Natl Acad Sci U S A **89:**718-722.

175. **Head CG, Tardy A, Kenney LJ.** 1998. Relative binding affinities of OmpR and OmpR-phosphate at the *ompF* and *ompC* regulatory sites. J Mol Biol **281:**857-870.

176. **Da Re SS, Deville-Bonne D, Tolstykh T, M Vr, Stock JB.** 1999. Kinetics of CheY phosphorylation by small molecule phosphodonors. FEBS Lett **457:**323-326.

177. **Mayover TL, Halkides CJ, Stewart RC.** 1999. Kinetic characterization of CheY phosphorylation reactions: comparison of P-CheA and small-molecule phosphodonors. Biochemistry **38:**2259-2271.

178. **McCleary WR.** 1996. The activation of PhoB by acetylphosphate. Mol Microbiol **20:**1155-1163.

179. **Klein AH, Shulla A, Reimann SA, Keating DH, Wolfe AJ.** 2007. The intracellular concentration of acetyl phosphate in *Escherichia coli* is sufficient for direct phosphorylation of two-component response regulators. J Bacteriol **189:**5574-5581.

180. **Wolfe AJ.** 2005. The acetate switch. Microbiol Mol Biol Rev **69:**12-50.

181. **Gunsalus RP, Park SJ.** 1994. Aerobic-anaerobic gene regulation in *Escherichia coli*: control by the ArcAB and Fnr regulons. Res Microbiol **145:**437-450.

182. **Sengupta N, Paul K, Chowdhury R.** 2003. The global regulator ArcA modulates expression of virulence factors in *Vibrio cholerae*. Infect Immun **71:**5583-5589.

183. **Serna A, Espinosa E, Camacho EM, Casadesus J.** 2010. Regulation of bacterial conjugation in microaerobiosis by host-encoded functions ArcAB and *sdhABCD*. Genetics **184:**947-958.

184. **Zbell AL, Benoit SL, Maier RJ.** 2007. Differential expression of NiFe uptake-type hydrogenase genes in *Salmonella enterica* serovar Typhimurium. Microbiology **153:**3508-3516.

185. **Taki K, Abo T, Ohtsubo E.** 1998. Regulatory mechanisms in expression of the *traY-I* operon of sex factor plasmid R100: involvement of *traJ* and *traY* gene products. Genes Cells **3:**331-345.

186. **Loui C, Chang AC, Lu S.** 2009. Role of the ArcAB two-component system in the resistance of *Escherichia coli* to reactive oxygen stress. BMC Microbiol **9:**183.

187. **Miller JH.** 1992. A short course in bacterial genetics : a laboratory manual and handbook for *Escherichia coli* and related bacteria. Cold Spring Harbor Laboratory Press, Plainview, N.Y.

188. **Horton RM, Cai ZL, Ho SN, Pease LR.** 1990. Gene splicing by overlap extension: tailor-made genes using the polymerase chain reaction. BioTechniques **8:**528-535.

189. **Adin DM, Engle JT, Goldman WE, McFall-Ngai MJ, Stabb EV.** 2009. Mutations in *ampG* and Lytic Transglycosylase Genes Affect the Net Release of Peptidoglycan Monomers from *Vibrio fischeri*. J Bacteriol **191:**2012-2022.

190. **Barak R, Eisenbach M.** 2004. Co-regulation of Acetylation and Phosphorylation of CheY, A Response Regulator in Chemotaxis of *Escherichia coli*. J Mol Biol **342:**375-381.